UNCLASSIFIED

AD NUMBER

AD864172

LIMITATION CHANGES

TO:

Approved for public release; distribution is unlimited.

FROM:

**Distribution authorized to U.S. Gov't. agencies and their contractors;
Administrative/Operational Use; 06 JAN 1970.
Other requests shall be referred to Air Force Technical Applications Center, Washington, DC 20330.**

AUTHORITY

AFTAC USAF ltr 25 Jan 1972

THIS PAGE IS UNCLASSIFIED

AD 864172

A LONG-PERIOD NOISE STUDY AT MURPHY DOME, ALASKA

(LRSM SITE FB-AK AND ALPA SITE 3-4)

6 January 1970

Prepared For

AIR FORCE TECHNICAL APPLICATIONS CENTER
Washington, D. C.

By

D. H. Von Seggern

SEISMIC DATA LABORATORY

Under

Project VELA UNIFORM

DDC
RETURNED
JAN 28 1970
B

Sponsored By

ADVANCED RESEARCH PROJECTS AGENCY
Nuclear Monitoring Research Office
ARPA Order No. 624

Reproduced by the
CLEARINGHOUSE
for Federal Scientific & Technical
Information Springfield Va. 22151

This document is subject to special export controls and each transmittal to foreign governments or foreign nationals may be made only with prior approval of Chief, AFTAC. VSC

Alexandria, Va. 22314

BEST
AVAILABLE COPY

A LONG-PERIOD NOISE STUDY AT MURPHY DOME, ALASKA

(LRSM Site FB-AK and ALPA Site 3-4)

SEISMIC DATA LABORATORY REPORT NO. 247

AFTAC Project No.:	VELA T/9706
Project Title:	Seismic Data Laboratory
ARPA Order No.:	624
ARPA Program Code No.:	9F10
Name of Contractor:	TELEDYNE INDUSTRIES, INC.
Contract No.:	F33657-69-C-0913-PZ01
Date of Contract:	2 March 1969
Amount of Contract:	$ 2,000,000
Contract Expiration Date:	1 March 1970
Project Manager:	Royal A. Hartenberger (703) 836-7647

P. O. Box 334, Alexandria, Virginia

AVAILABILITY

This document is subject to special export controls and each transmittal to foreign governments or foreign nationals may be made only with prior approval of Chief, AFTAC.

This research was supported by the Advanced Research Projects Agency, Nuclear Monitoring Research Office, under Project VELA-UNIFORM and accomplished under technical direction of the Air Force Technical Applications Center under Contract F33657-69-C-0913-PZ01.

Neither the Advanced Research Projects Agency nor the Air Force Technical Applications Center will be responsible for information contained herein which may have been supplied by other organizations or contractors, and this document is subject to later revision as may be necessary.

TABLE OF CONTENTS

	Page No.
ABSTRACT	
INTRODUCTION	1
INSTRUMENTATION	1
SPECTRAL COMPUTATIONS	2
SYSTEM NOISE	4
SEISMIC NOISE	5
Spectra of Noise at Murphy Dome	5
Coherence with Microbarograph Recordings	6
Direction of Propagating Noise	8
SIGNALS	8
CONCLUSION	11
REFERENCES	

LIST OF FIGURES

Figure Title	Figure No.
LRSM and ALPA long-period system response curves.	1
System noise - raw Triax, transformed Triax, and ALPs traces.	2
Seismic noise - raw Triax, transformed Triax, and ALPs traces.	3
Vertical and east component noise spectra - samples before March 1, 1969.	4a
Vertical and east component noise spectra - samples after March 1, 1969.	4b
Power spectra of microbarograph and seismograph recordings on 13 January 1969.	5a
Coherence between microbarograph and seismograph recordings on 13 January 1969.	5b
Power spectra of microbarograph and seismograph recordings on 21 February 1969.	6a
Coherence between microbarograph and seismograph recordings on 21 February 1969.	6b
Power spectra of microbarograph and seismograph recordings on 18 February 1969.	7a
Coherence between microbarograph and seismograph recordings on 18 February 1969.	7b
Coherence of vertical and rotated horizontal components on 13 January 1969.	8
Coherence of vertical and rotated horizontal components on 9 February 1969.	9
Coherence of vertical and rotated horizontal components on 2 June 1969.	10

LIST OF FIGURES (Cont'd.)

Figure Title	Figure No.
Recorded vertical, radial, and transverse components for the signals analyzed (10 pages).	11
Power spectra of body waves recorded simultaneously on the ALPs and Triax systems.	12
Power spectra of Love waves recorded simultaneously on the ALPs and Triax systems (2 pages).	13
Power spectra of Rayleigh waves recorded simultaneously on the ALPs and Triax systems (3 pages).	14
Power spectra of Rayleigh waves recorded simultaneously on the ALPs vertical and radial components (3 pages).	15
Coherence between ALPs and Triax components for several signals (3 pages).	16
Coherence between ALPs vertical and ALPs radial components for several signals (2 pages).	17

LIST OF TABLES

Table Title	Table No.
Abbreviations for Components of Motion	1
Confidence Limits on Coherence	2
Ncise Sample Times	3
Epicenter Data for Signals Analyzed	4

ABSTRACT

Long-period signals and noise samples recorded at Murphy Dome, Alaska, on standard LRSM instruments and the Geotech triaxial seismometer were subjected to spectral analysis. System noise tests showed that recorded seismic noise was limited to a band from .02 to 0.3 cps. Spectra representing many recording periods between January and August 1969 revealed the background noise to be of variable character and the RMS to range from 2.5 millimeters to 5.2 millimeters on a trace magnified 10^5 times with the standard LRSM system response. Due to its location at depth the triaxial instrument significantly reduced background noise on horizontal components caused by atmospheric pressure changes. Coherence between triaxial components of motion and corresponding LRSM components was excellent for most signals analyzed.

INTRODUCTION

A long-period triaxial seismometer has been in operation at Murphy Dome, Alaska, since December 1968 at various depths to 175 feet within a borehole. During this time a LRSM site (FB-AK) has been maintained at the same location. Thus, there is the opportunity to compare seismic background samples and signals as recorded by the triaxial instrument with those recorded by the standard long-period instruments of the LRSM program on the surface. Further, a microbarograph has been operating, and the effects of atmospheric pressure changes on the background noise can be quantitatively assessed.

INSTRUMENTATION

Three Advanced Long Period seismometers (hereafter termed "ALPs") as described by Geotech (1964) were operated at the surface. These were oriented in the vertical, north, and east directions. The long-period triaxial seismometer (hereafter termed "Triax") as described by Geotech (1969) was emplaced in a borehole. Transformation of triaxial components into vertical, north, and east motion is straightforward and is accomplished at the site. The relations are such that magnifications of the three transformed components will be identical if the three separate triaxial components are operated at equal gains. Table 1 lists the abbreviations used in this report to designate the various ALPs and Triax components. Relative response curves for both systems have been matched since operation began. Prior to March 1, 1969, the response for both systems was of the standard LRSM long-period type, Figure 1; and after March 1, 1969, the response of both systems was altered to that also shown in Figure 1, which will be referred to as the "ALPA" (Advanced Long-Period Array) response. Both responses are uncertain outside

the period band from 10 to 100 seconds, but smooth attenuation rates can be assumed. Since spectra shown in this report will be reduced to absolute ground motion at 25 seconds period only and will not be corrected for system response relative to this period, these curves must be kept in mind in viewing actual spectra representing recording times before and after March 1, 1969.

The microbarograph in use at Murphy Dome, Alaska, is Geotech's commercial model. Its system response is sufficiently flat over the frequency range of interest (.008 to .5 cps) that spectra of recordings from this instrument are representative of absolute pressure changes at all frequencies.

SPECTRAL COMPUTATIONS

All the data for this report were band-pass filtered between .002 and 1.0 cps with 24 db/octave cutoff on both ends and were digitized at a rate of one sample per second. Since the Cooley-Tukey fast Fourier transform technique was employed, record lengths were fixed at an even power of two. All noise samples analyzed consisted of 2048 points, and signals analyzed varied from 128 to 2048 points. Spectra were smoothed by the Hanning function and decimated by two successively until a final spectra of 64 points plus the DC term remained, representing 0.0 to 0.5 cps in frequency increments of .0078 cps. The DC value is ignored and the first point of the spectra corresponds to a period of 128 seconds in the plots shown later. Power spectra of the seismic traces are reduced to absolute ground motion at 25 seconds period only by applying a demagnification factor determined from calibration data at this period. Microbarograph spectra have been reduced to absolute pressure changes.

Coherencies were computed from the smoothed power spectra

according to the formula

$$\gamma(f) = \left[\frac{|P_{12}(f)|^2}{P_{11}(f) \cdot P_{22}(f)} \right]^{\frac{1}{2}}$$

where P_{ii} is the power spectrum of the first or second trace and P_{12} is the cross-power spectra of the two traces.

Spectra computed in this manner represent only a finite sample of a noise process. Assuming the noise to be Gaussian and stationary (see VESIAC Advisory Report, 1962, for discussions) we can utilize the method of Jenkins and Watts (1968) to define confidence limits on the computed values of the spectral estimates. We find that for 2048 point samples, the 95% confidence limits at any frequency for an estimate of power equal to 1.00 μ^2/cps are 0.65 and 1.75μ^2/cps. The interval defined by these limits at 1.00μ^2/cps can be moved up or down on the logarithmic plot of power without changing its visual length although the absolute values of the limits will of course be proportional to the particular power estimate under consideration. The 95% confidence limits will be shown on all noise spectra.

Of equal importance in this study are the confidence limits on the estimates of noise coherence. We follow Bendat and Piersol (1966) in calculating 95% confidence limits again assuming a stationary Gaussian noise process, and these limits are tabulated in Table 2 for several values of γ in the range where their formula is applicable. Below $\gamma = 0.60$, no confidence limits can be estimated; but from Jenkins and Watts, a level below which the hypothesis of actual zero coherence can be accepted in 95% of the cases is $\gamma = 0.42$ for our samples of 2048 points. Thus only points above 0.42 bear significant evidence that the sampled noise processes have non-zero coherence over the infinite time interval.

SYSTEM NOISE

An evaluation of system noise is a prerequisite to proper interpretation of seismic noise spectra. For the ALPs and Triax systems, this was accomplished by substituting a resistor for the seismometer input. Power spectra of all nine recorded traces (including the raw triaxial seismometer components) during this dummy-load interval of recording are shown in Figure 2. The Triax recording system shows about 16 db more system noise than the ALPs. The two sharp peaks at about 0.2 and 0.4 cps are believed to originate from the mechanical functioning of the tape recorder or playback equipment. Comparison of power levels in Figure 2 with power levels from the same channels during a period of normal seismic recording in Figure 3 indicates the portion of the spectra which is dominated by system noise. It is evident that the frequencies outside the band of .02 to .20 cps for the Triax or .02 to .30 for the ALPs comprise system noise and that little or no seismic noise information can be obtained outside these bands. Figure 3 itself reveals the higher system noise on the Triax when the seismic noise is aligned on the vertical (power) scale between the Triax and the ALPs systems. (It became apparent when further seismic noise spectra were computed that the system noise on the Triax was greater than on the ALPs only at certain times, and thus there is no inherently higher noise level for the Triax system). Lower power levels of seismic noise can be studied if gains are adjusted to record the instrument output at a higher level relative to the system noise, which is mostly tape-generated. This report will show one spectra for which the gains were increased by a factor of 3; all other noise spectra represent normal recording with background noise set to a standard recording level in the LRSM program (Geotech, 1962).

SEISMIC NOISE

Noise samples at selected dates from January 1969 through August 1969 were processed. Not only was the spectral content of the noise assessed but also some particular investigations such as of the coherence between seismograph and microbarograph recordings and of the propagation direction of assumed Rayleigh-mode noise were undertaken.

Spectra of Noise at Murphy Dome

Dates and time windows for 2048 point samples of noise at Murphy Dome are listed in Table 3. These samples represent a wide variety of noise character on film records--low to high microseisms, isotropic noise, low to high accompanying atmospheric pressure fluctuations, and some relatively quiet periods. The power spectra of vertical and east components for these samples are shown in Figures 4a and 4b according to whether they represent time prior to or after March 1, 1969, respectively, so that the difference in the relative response curves of Figure 1 may be taken into account. At most the difference in system response will only effect the power spectra values by a factor of 2. Except for cases as marked in Table 3, the ALPs recordings were used in the spectral calculations. The dominance of two peaks in the seismic noise is evident--the first represents high recorded amplitudes at periods from 14 to 20 seconds and the second represents periods from 7 to 9 seconds. For three spectra in Figure 4b from the May, June, and August samples, both these peaks are very subdued, and very long period noise (>20 seconds period) accounts for maximum recorded amplitudes. This particular noise may not be of seismic origin, and moderate microbarograph levels suggest that the recording system is

responsible for this very long-period noise. The 14-20 second peak maintains a rather constant amplitude over the entire January to March time period, but the 7-9 second peak is more variable, ranging over 10 db on the power scale even when neglecting the May, June, and August samples which have quite different character. Approximate RMS values for the vertical component have been calculated on the noise samples having highest and lowest apparent amplitudes by numerically integrating the power density spectra. The sample with the highest noise level, 18 February, has an RMS of approximately 5.2 millimeters assuming a film magnification of 10^5, and the sample with lowest noise level, 10 January, has an RMS of about 2.5 millimeters assuming the same magnification. These values of RMS from the integrated spectra agreed with RMS values calculated directly from the corresponding digitized time series.

Coherence with Microbarograph Recordings

Sorrells (1969) has theoretically predicted the response of layered media to atmospheric pressure fluctuations and has found that this may significantly contribute to background noise on long-period recordings, especially for surface instruments. Capon (1969) has demonstrated empirically with LASA data that this phenomenon is a partial component of observed background. Data taken at Murphy Dome corroborates this fact. Figures 5, 6, and 7 illustrate the effects of atmospheric pressure on three different dates. Figures 5a, 6a, and 7a show the power spectra of the microbarograph, ALPs, and Triax recordings for each of the dates; and Figures 5b, 6b, and 7b show the corresponding coherence plots between each of the six seismic components of motion and the microbarograph recording. The three cases are ordered according to increasing barometric

activity. For the first case, 13 January, in Figure 5b there is significant coherence between the microbarograph and the ALPs east component only; this results in a higher noise level shown in the spectra of this ALPs component in Figure 5a for the frequency band where coherence is good. Figure 6a shows a similar increase in noise level on the east component on 21 February due to the atmospheric pressure coupling with the ground as evidenced in the coherence plot in Figure 6b for the east component. The last case, on 18 February, reveals the effects of very high atmospheric pressure fluctuations in Figures 7a and 7b. Coherence plots shown in Figure 7b are high for the surface instruments in the period band of 20 to 128 seconds; and the surface vertical instrument has significant coherence with the microbarograph at periods of about 30 seconds, unlike the previous two cases, although this does not result in a higher noise level at that period for the ALPs recording as opposed to the Triax recording in Figure 7a. The fact that all three cases show little or no coherence between the microbarograph and the vertical recordings while there is considerable coherence for the horizontal recordings is in agreement with the predictions of Sorrells which estimate that the effect on the vertical trace amplitude will be about one order of magnitude less than on the horizontal trace. For the horizontal instruments, the data show that pressure fluctuation having power densities greater than about $10\mu bar^2/cps$ contribute to the overall background noise level in a significant amount between periods of 16 and 128 seconds and that this atmospheric generated noise is greatly reduced (as much as 10 db in power) on the Triax horizontal component because of this instrument's 175 feet displacement from the surface, as predicted by Sorrells.

Direction of Propagating Noise

In Figures 8 through 10 we investigate the direction of noise propagation assuming microseisms having Rayleigh-mode character are being recorded. Normal north and east components were merely rotated in 30° increments to obtain radial components at 0°, 30°, 60°..., 180° orientations. Examination of phase angles of cross spectra between these and the vertical component allows us to choose between θ and θ + 180° as the direction of propagation after the approximate (±20°) line of propagation has been determined by the best coherence between vertical and horizontal components. In the first case taken from 13 January, Figure 8 shows that coherence was best for the horizontal component aligned along the 90°/270° direction, and phase angle information from the spectral program indicated 90° as the direction of approach. In the second case analyzed, 9 February in Figure 9, 120° was found to be the direction of approach. Both these samples then suggest microseisms from Atlantic Ocean sources. The definite peaking of the coherence spectra in Figures 8 and 9 along a particular direction validates the assumption of Rayleigh-mode energy propagating unidirectionally on these two dates. Peaks in the best coherence spectra for these two cases can be related to the power spectra peaks in the 14 to 20 second and 7 to 9 second period bands seen earlier in Figures 4a and 4b. Another noise sample on June 2, which was previously noted to be of different character, was analyzed and results are shown in Figure 10. Since no definte peaking in the coherence spectra as a whole can be found when the radial component is rotated, this seismic noise is not dominated by Rayleigh-mode microseisms.

SIGNALS

Several signals with a high S/N ratio from located events were processed through the spectral program. Horizontal components of motion were aligned parallel and perpendicular to the back azimuth to obtain radial and transverse components. Most signals analyzed were Rayleigh (LR) arrivals although some compressional (P), shear (S), and Love (LQ) arrivals were also analyzed. Table 4 lists pertinent epicenter information. All three components of both the ALPs and Triax are shown together for each arrival or set of arrivals in Figure 11 where they are ordered by date as in Table 4. The exact time window used for spectral calculations is indicated. The time traces are not scaled to relative ground motion; however, the spectra of these signals shown in Figures 12, 13, and 14 for body-wave, LQ, and LR arrivals respectively are scaled to true relative motion. We do not expect differences to exist in power levels between the ALPs and Triax instruments--as is apparent in these comparative spectra for a well-recorded, high S/N ratio arrival. We must accept inevitable errors in calibration even though utmost care is exercised in all the processes involving reduction of data to true ground motion. However, in the case of comparing the vertical and radial components of Rayleigh motion, as shown in Figure 15, the sytematically lower power level on the radial component can be interpreted as the effect of the ellipticity factor for Rayleigh-mode particle motion.

The coherence between ALPs and Triax components shown by Figure 11 in the time domain seems excellent. To reinforce this conclusion, coherence (γ) was calculated in the spectral program between the two systems for all the signals. In most cases coherence was nearly unity for a broad band of frequencies; Figure 16 illustrates typical coherence spectra between these two types of instruments for body and surface waves.

Theoretically, the coherence between vertical and radial components of motion during passage of a Rayleigh-mode signal should be unity, but Figure 17 shows that for several signals this coherence is poor over most of the whole frequency band shown and good only for a small band where the signal peaks. We attribute this to contamination of the Rayleigh wave by laterally-refracted LQ waves on the radial trace and by late-arriving body-wave phases on both the vertical and radial traces.

One further aspect of the signal analysis concerns the spectral content itself. We find from Figures 12 to 14 that the signal spectra of body and surface waves peaks in the range of 16 to 30 seconds period. A comparison with the seismic noise spectra shown earlier shows that this range overlaps the noise spectra where it is rapidly decreasing toward the longer periods in most cases. Thus the system responses employed, Figure 1, are nearly optimum filters in the recording of film records which will have easily identifiable valid seismic signals. There does appear to be sufficient long-period energy with periods greater than 30 seconds in the signals analyzed to warrant its exploitation by a system response which does not cut down the longer periods as rapidly as that presently employed. Although this would do little to enhance the recorded signals for visual identification, the long-period energy would be recorded above the system noise level so that this portion of the spectra could be used in later analysis. In this regard the change from the LRSM to ALPA response in Figure 1 was an improvement.

CONCLUSION

The seismic background at Murphy Dome shows variable character but normally has peaks at periods of about 16 and 8 seconds which are somewhat classical phenomena in seismology. From the limited samples studied the RMS level on a record varied by a factor of two at most. The overall level of the seismic background can best be measured by the peaks at periods of about 16 and 8 seconds. The 16-second peak, when corrected for the system response, represents about 0.2 microns of ground motion. This compares with about 0.1 microns at LASA as shown for just one sample by Capon (1969) and with also about 0.1 microns as the "world average" given by Oliver in the VESIAC Advisory Report (1962) on seismic noise. The peak at about 8 seconds is more variable in amplitude at Murphy Dome but represents on the average a grourd amplitude of about 1 micron which is again about twice that of the "world average" given by Oliver. Two noise samples from Murphy Dome revealed the propagation of Rayleigh-mode energy; one other sample with quite a different power spectra did not. The system noise limits information on seismic noise to the band from about .02 to 0.3 cps; this is not, however, a serious problem since our interest does not extend beyond these limits as far as detecting long-period signals from teleseismic events is concerned.

The spectral analysis of several signals, both body and surface waves, showed the system response to be ideally suited to the emphasis of ordinary signals over background noise at Murphy Dome.

The comparison of the ALPs and Triax system was a salient feature of this report. Coherence between ALPs and Triax components was shown to be excellent both in the time and frequency domains for many signals with high S/N ratios. In

addition to providing a recorded trace which matches the standard LRSM recording of the same signal, the Triax system has accomplished a very significant reduction of horizontal-component noise generated by atmospheric pressure fluctuations due to its location at depth. This reduction was as much as 10 db, and this affects the period range of commonly recorded signals at Murphy Dome.

REFERENCES

Capon, J., Investigations of long-period noise at the Large Aperture Seismic Array, J. Geophys. Res., 74, 3182-3194, 1969.

Bendat, Julius S., and Alan G. Piersol, Measurement and Analysis of Random Data, John Wiley and Sons, Inc., New York, 1966.

Geotech, Interpretation of LRSM seismic data, Technical Report No. 62-14, 1962.

Geotech, Operation and calibration of advanced long-period system, Technical Report No. 64-9[illegible], 1964.

Geotech, Long-period triaxial seismograph development, final report, Project VT/6706, Technical Report No. 69-17, 1969.

Jenkins, Gwilym M., and Donald G. Watts, Spectral Analysis and Its Applications, Holden-Day, San Francisco, 1968.

Sorrells, G.G., Long-period seismic noise and atmospheric pressure variations. Part I. The response of an isotropic half-space to a plane pressure wave, Geotech, A Teledyne Company, Technical Note 3/69, 1969.

VESIAC, Problems in seismic background noise, Advisory Report 4410-32-X, edited by VESIAC staff, Acoustic and Seismic Laboratory, The University of Michigan, 1962.

TABLE 1

Abbreviations for Components of Motion

Symbol	Component
Z	ALPS vertical
ZT	Triax vertical
N	ALPs north
NT	Triax north
E	ALPs east
ET	Triax east
R	ALPs radial
RT	Triax radial
T	ALPs transverse
TT	Triax transverse
TR1	First raw Triax
TR2	Second raw Triax
TR3	Third raw Triax
MBG	Microbarograph

TABLE 2

Confidence Limits on Coherence

Computed γ	95% lower limit	95% upper limit
.6	.17	.78
.7	.34	.84
.8	.53	.90
.9	.75	.95
.95	.87	.98
.975	.93	.99

TABLE 3

Noise Sample Times

Date (1969)	Time Windows 2048 seconds starting at
10 January	08:20:00
13 January	03:00:00*
9 February	09:20:00*
11 February	14:00:00*
18 February	13:30:00*
21 February	22:45:00*
14 March	07:45:00
16 March	05:45:00
30 May	00:10:00
2 June	02:00:00
19 August	20:45:00+

* Triax components used for spectra

+ Gain set 3 times greater than normal

TABLE 4

Epicenter Data for Signals Analyzed

Date (1969)	Origin Time (Z)	Coordinates	Distance (Degrees)	Back Azimuth
10 January	03:20:58	29N, 131E	60.2	275°
13 January	08:54:58	8S, 159E	82.5	233°
15 January	07:31:18	5S, 134E	89.3	257°
9 January	15:34:43	22N, 101E	78.6	298°
12 February	15:39:50	56N, 163E	25.0	272°
14 March	08:47:23	13N, 87W	66.3	111°
5 June	20:39:56	11N, 41W	87.3	70°
6 June	16:15:57	12N, 88W	66.8	112°
8 June	14:49:26	53N, 160E	28.3	270°
9 June	06:51:15	3S, 143E	83.8	249°

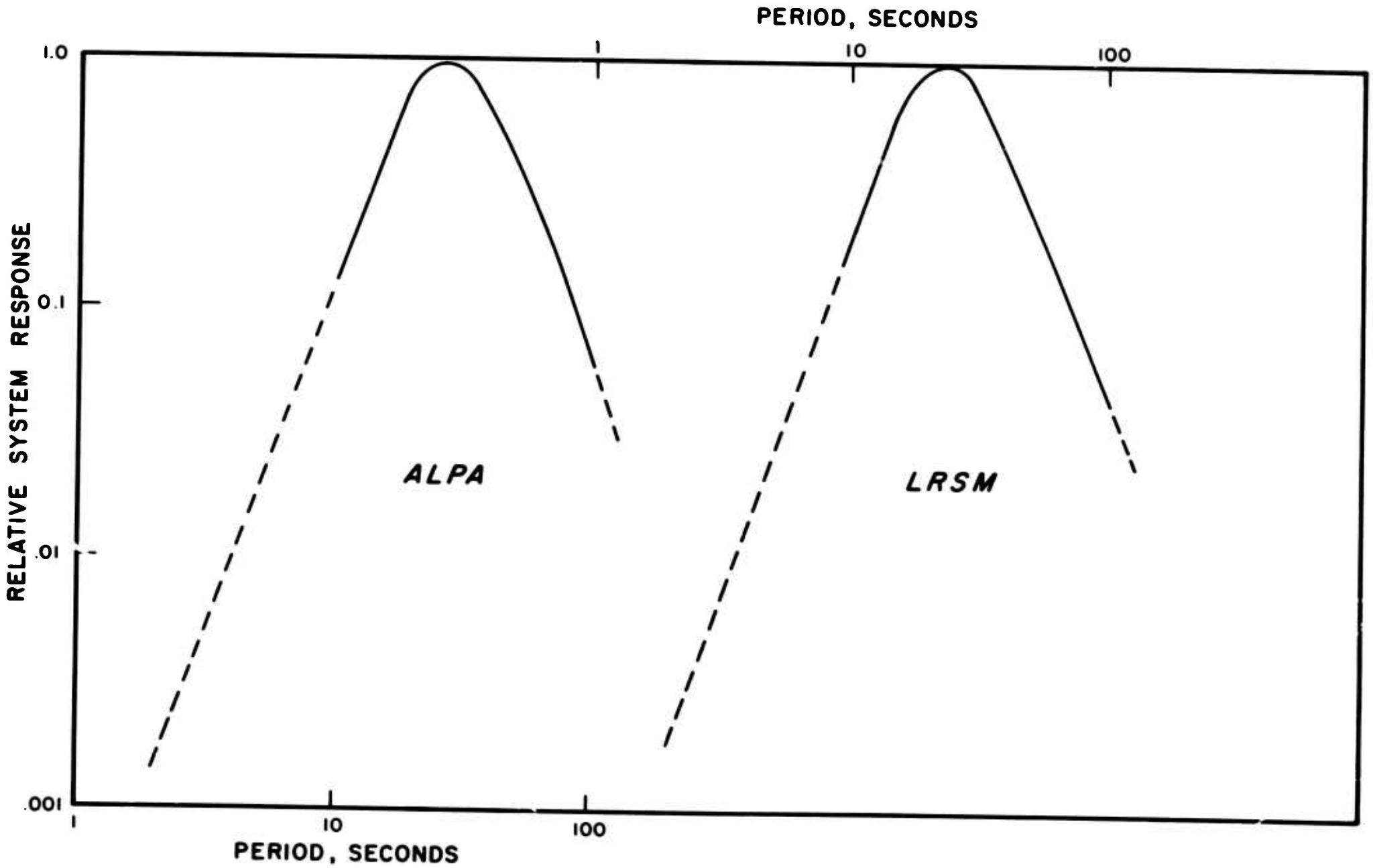

Figure 1. LRSM and ALPA long-period system response curves.

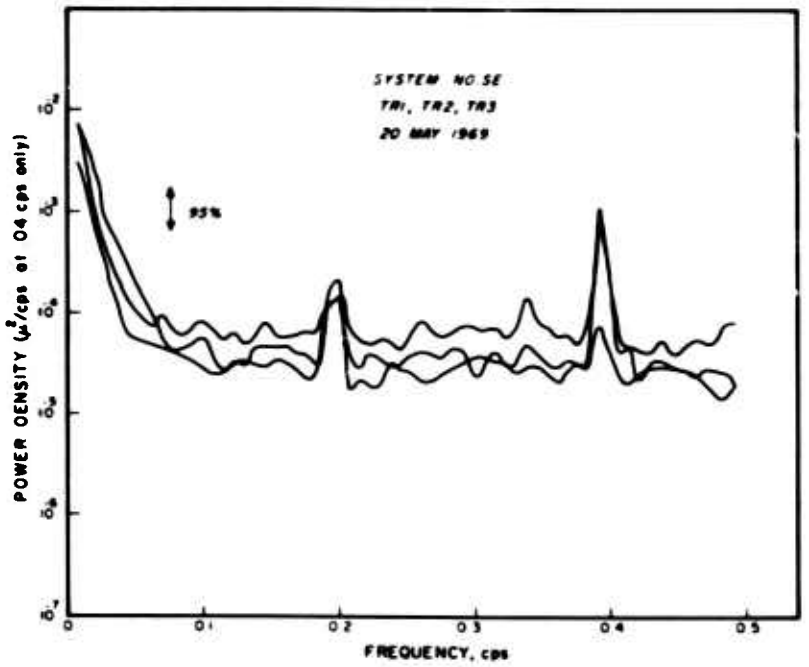

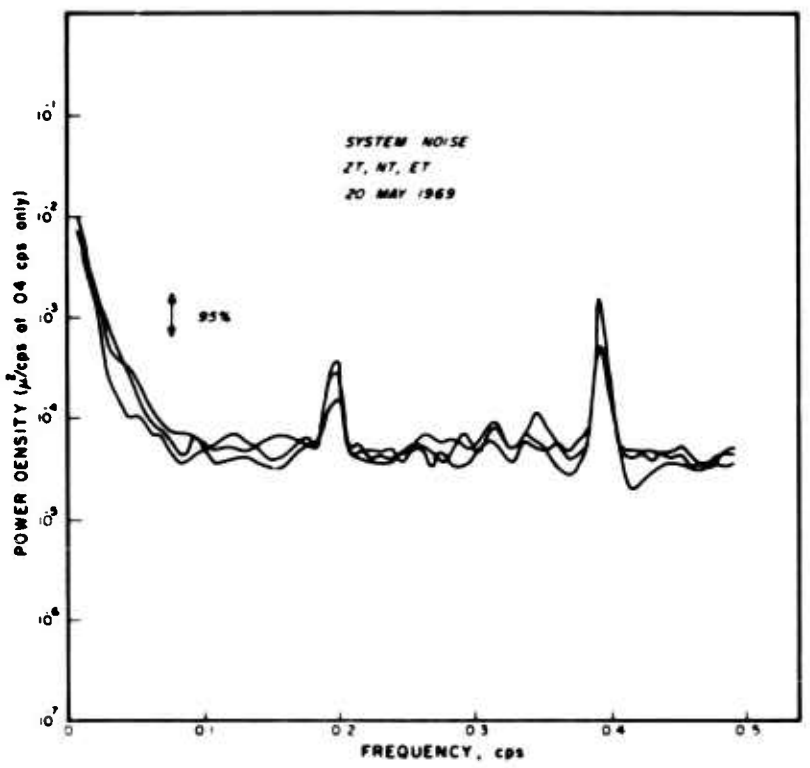

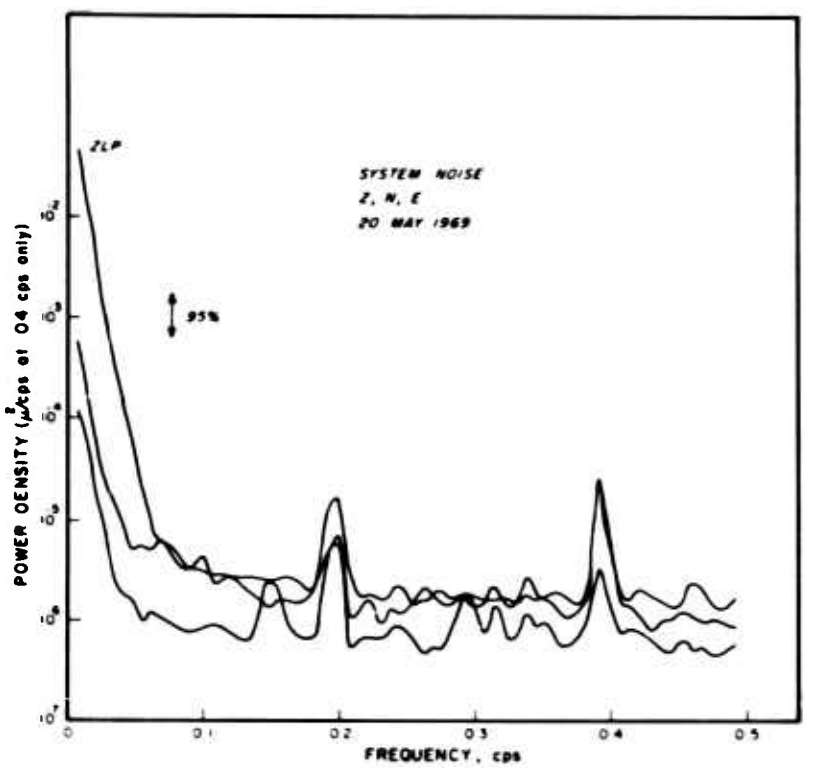

FIGURE 2. SYSTEM NOISE - RAW TRIAX, TRANSFORMED TRIAX, AND ALPS TRACES.

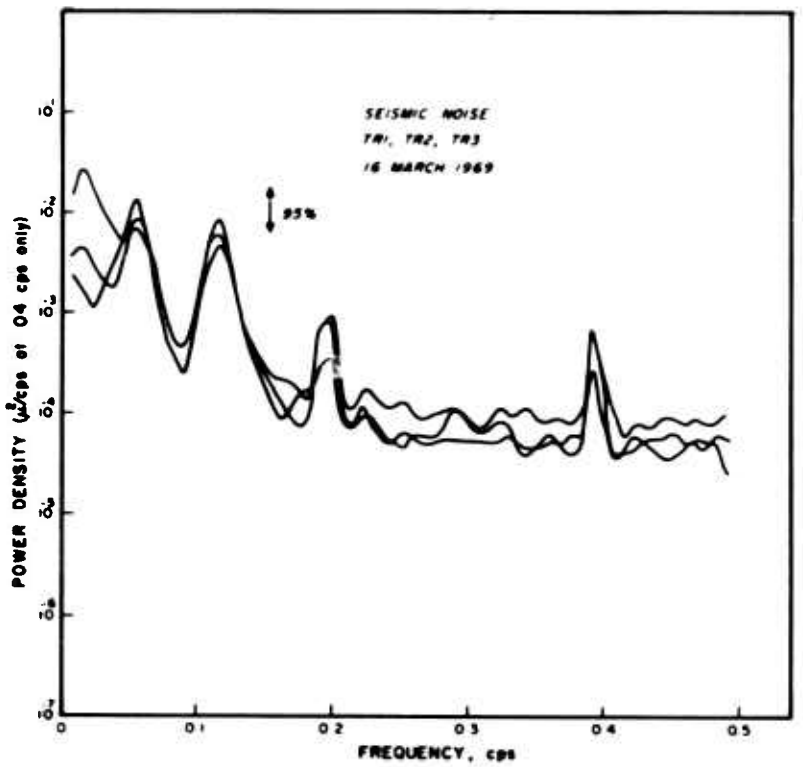

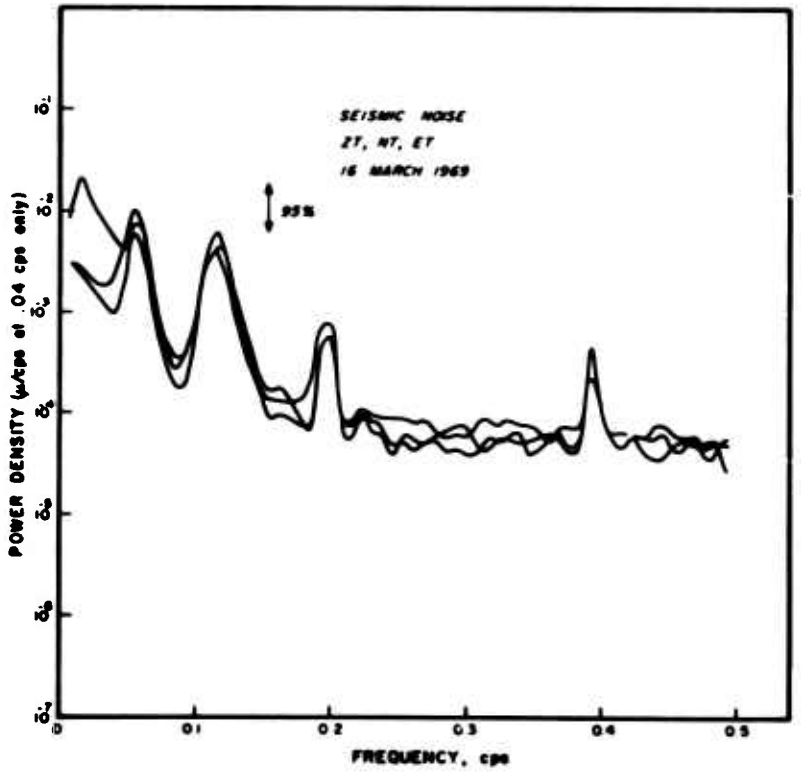

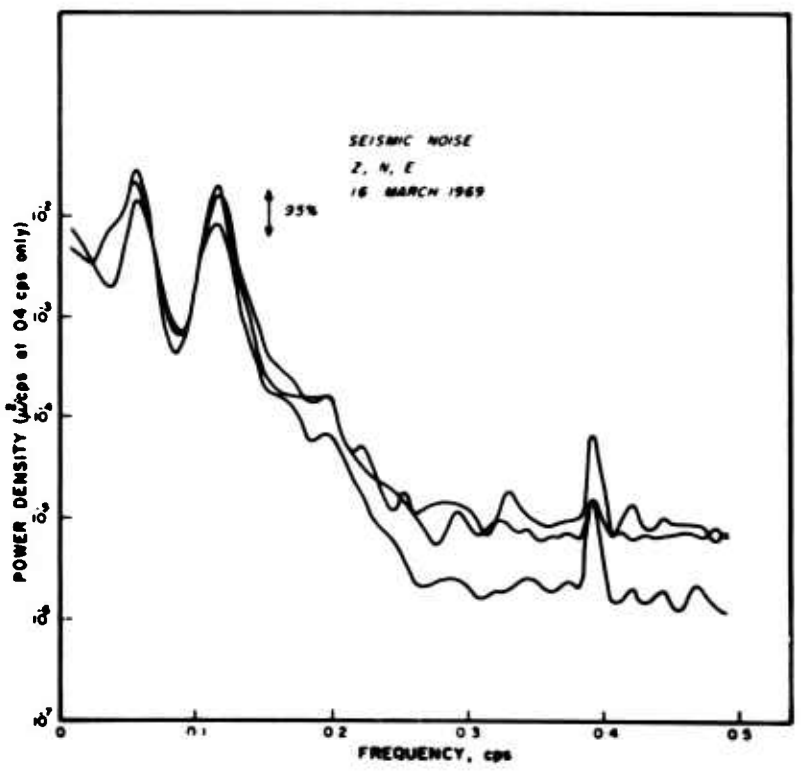

FIGURE 3. SEISMIC NOISE - RAW TRIAX, TRANSFORMED TRIAX, AND ALPS TRACES.

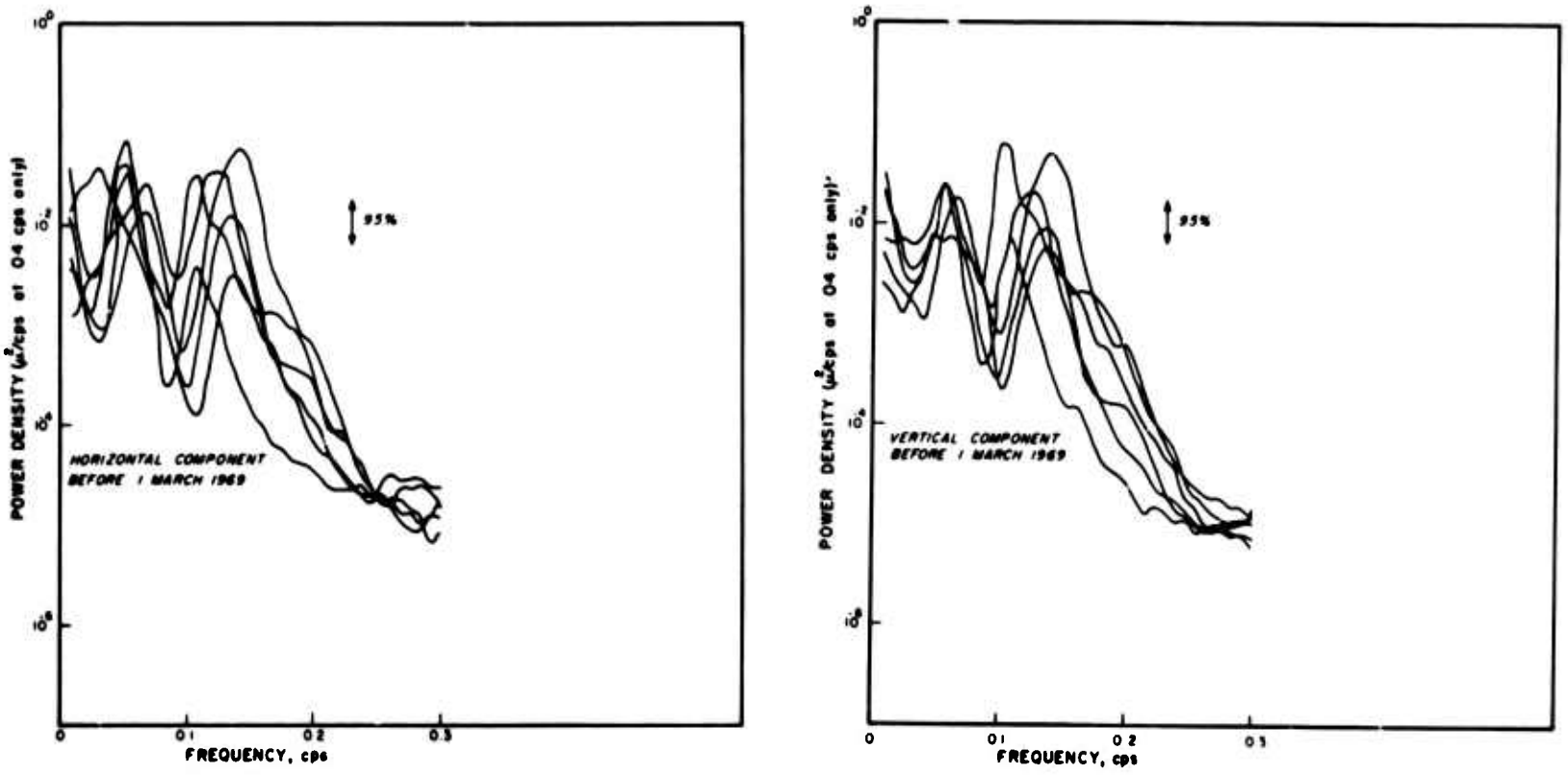

FIGURE 4A. VERTICAL AND EAST COMPONENT NOISE SPECTRA - SAMPLES BEFORE 1 MARCH 1969.

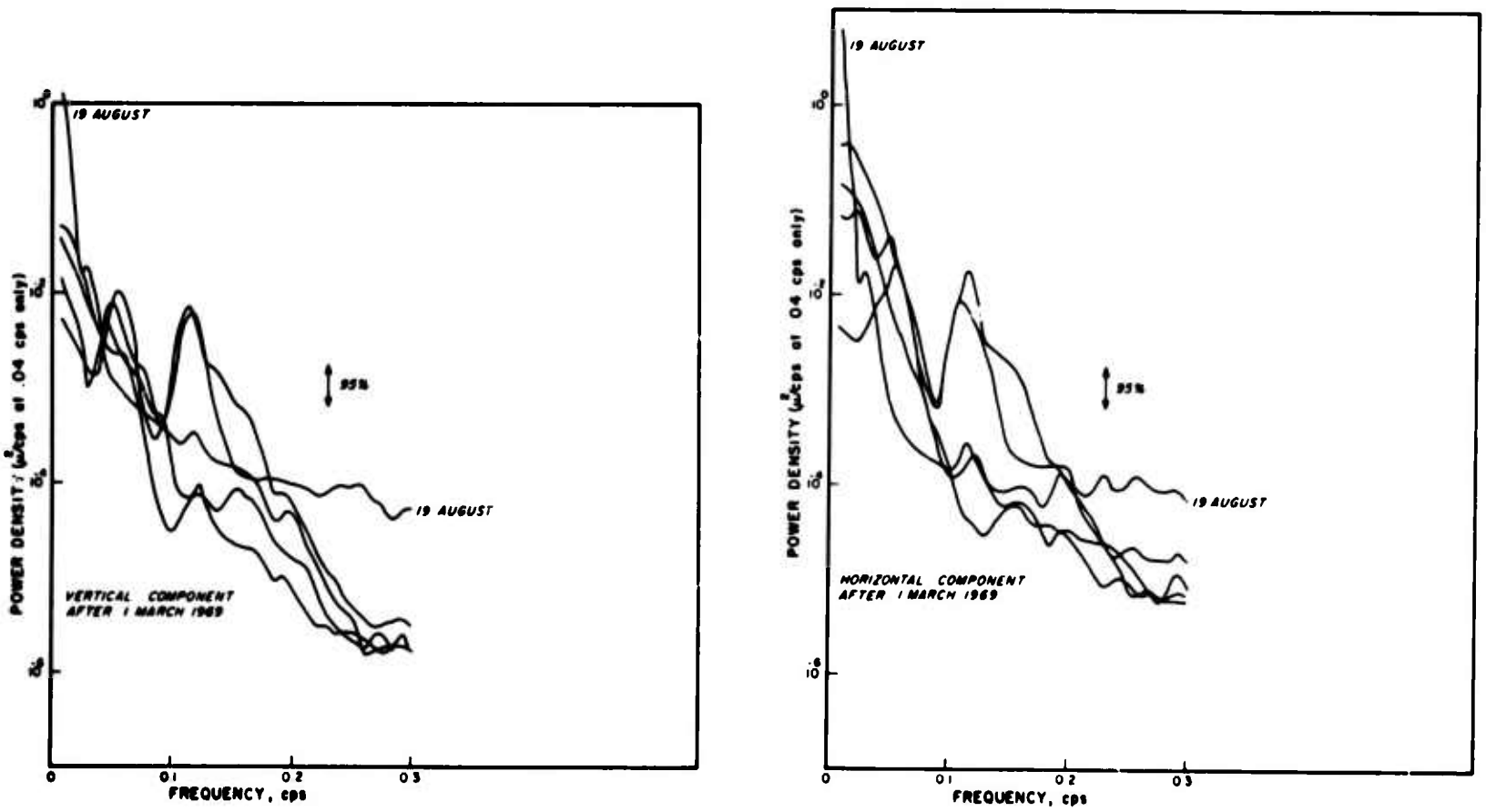

FIGURE 4B. VERTICAL AND EAST COMPONENT NOISE SPECTRA - SAMPLES AFTER 1 MARCH 1969.

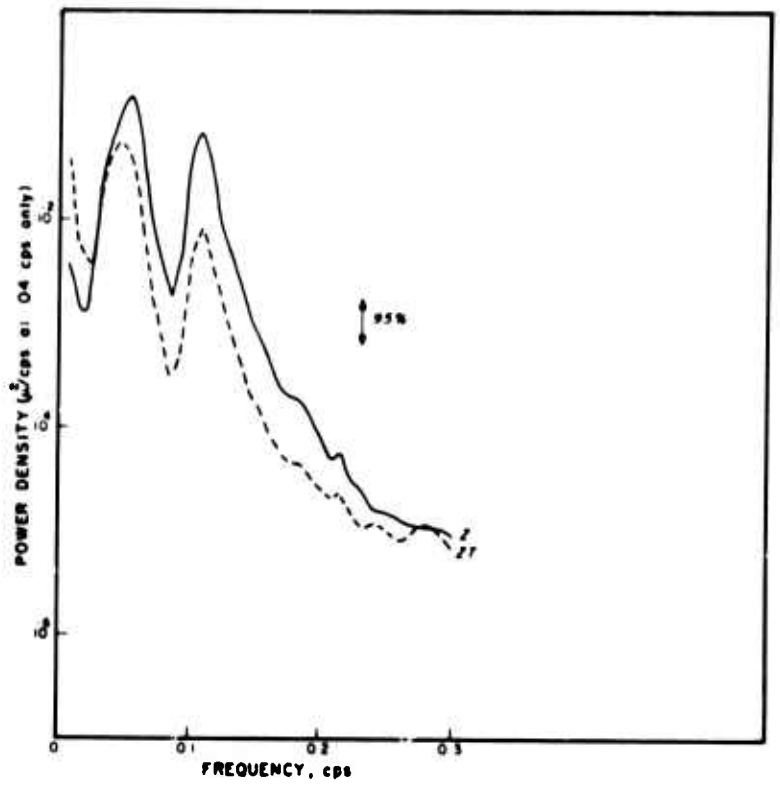

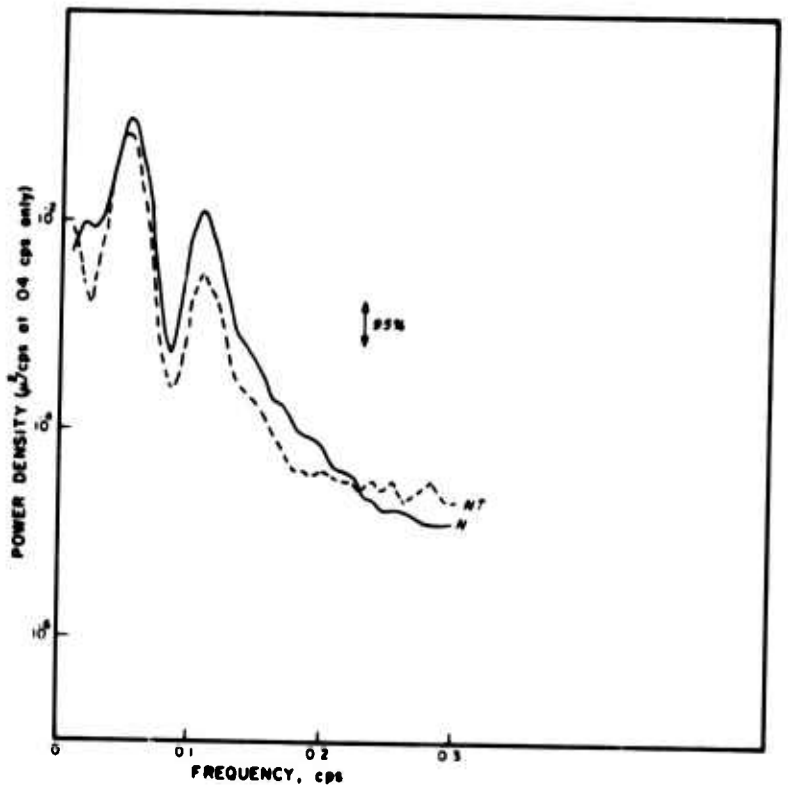

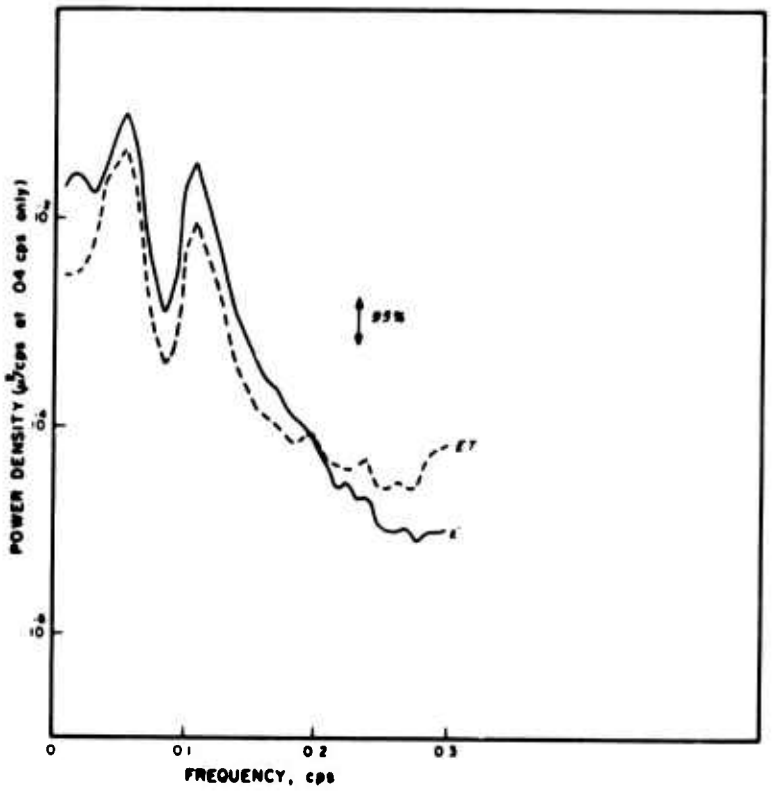

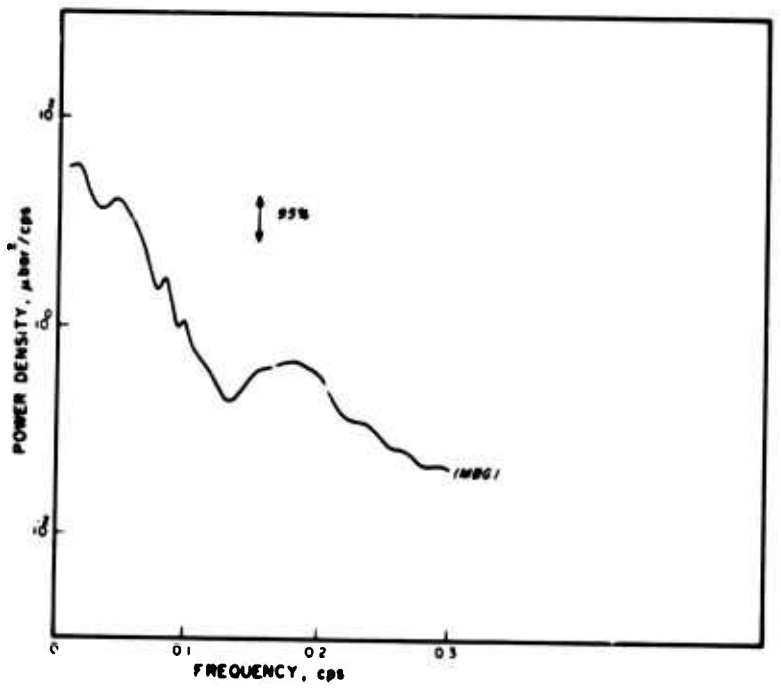

FIGURE 5A. POWER SPECTRA OF MICROBAROGRAPH AND SEISMOGRAPH RECORDINGS ON 13 JANUARY 1969.

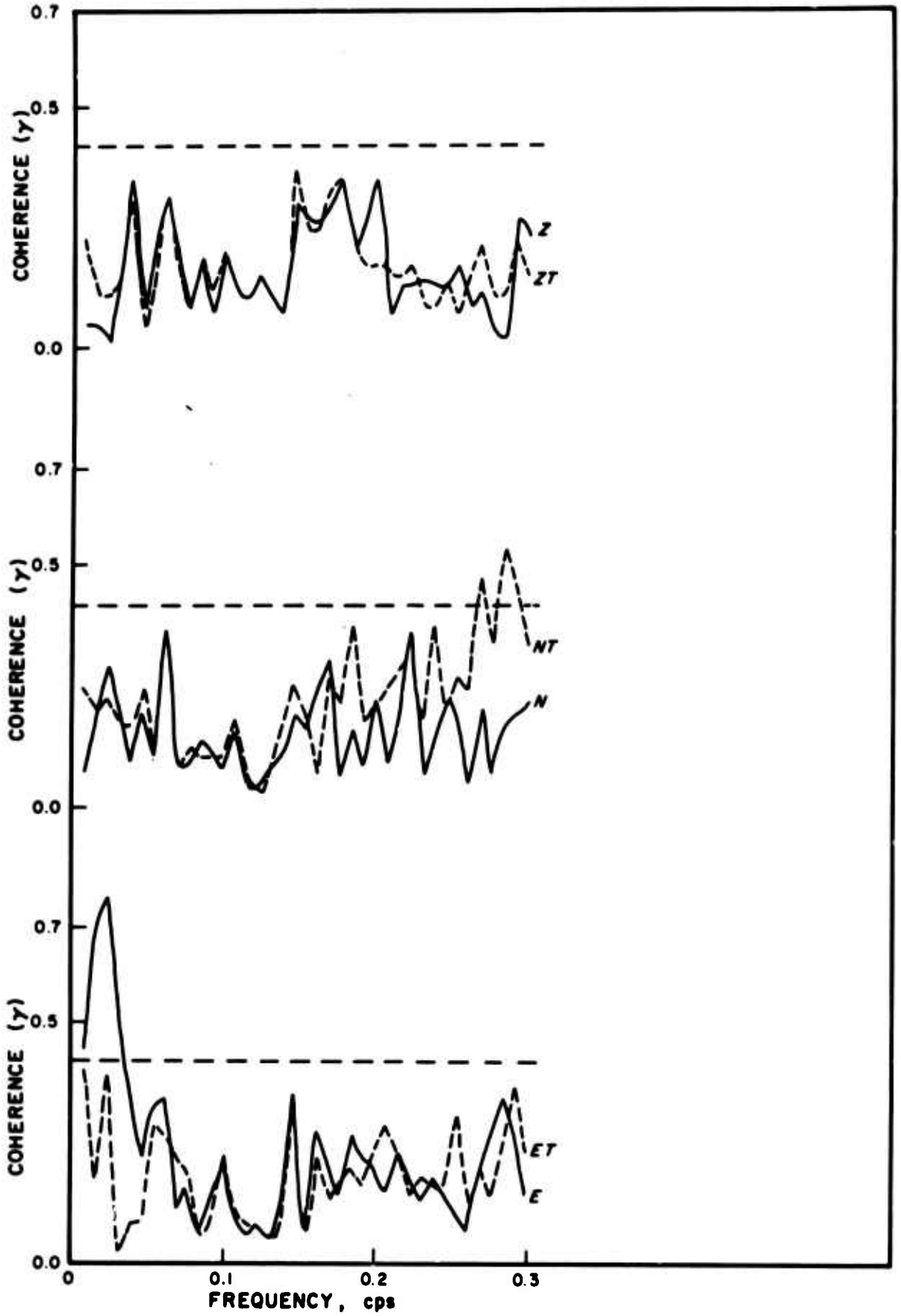

FIGURE 5B. COHERENCE BETWEEN MICROBAROGRAPH AND SEISMOGRAPH RECORDINGS ON 13 JANUARY 1969.

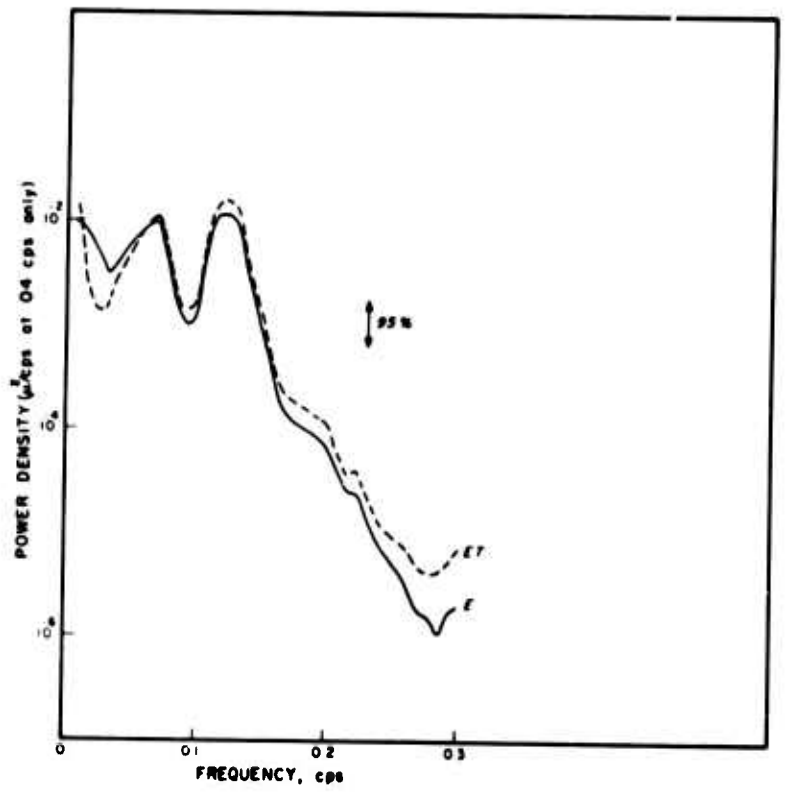

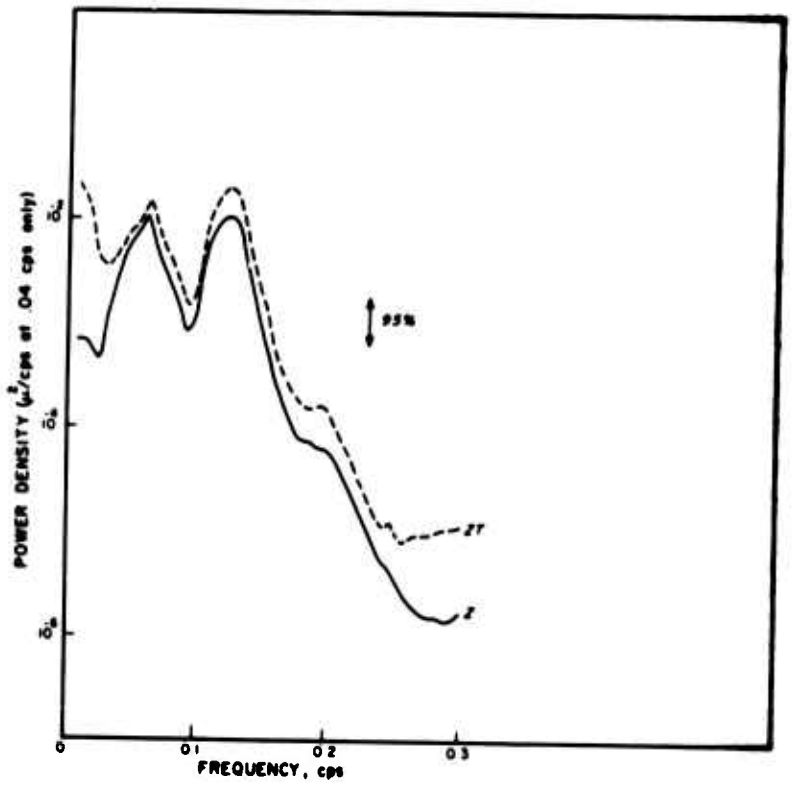

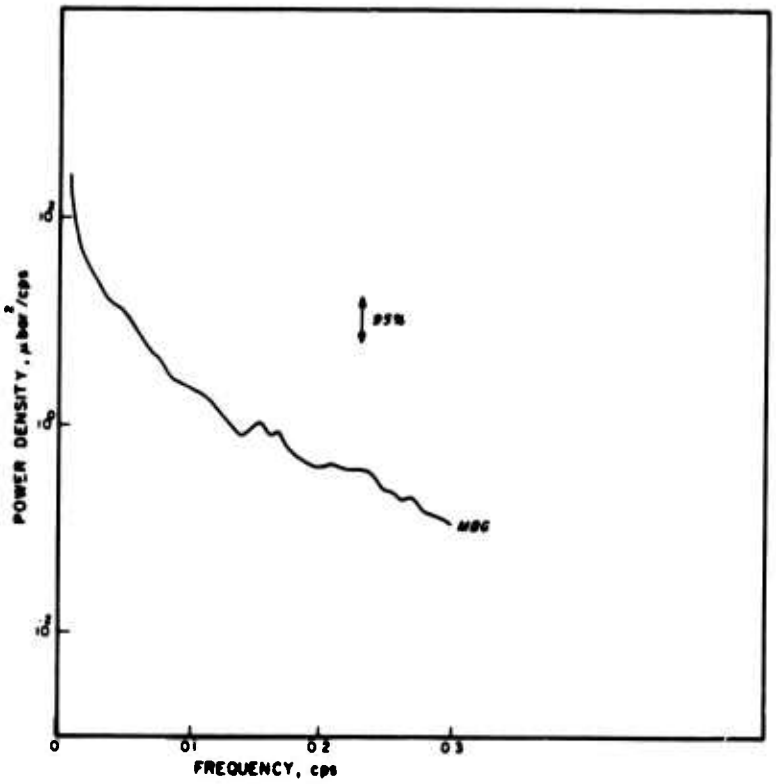

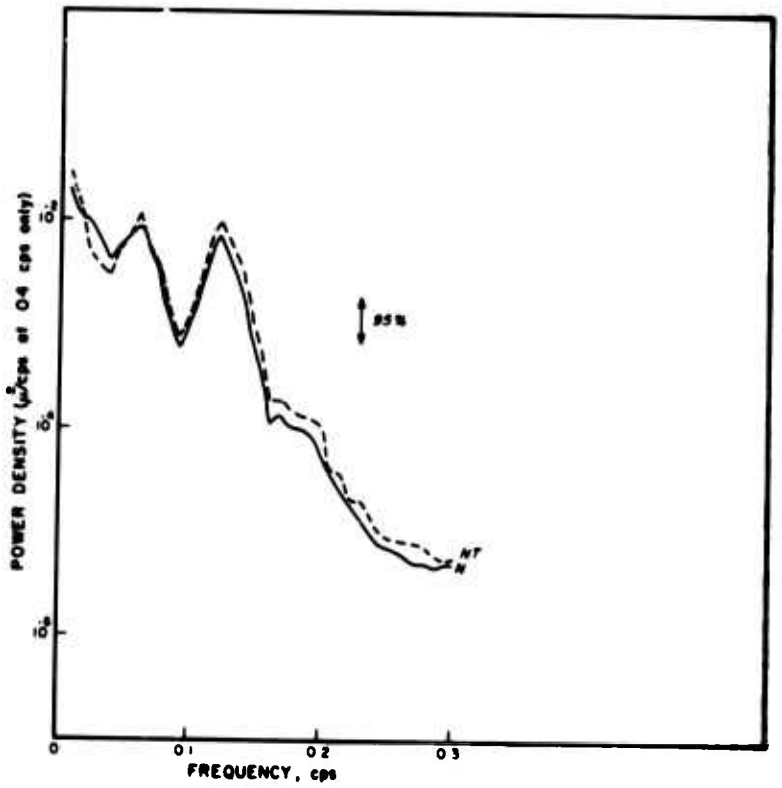

FIGURE 6A. POWER SPECTRA OF MICROBAROGRAPH AND SEISMOGRAPH RECORDINGS ON 21 FEBRUARY 1969.

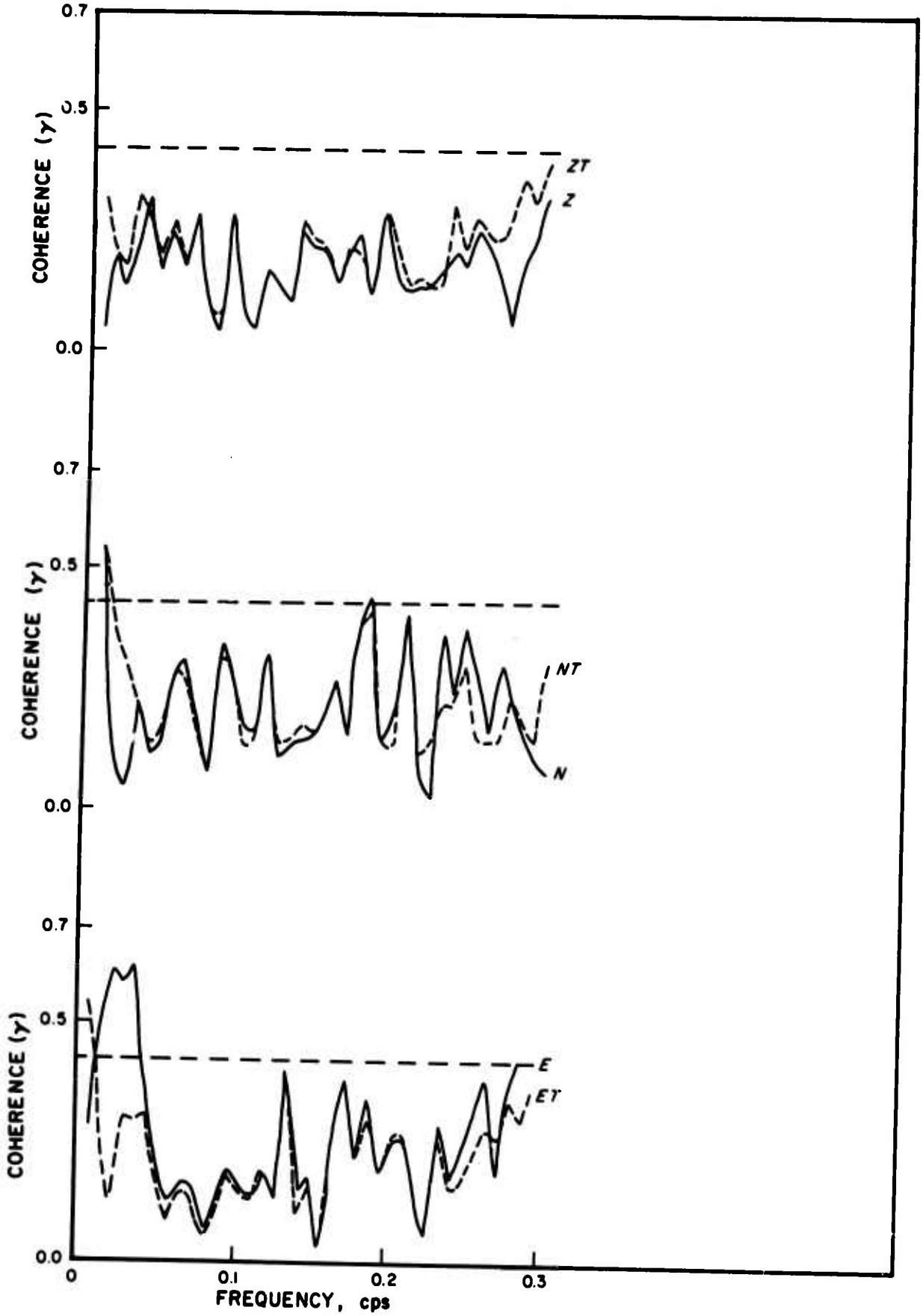

FIGURE 6B. COHERENCE BETWEEN MICROBAROGRAPH AND SEISMOGRAPH RECORDINGS ON 21 FEBRUARY 1969.

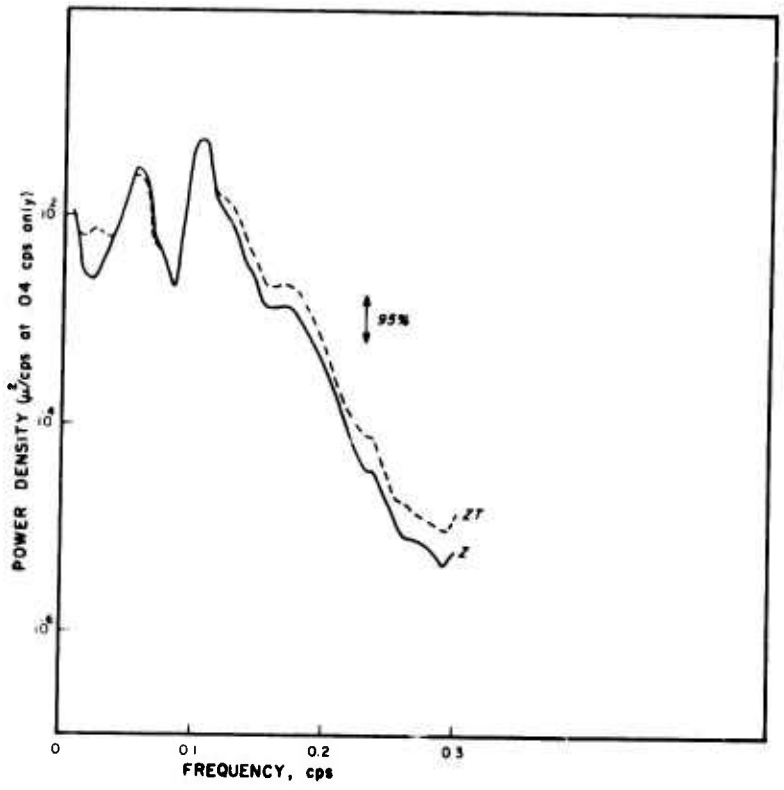

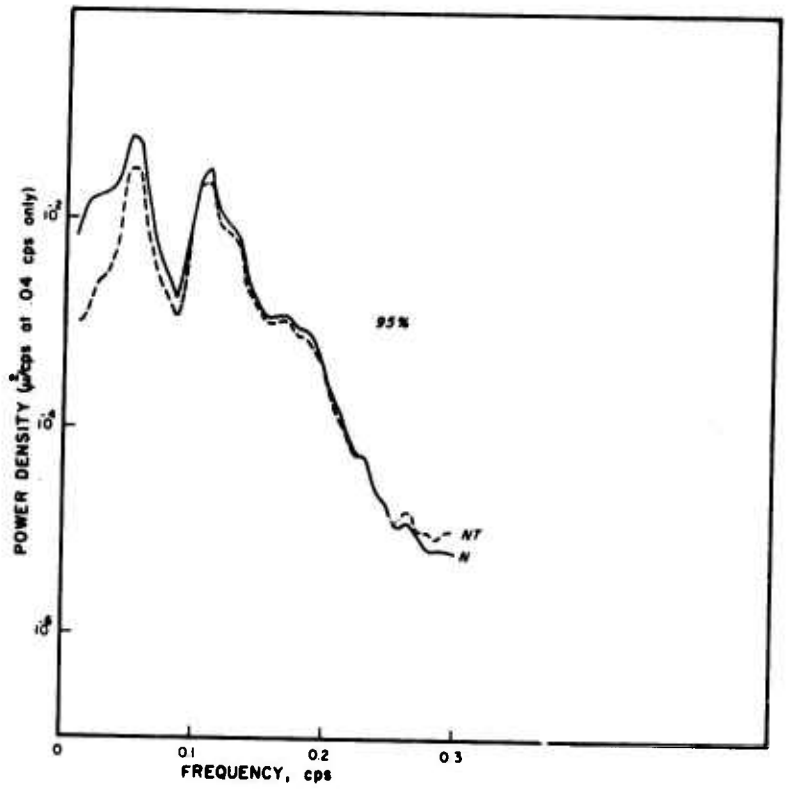

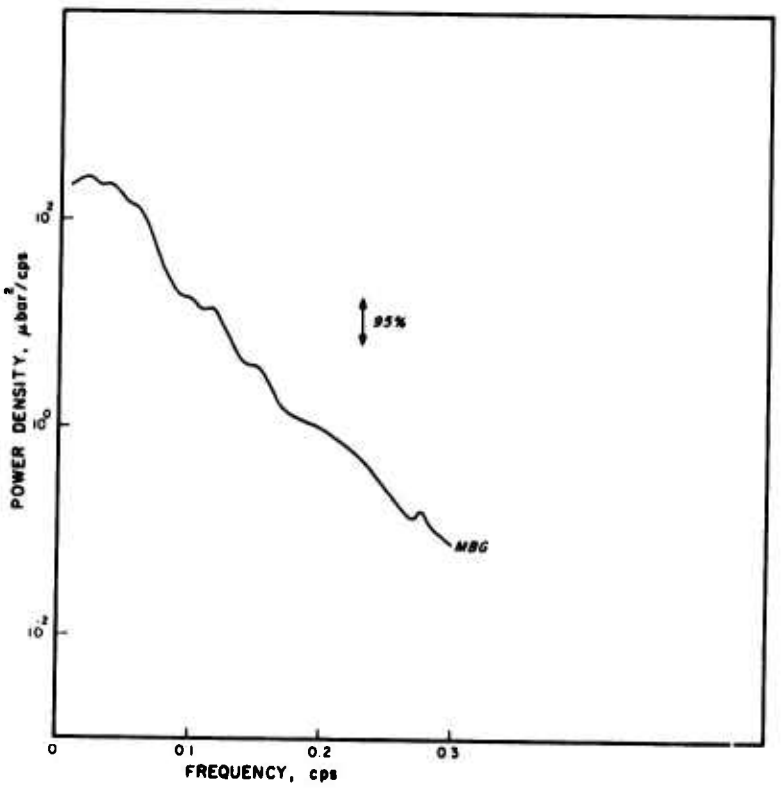

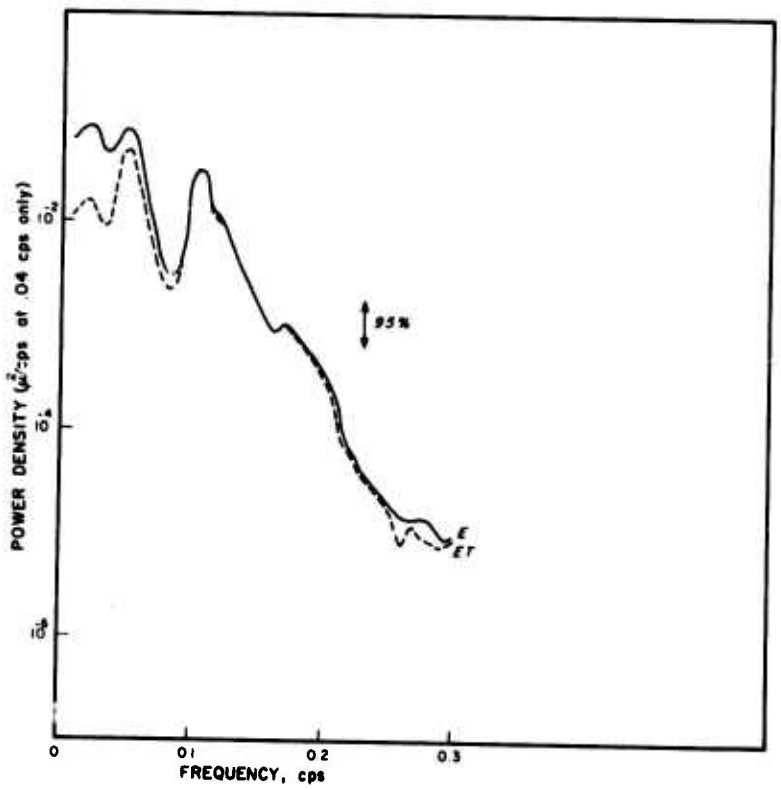

FIGURE 7A. POWER SPECTRA OF MICROBAROGRAPH AND SEISMOGRAPH RECORDINGS ON 18 FEBRUARY 1969.

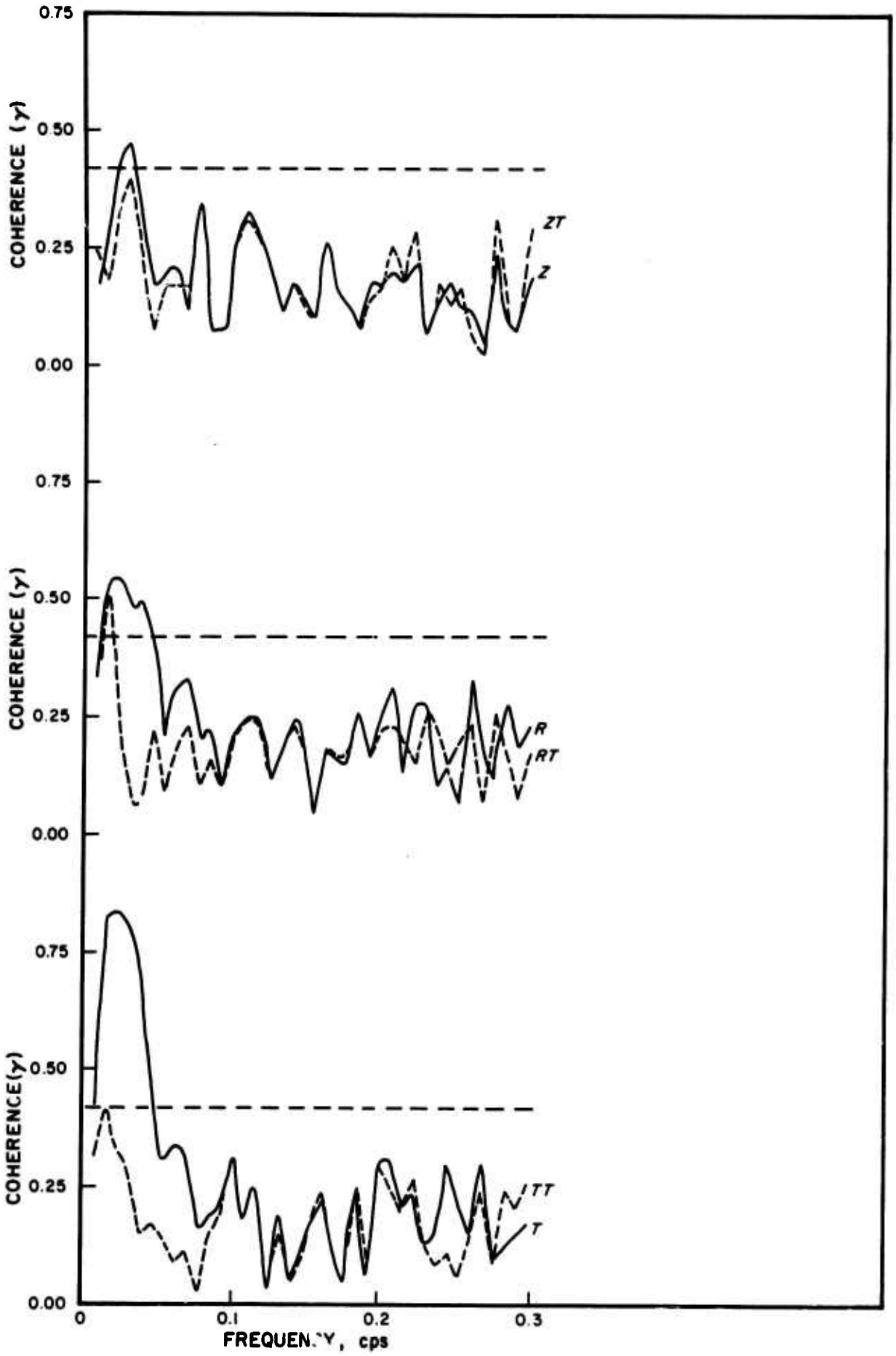

FIGURE 7B. COHERENCE BETWEEN MICROBAROGRAPH AND SEISMOGRAPH RECORDINGS ON 18 FEBRUARY 1969.

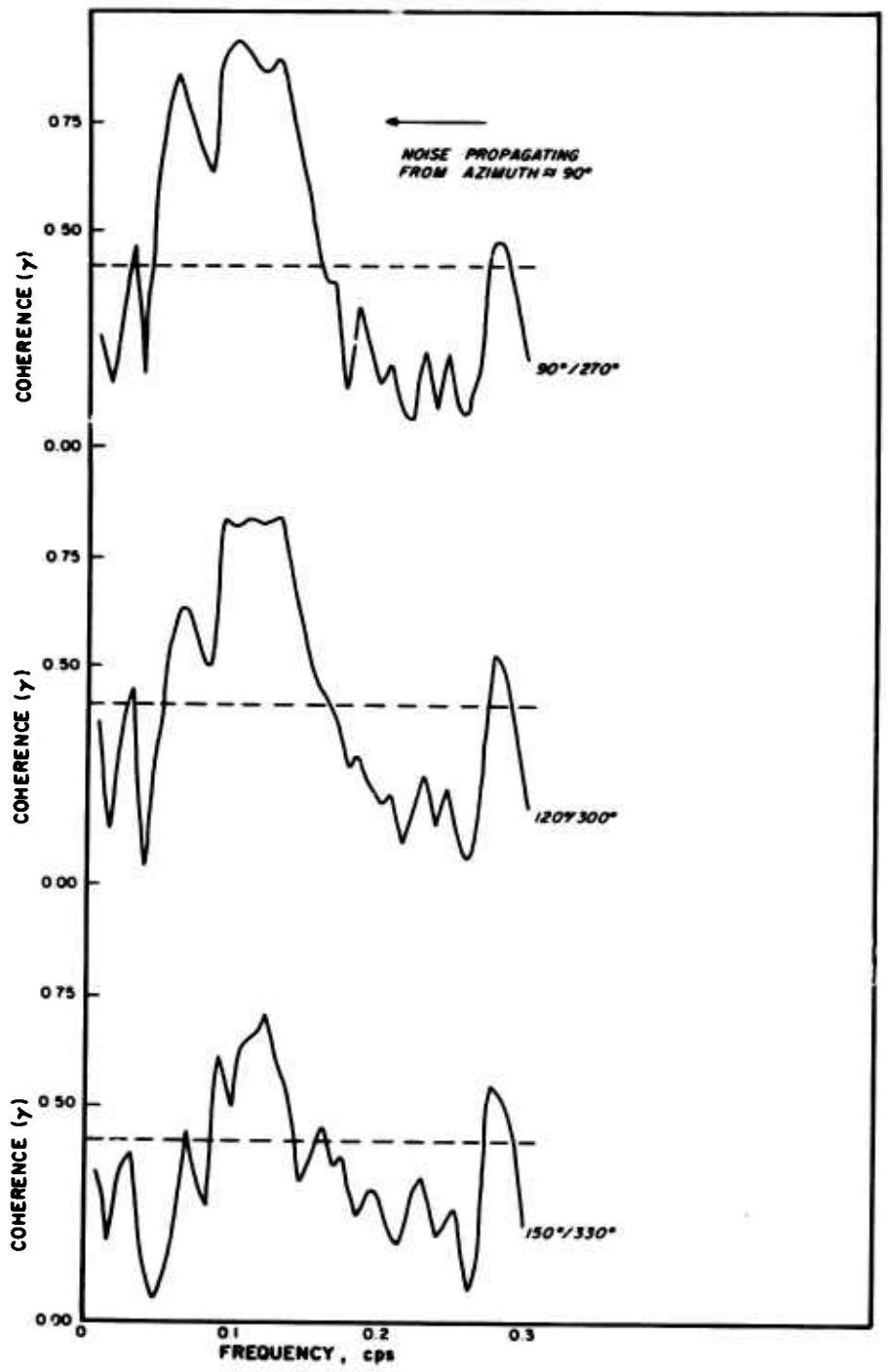

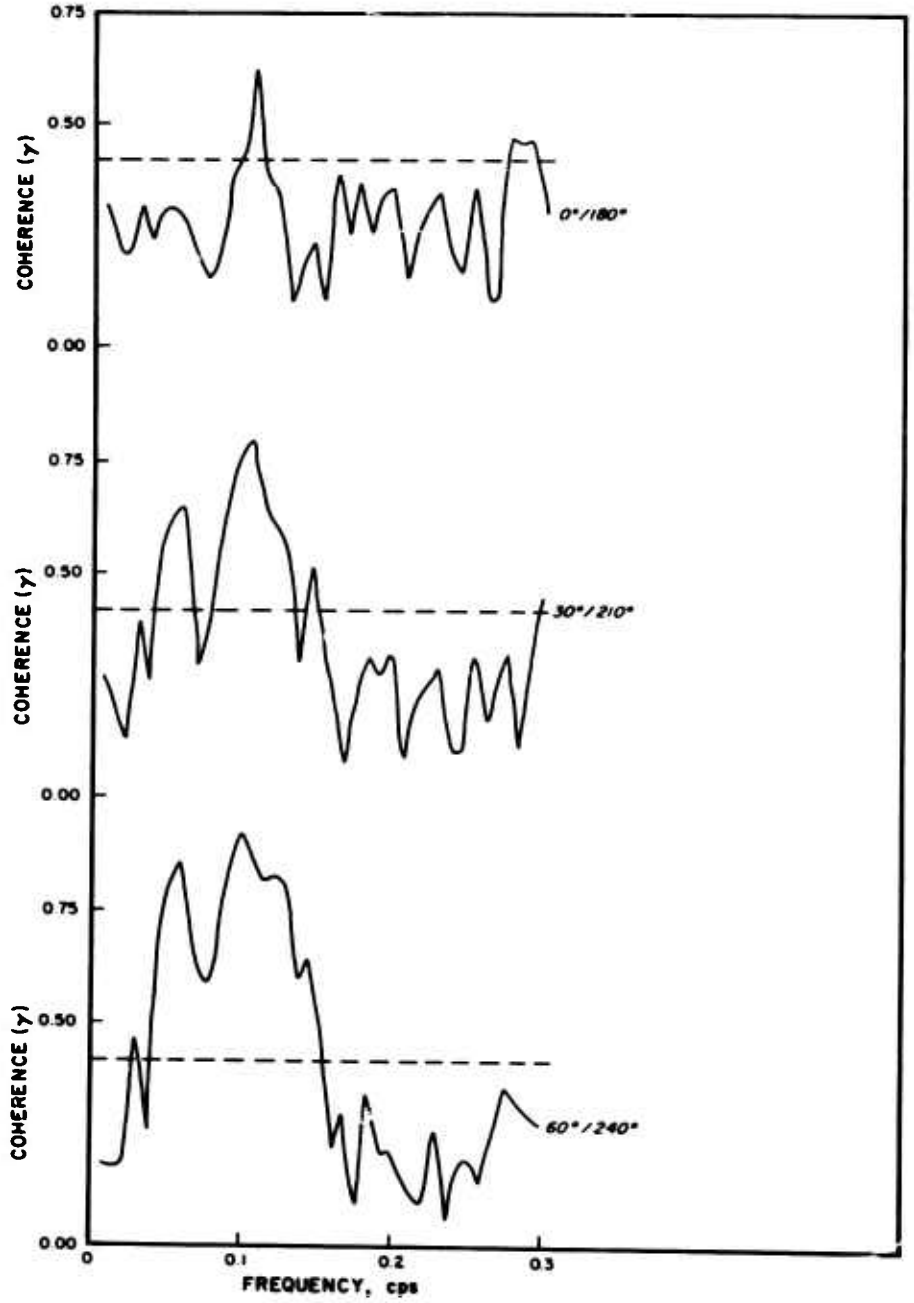

FIGURE 8. COHERENCE OF VERTICAL AND ROTATED HORIZONTAL COMPONENTS ON 13 JANUARY 1969.

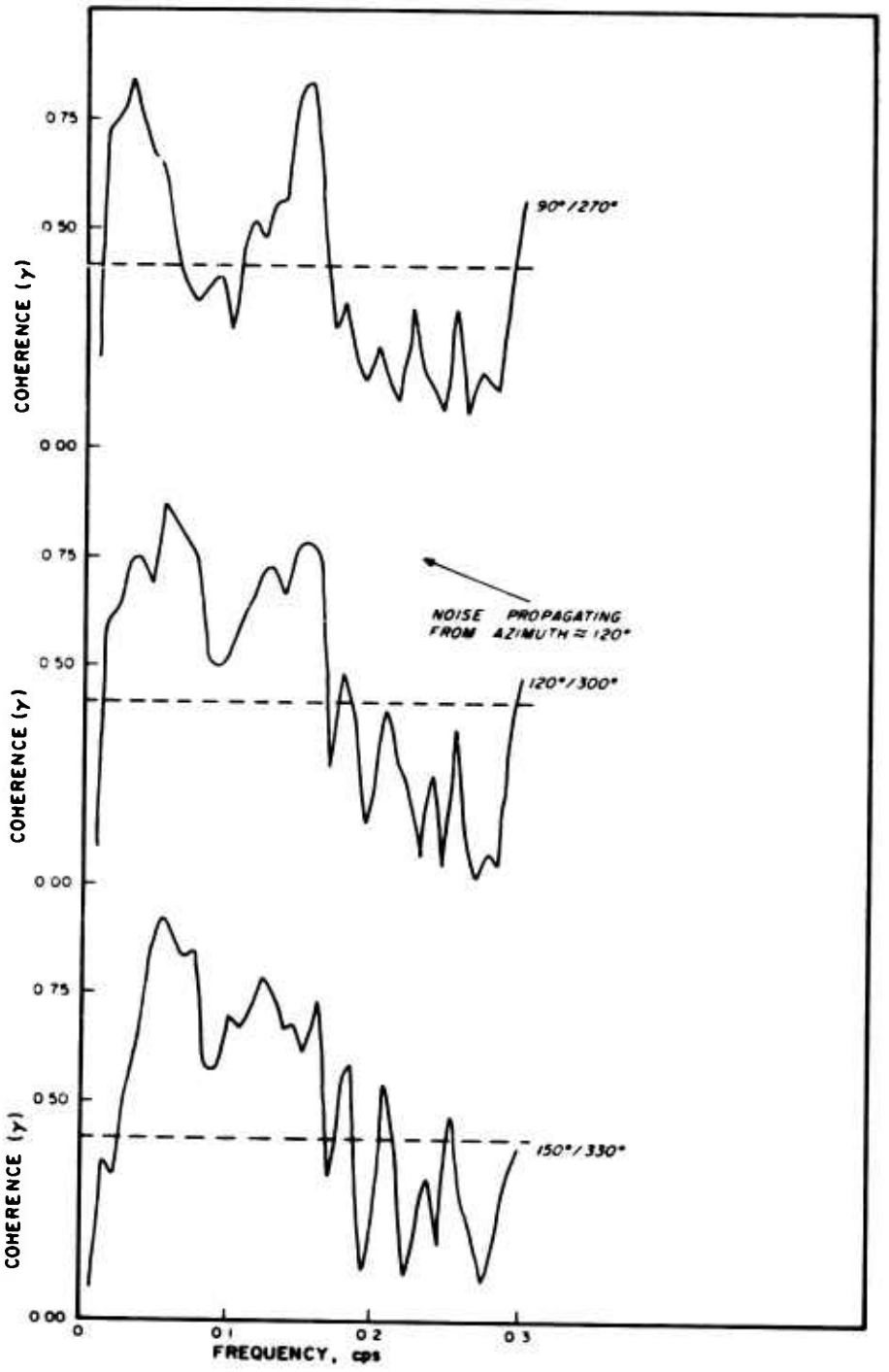

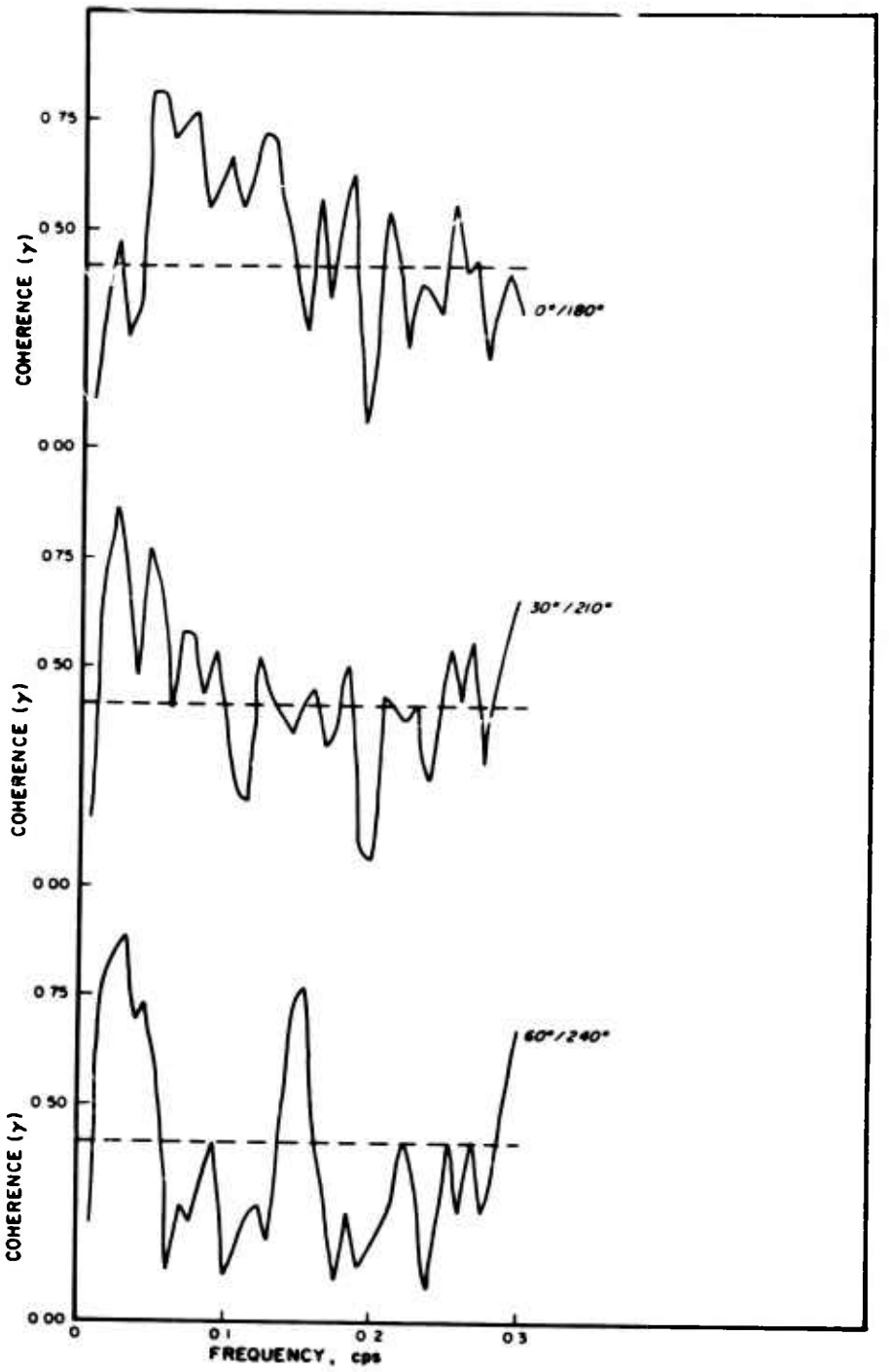

FIGURE 9. COHERENCE OF VERTICAL AND ROTATED HORIZONTAL COMPONENTS ON 9 FEBRUARY 1969.

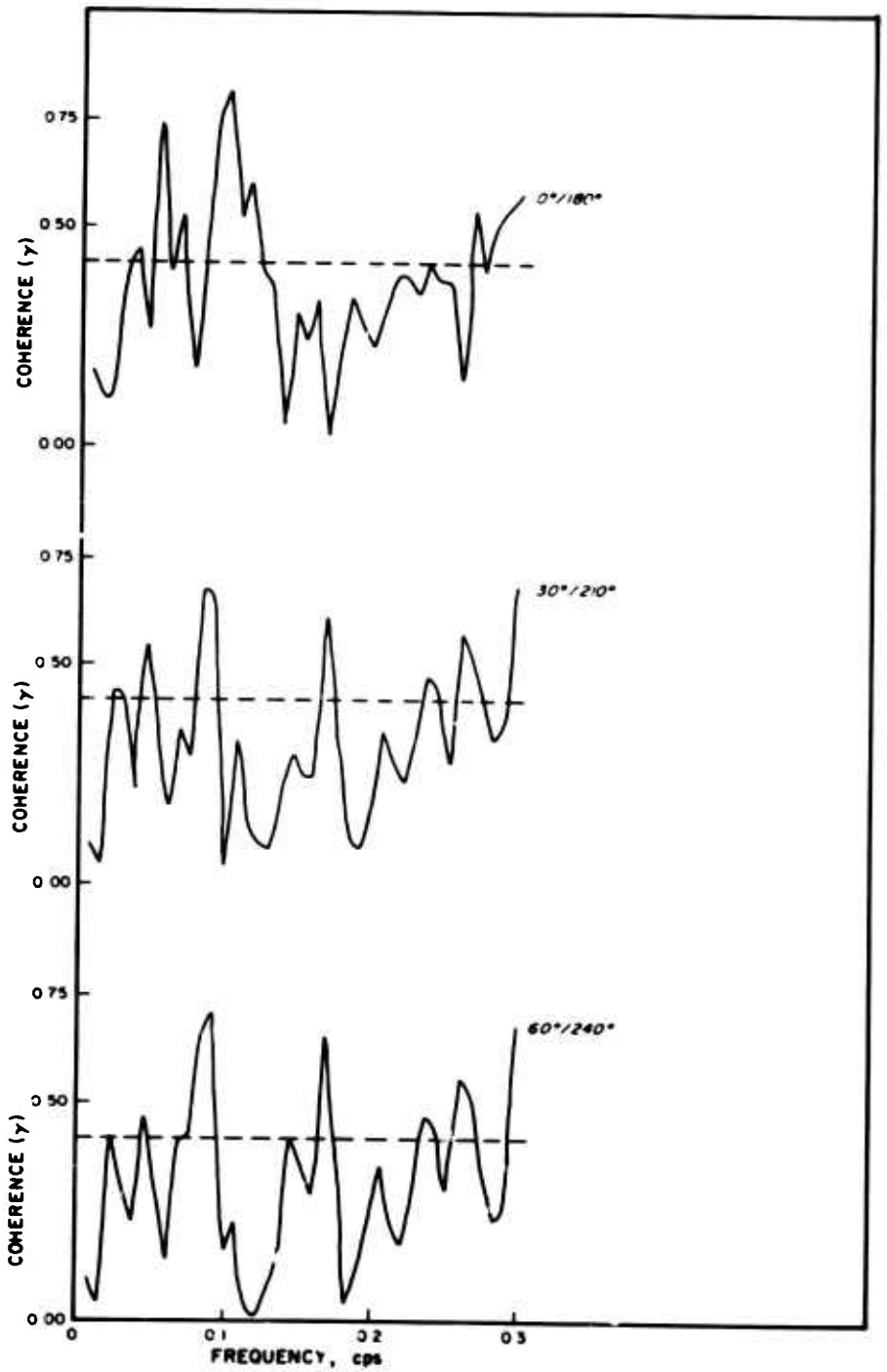

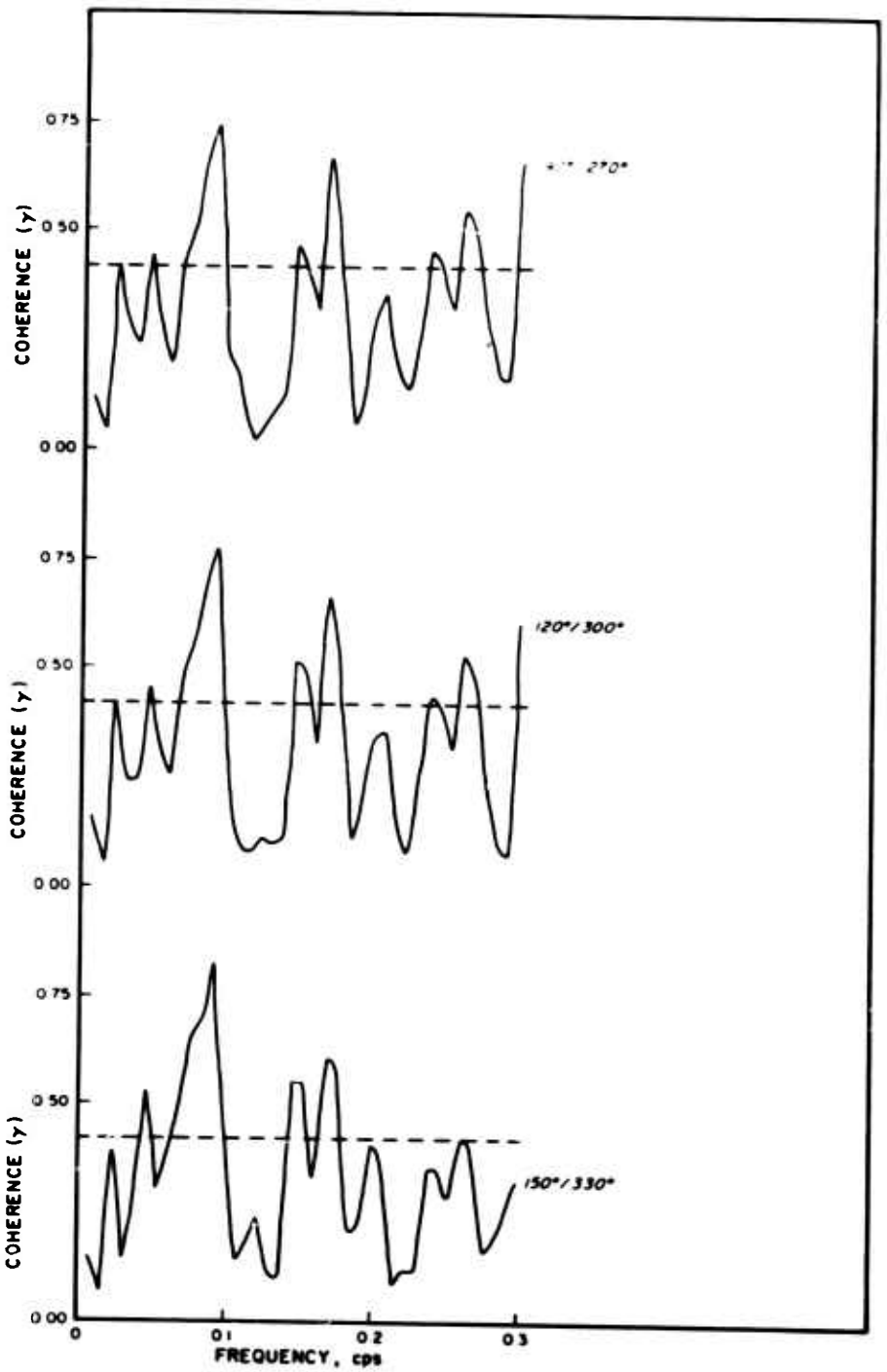

FIGURE 10. COHERENCE OF VERTICAL AND ROTATED HORIZONTAL COMPONENTS ON 2 JUNE 1969.

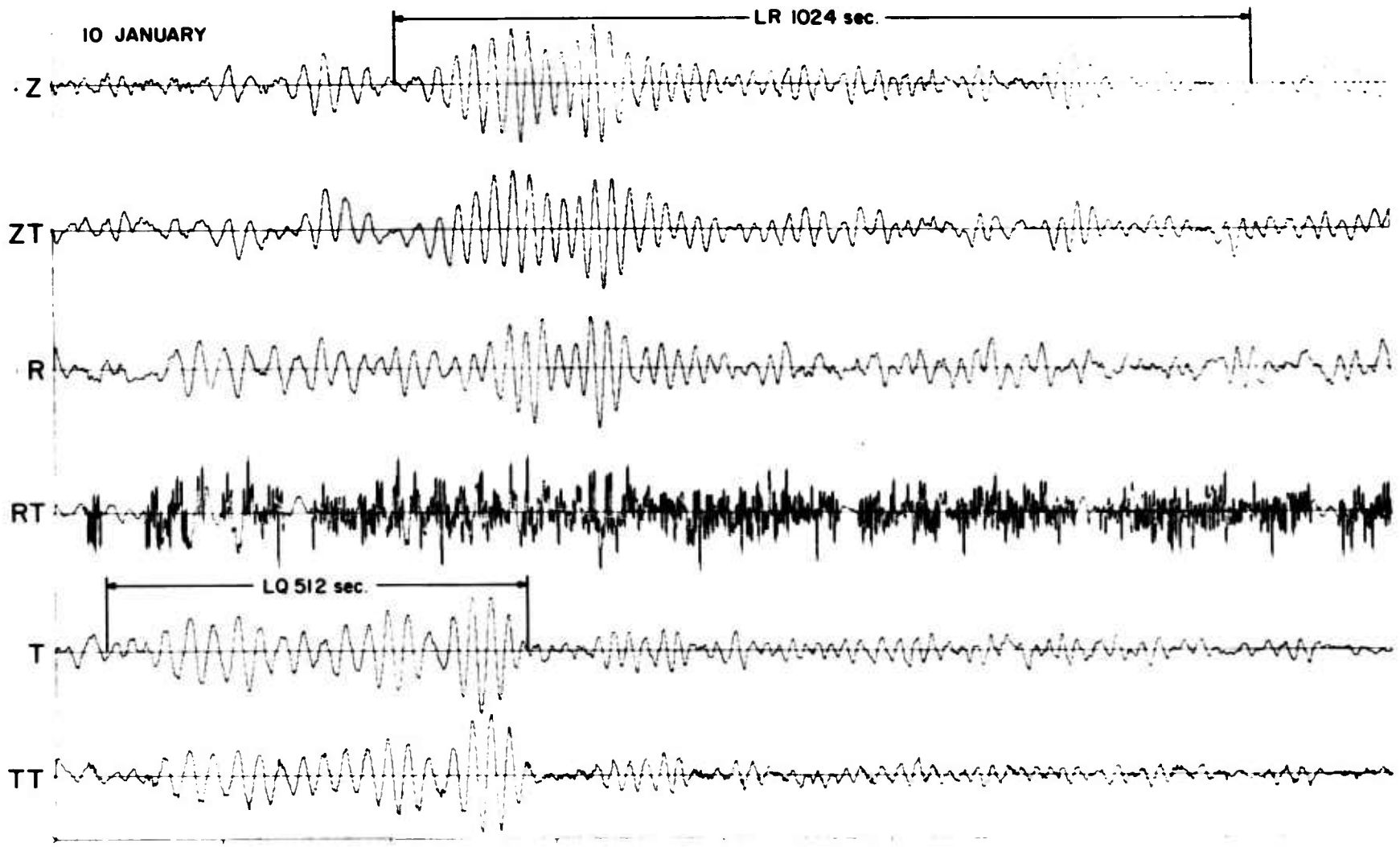

FIGURE 11. RECORDED VERTICAL, RADIAL, AND TRANSVERSE COMPONENTS FOR THE SIGNALS ANALYZED.

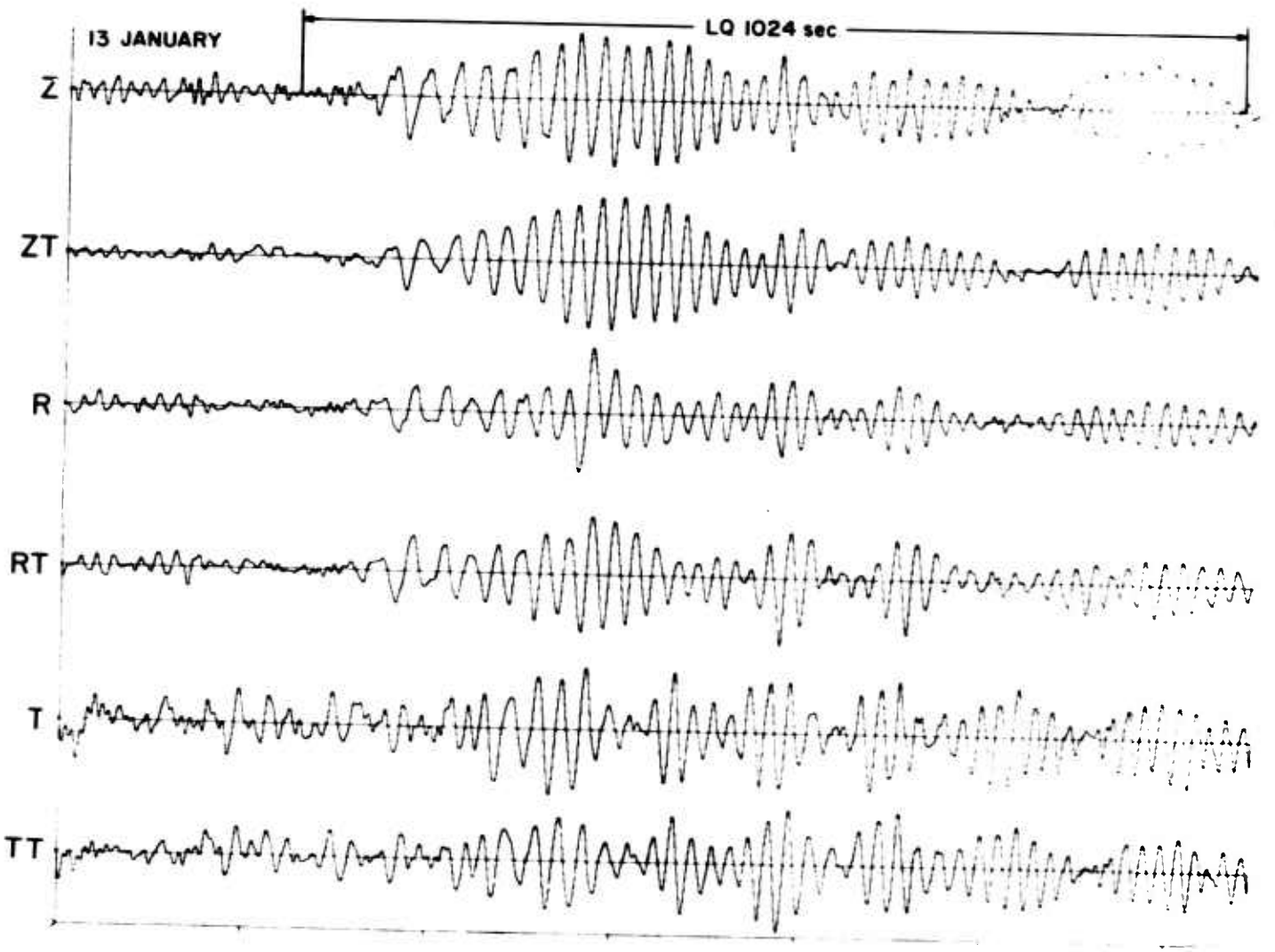

FIGURE 11. (CONT'D.) RECORDED VERTICAL, RADIAL, AND TRANSVERSE COMPONENTS FOR THE SIGNALS ANALYZED.

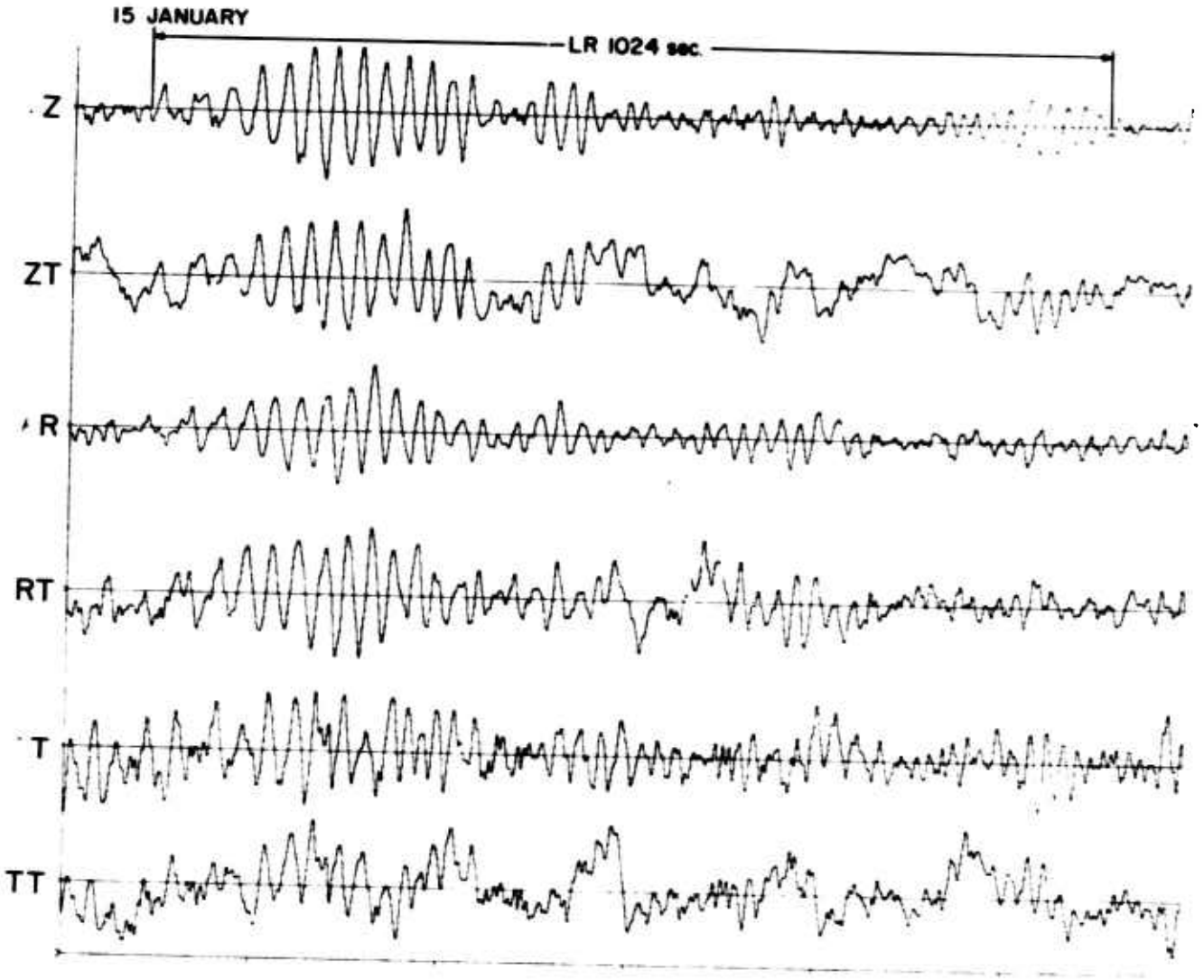

FIGURE 11. (CONT'D.) RECORDED VERTICAL, RADIAL, AND TRANSVERSE COMPONENTS FOR THE SIGNALS ANALYZED.

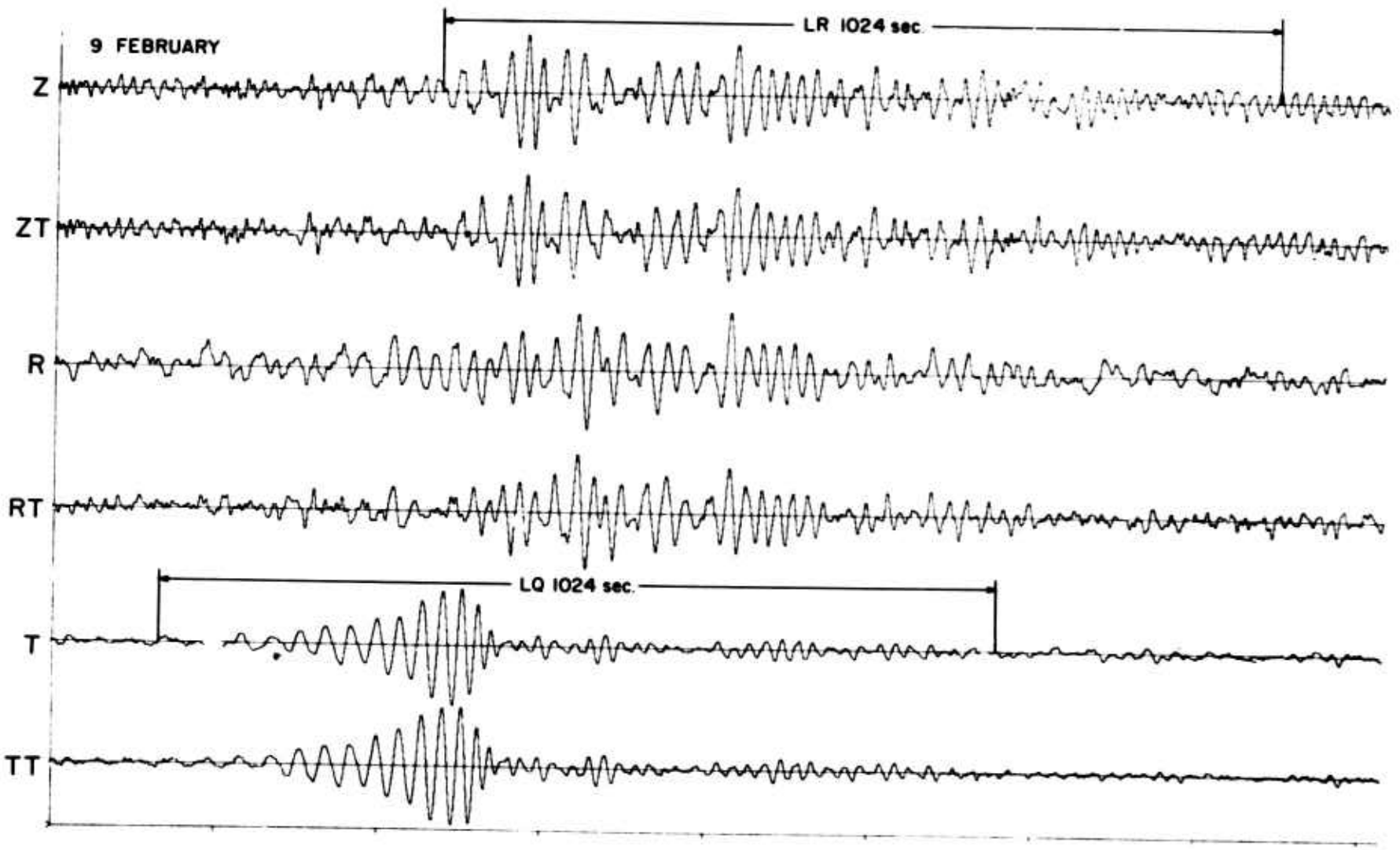

FIGURE 11. (CONT'D.) RECORDED VERTICAL, RADIAL, AND TRANSVERSE COMPONENTS FOR THE SIGNALS ANALYZED.

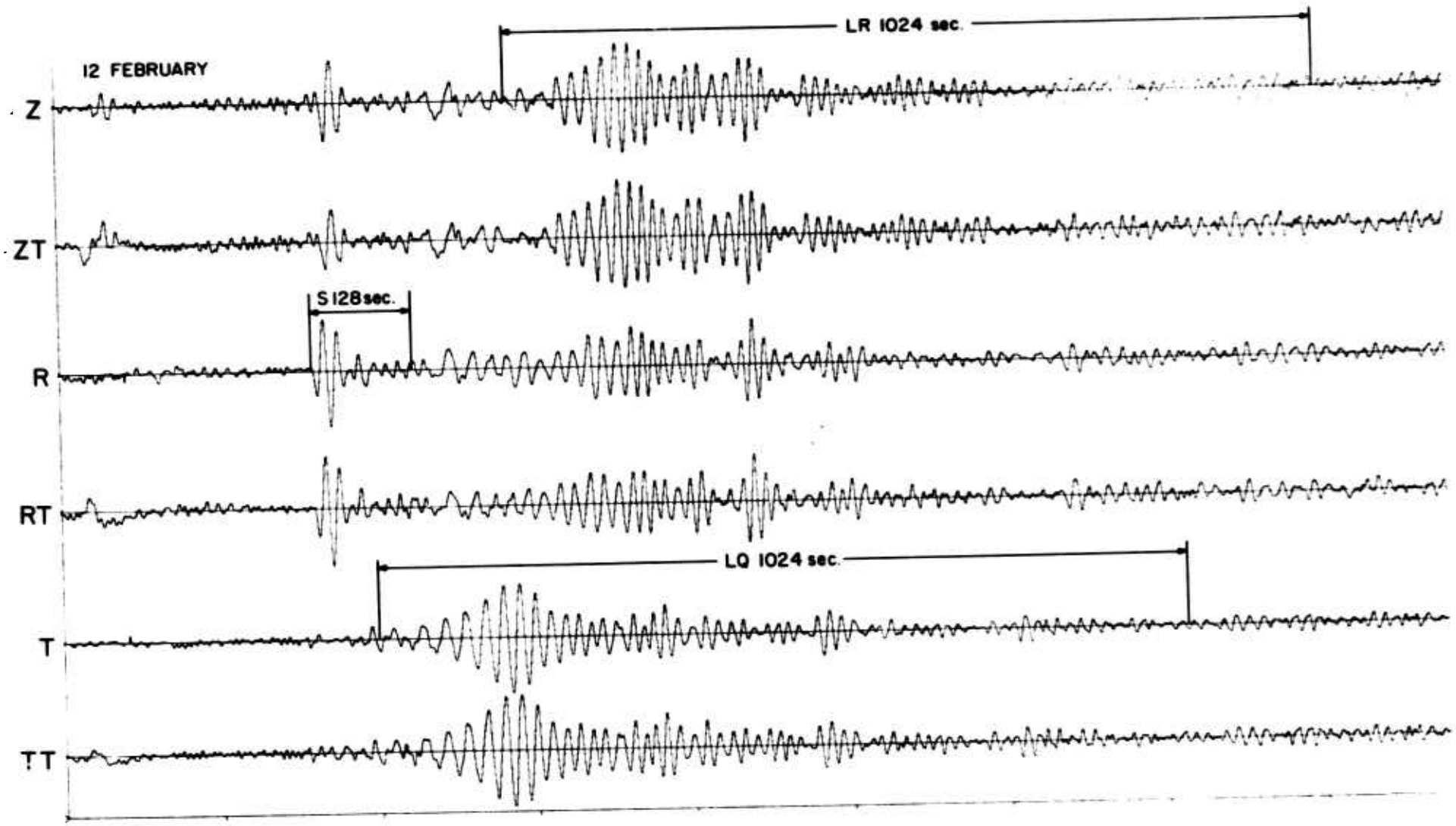

FIGURE 11. (CONT'D.) RECORDED VERTICAL, RADIAL, AND TRANSVERSE COMPONENTS FOR THE SIGNALS ANALYZED.

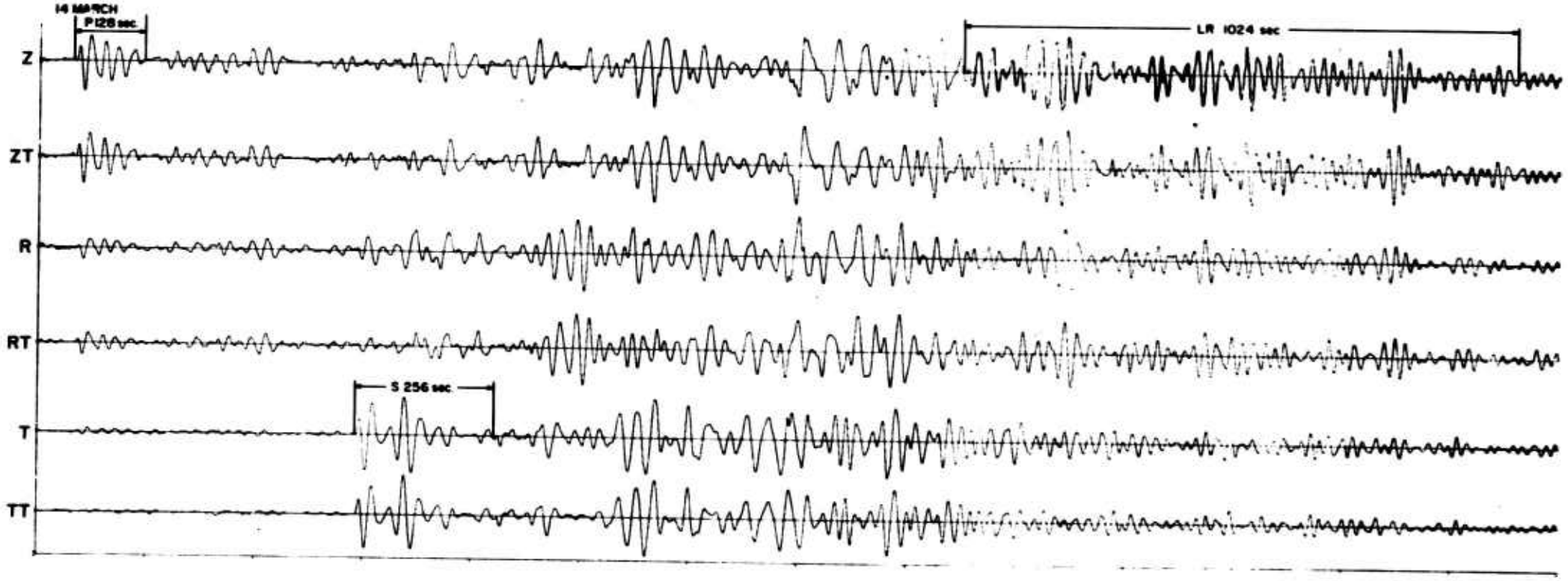

FIGURE 11. (CONT'D.) RECORDED VERTICAL, RADIAL, AND TRANSVERSE COMPONENTS FOR THE SIGNALS ANALYZED.

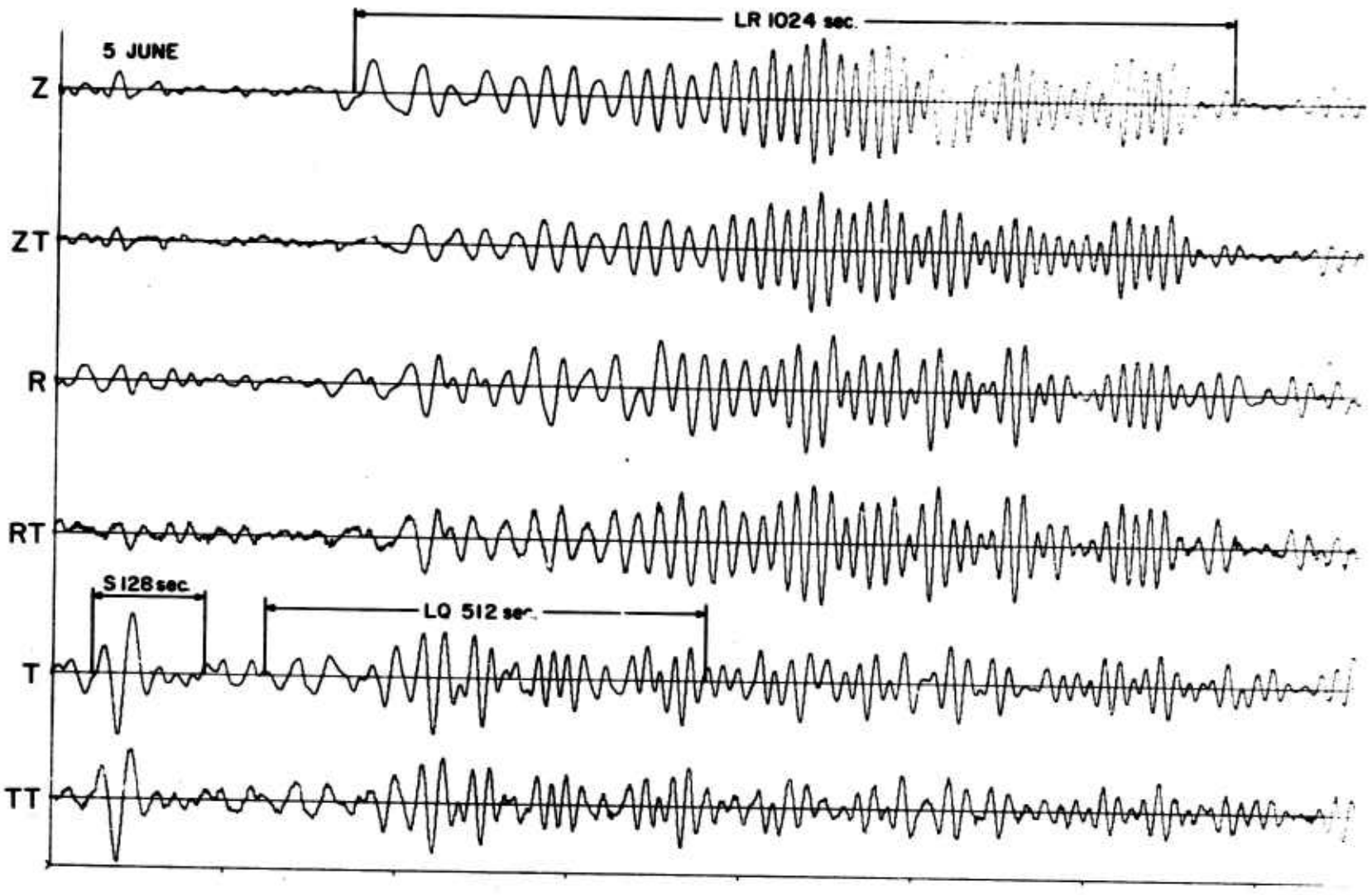

FIGURE 11. (CONT'D.) RECORDED VERTICAL, RADIAL, AND TRANSVERSE COMPONENTS FOR THE SIGNALS ANALYZED.

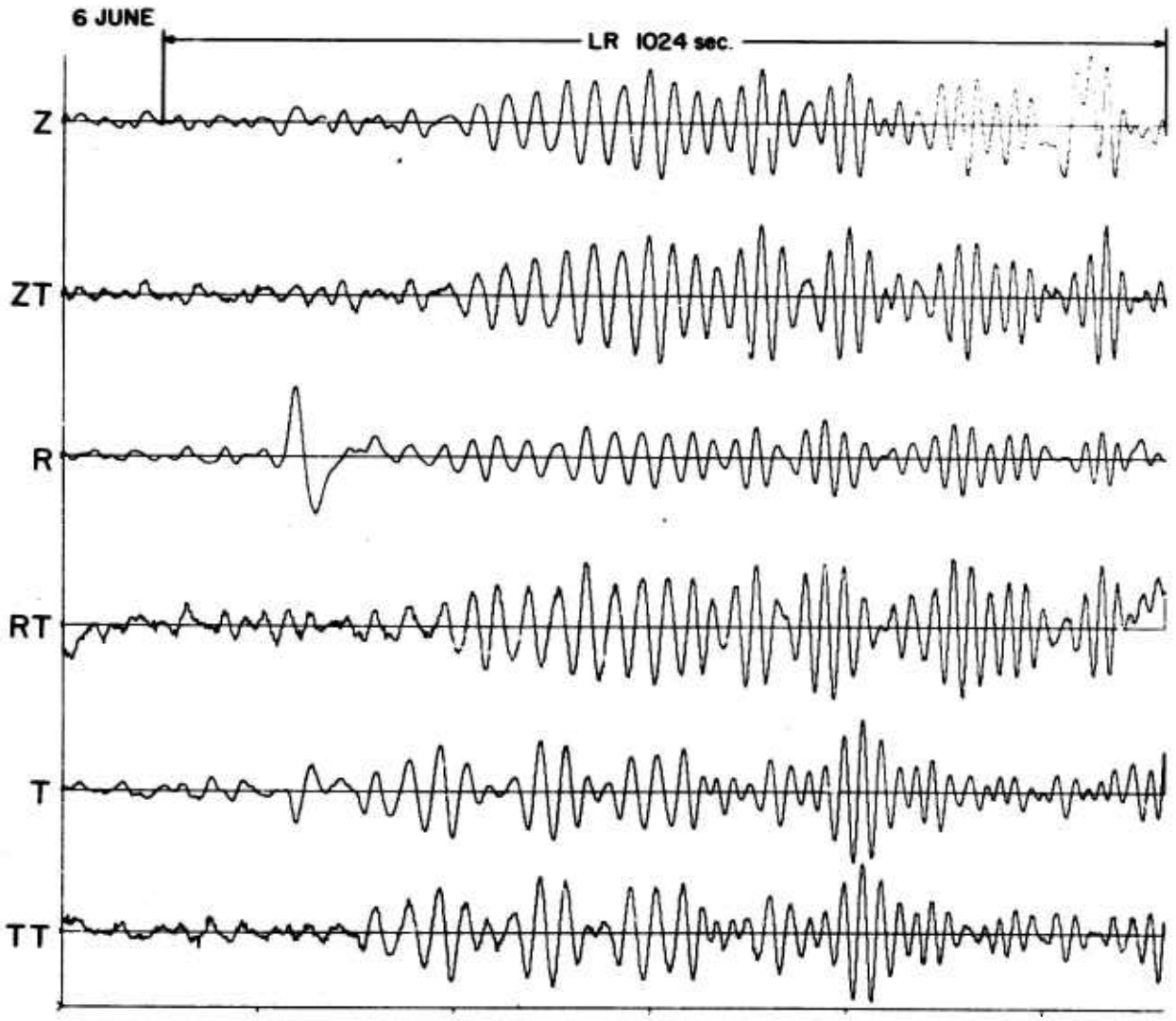

FIGURE 11. (CONT'D.) RECORDED VERTICAL, RADIAL, AND TRANSVERSE COMPONENTS FOR THE SIGNALS ANALYZED.

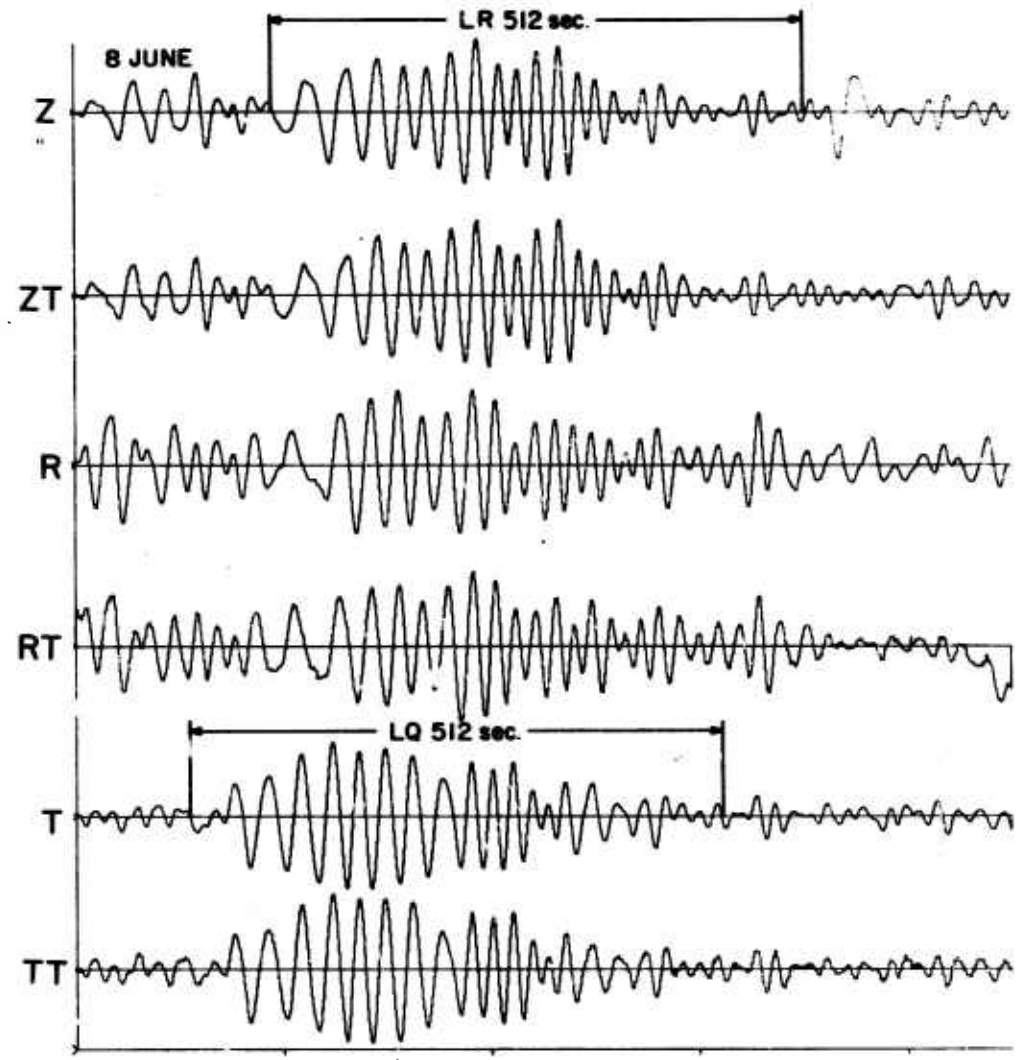

FIGURE 11. (CONT'D.) RECORDED VERTICAL, RADIAL, AND TRANSVERSE COMPONENTS FOR THE SIGNALS ANALYZED.

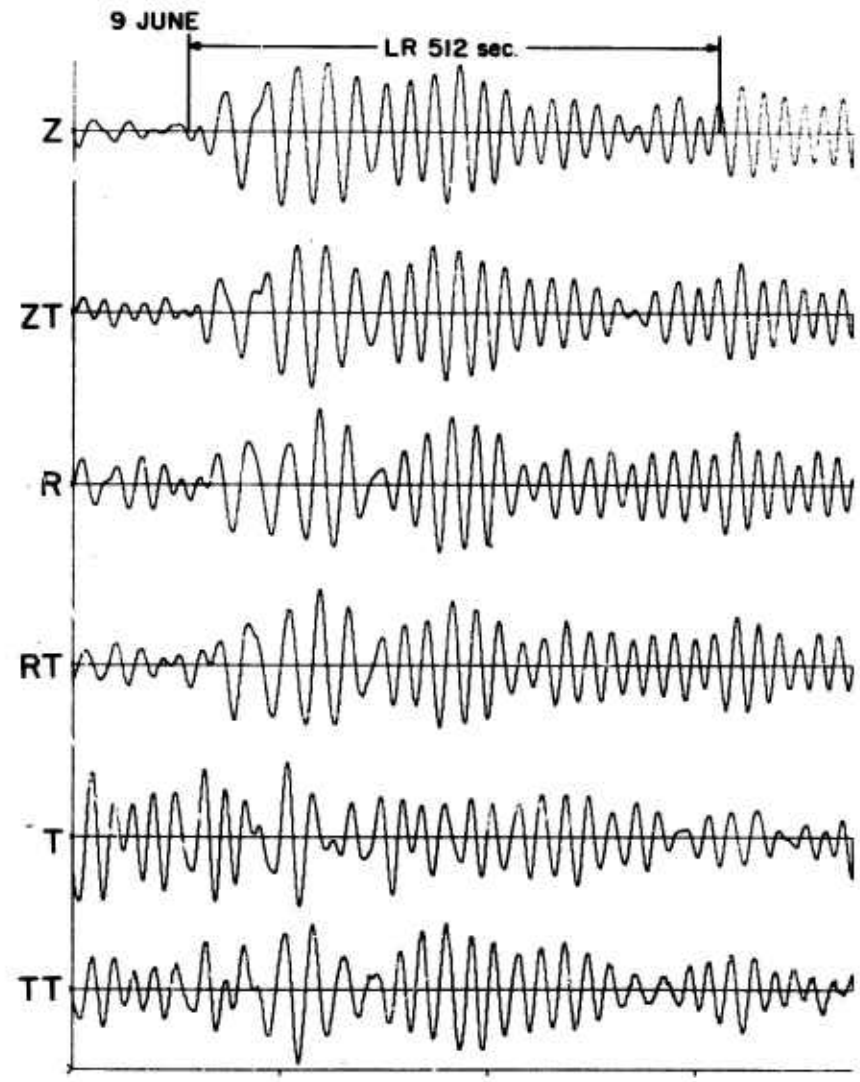

FIGURE 11. (CONT'D.) RECORDED VERTICAL, RADIAL, AND TRANSVERSE COMPONENTS FOR THE SIGNALS ANALYZED.

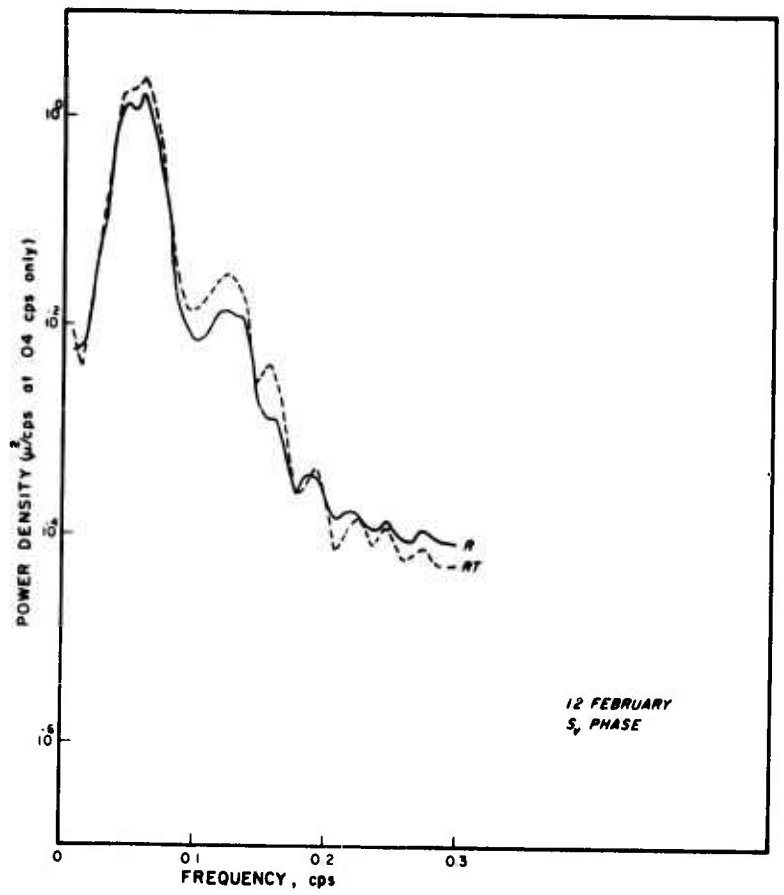

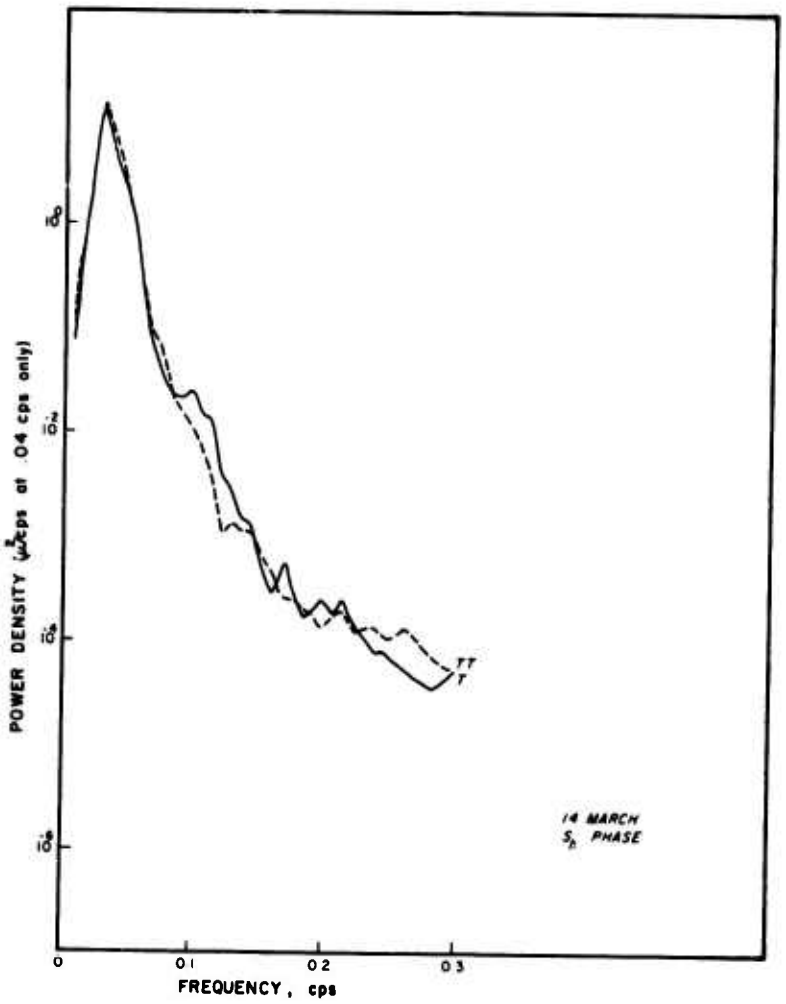

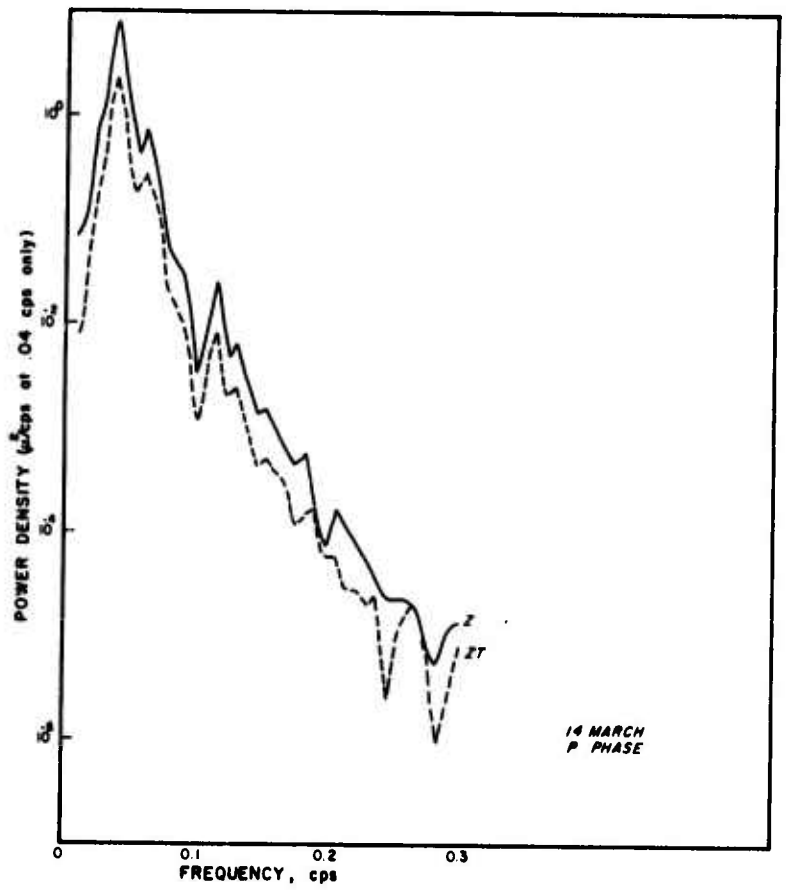

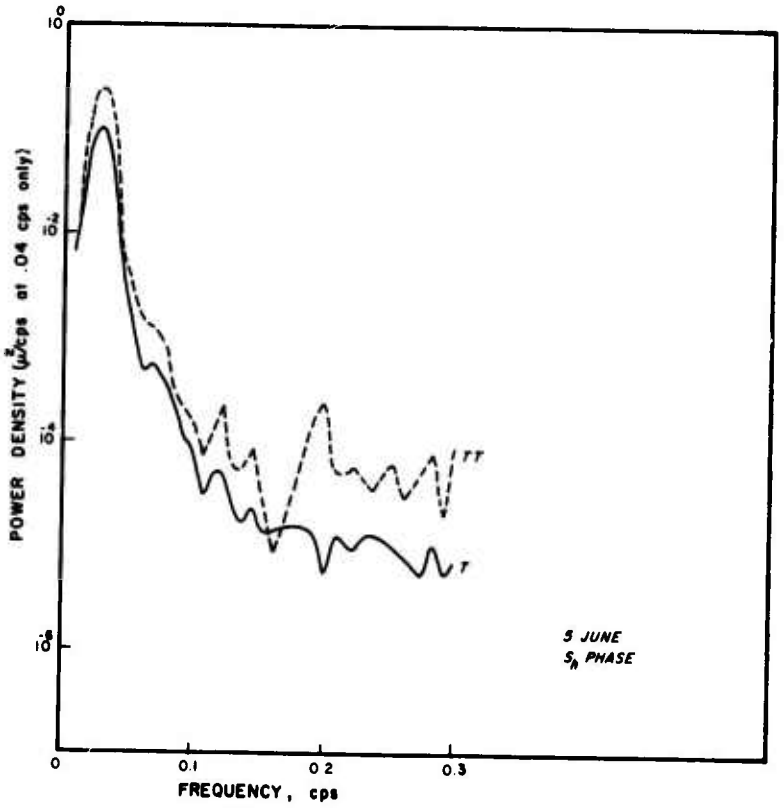

FIGURE 12. POWER SPECTRA OF BODY WAVES RECORDED SIMULTANEOUSLY ON THE ALPS AND TRIAX SYSTEMS.

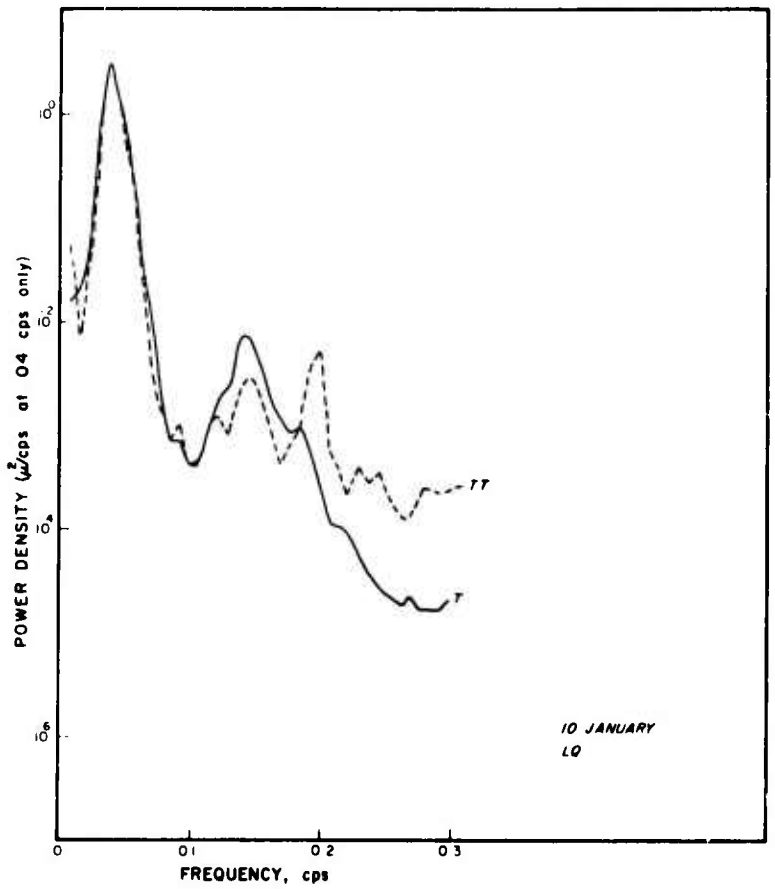

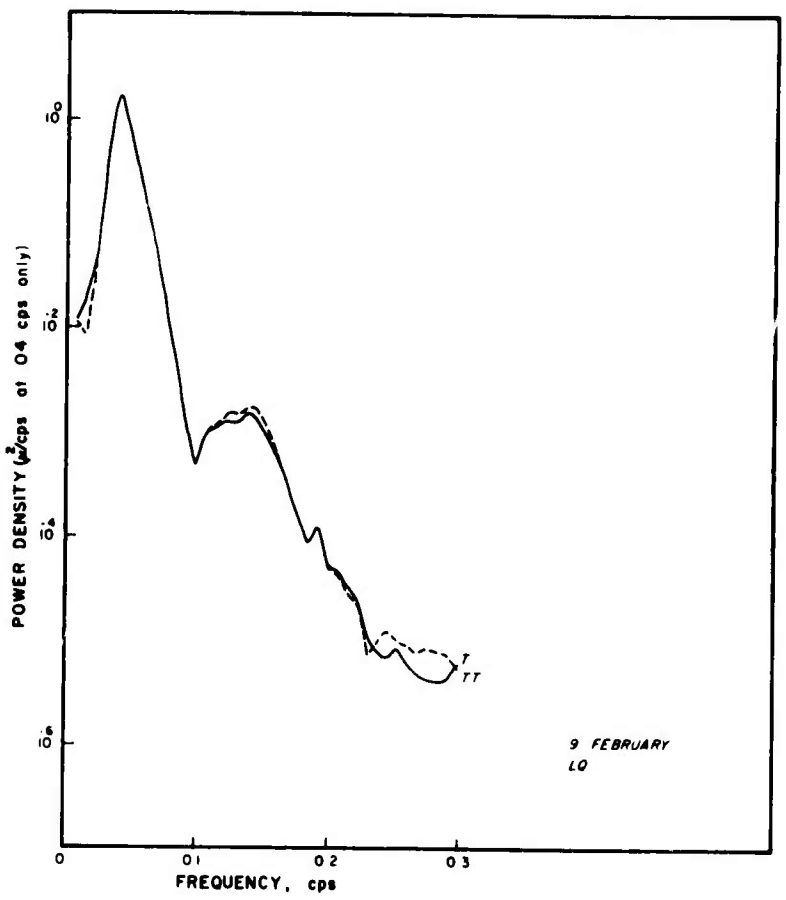

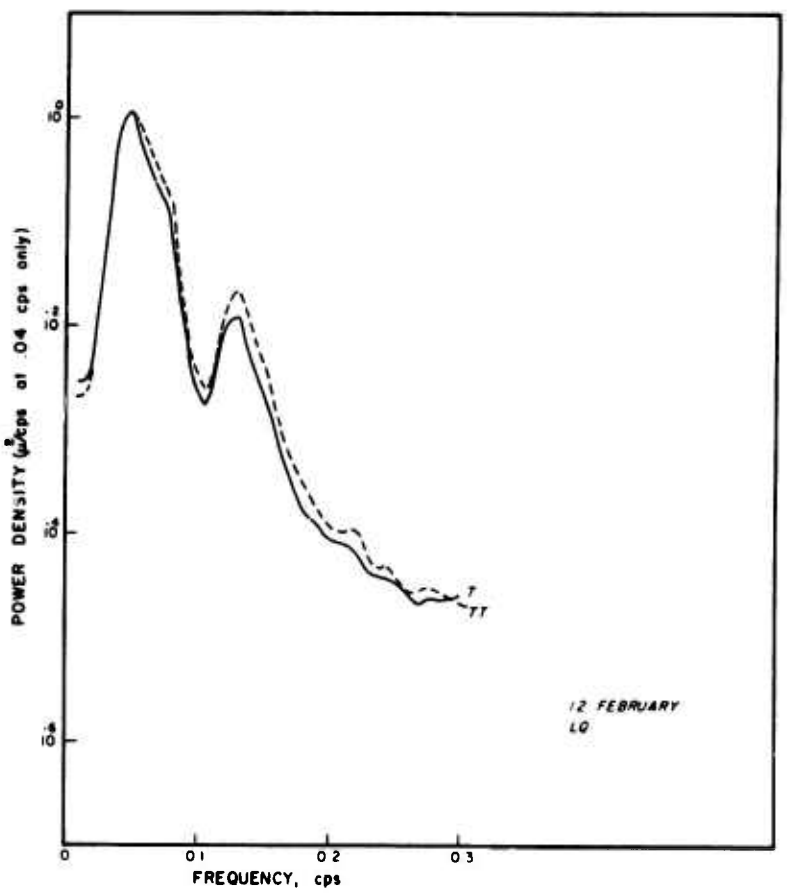

FIGURE 13. POWER SPECTRA OF LOVE WAVES RECORDED SIMULTANEOUSLY ON THE ALPS AND TRIAX SYSTEMS.

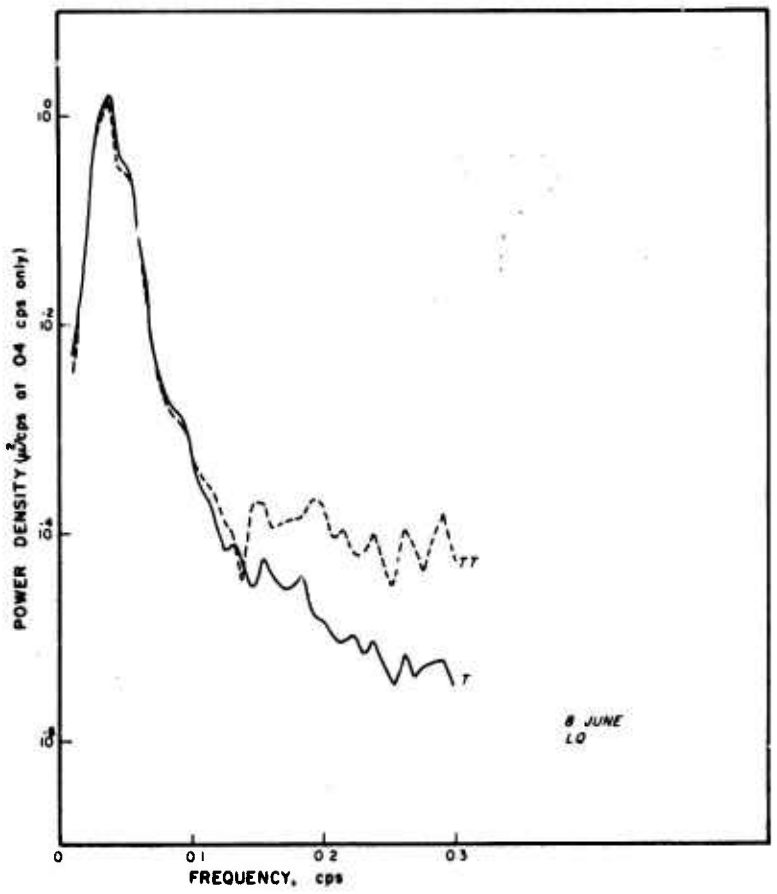

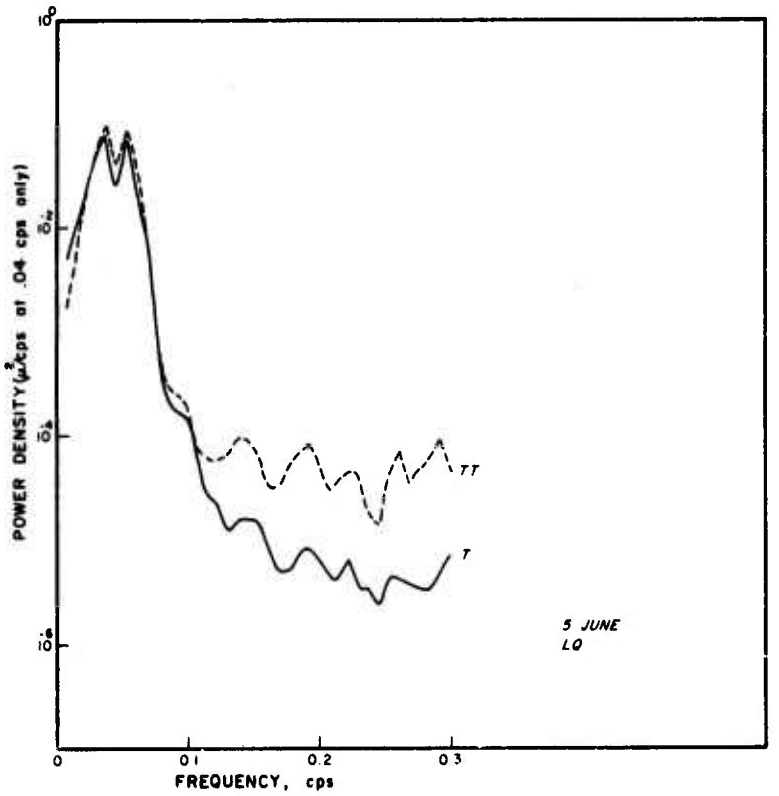

FIGURE 13 (CONT'D.). POWER SPECTRA OF LOVE WAVES RECORDED SIMULTANEOUSLY ON THE ALPS AND TRIAX SYSTEMS.

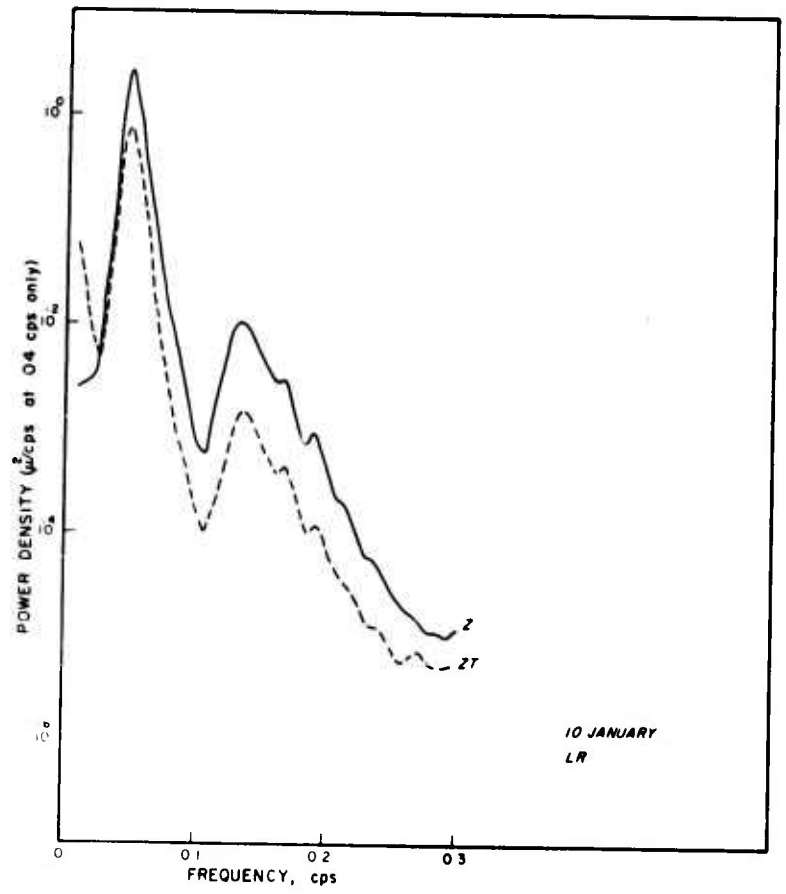

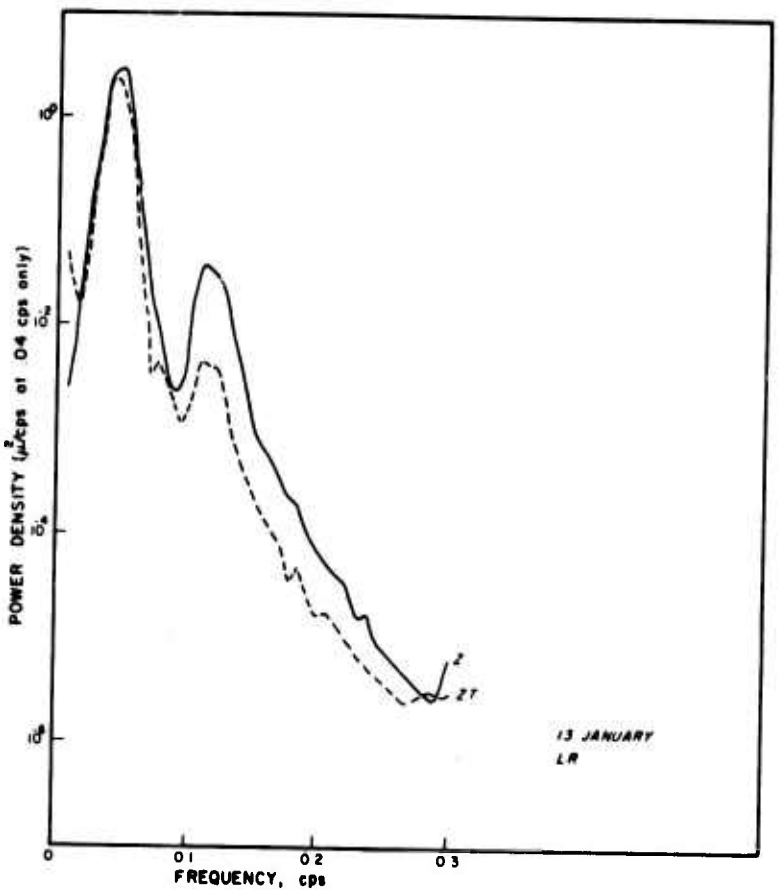

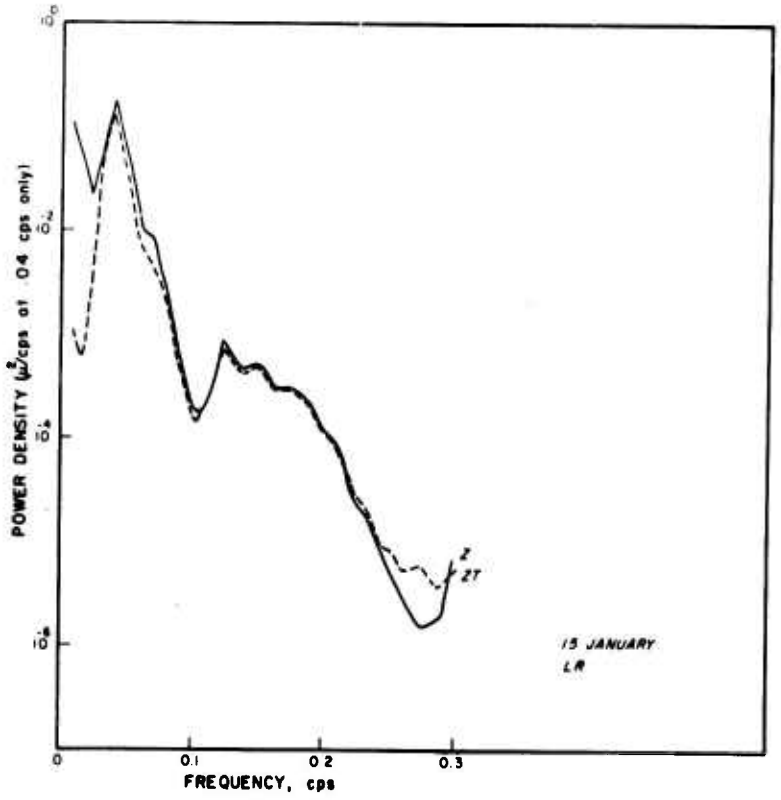

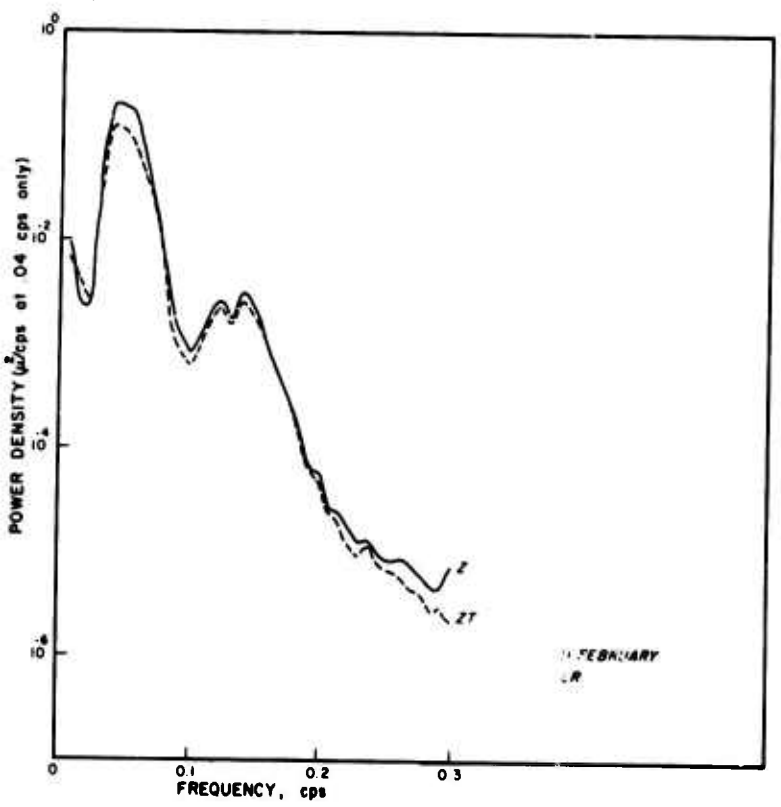

FIGURE 14. POWER SPECTRA OF RAYLEIGH WAVES RECORDED SIMULTANEOUSLY ON THE ALPS AND TRIAX SYSTEMS.

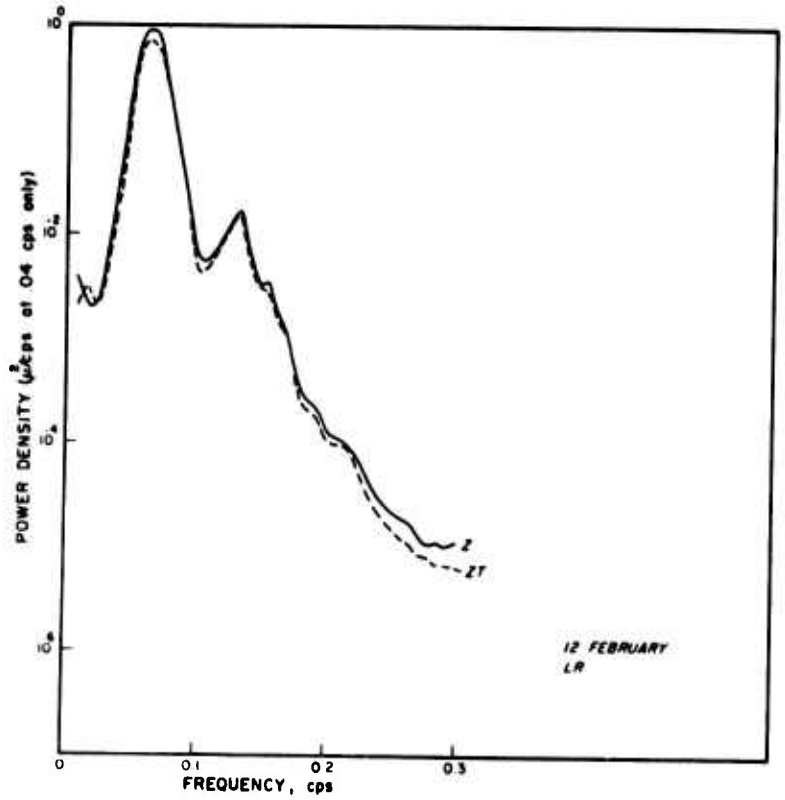

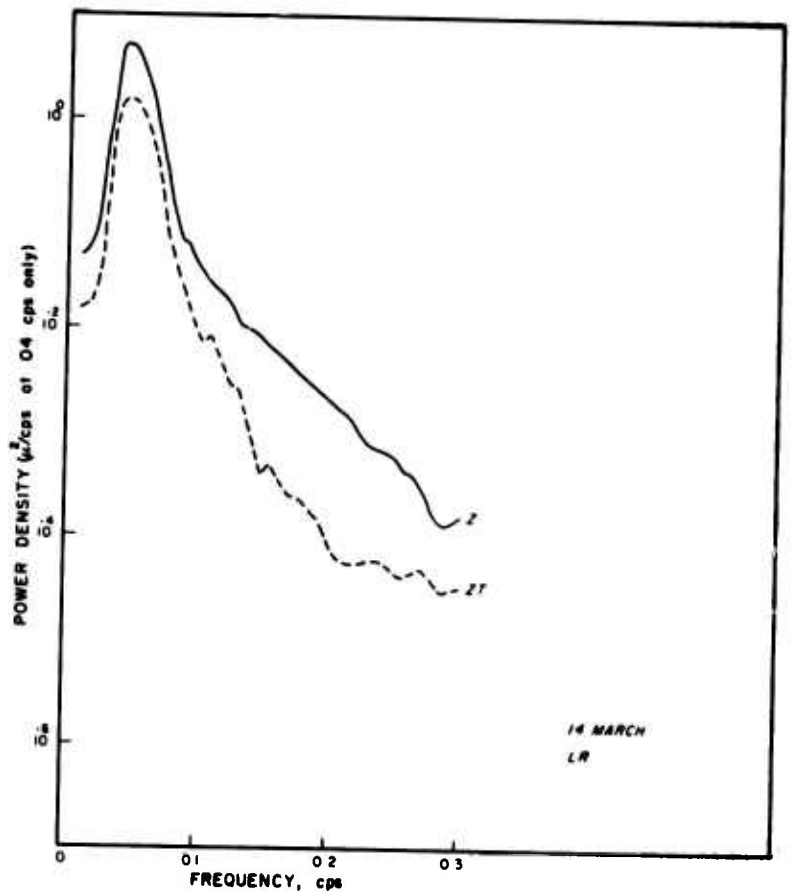

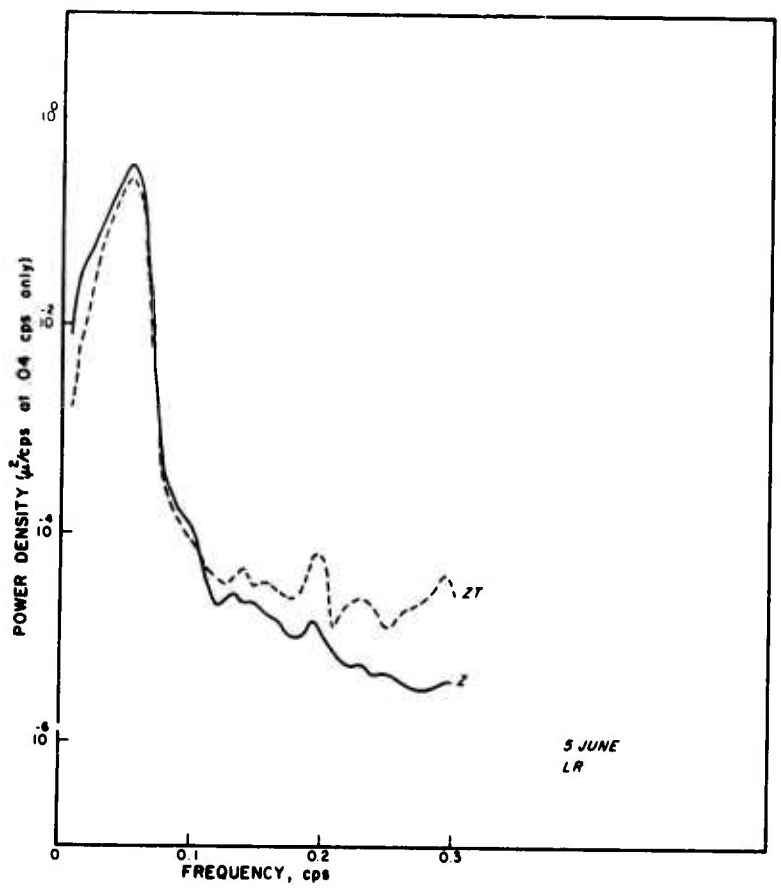

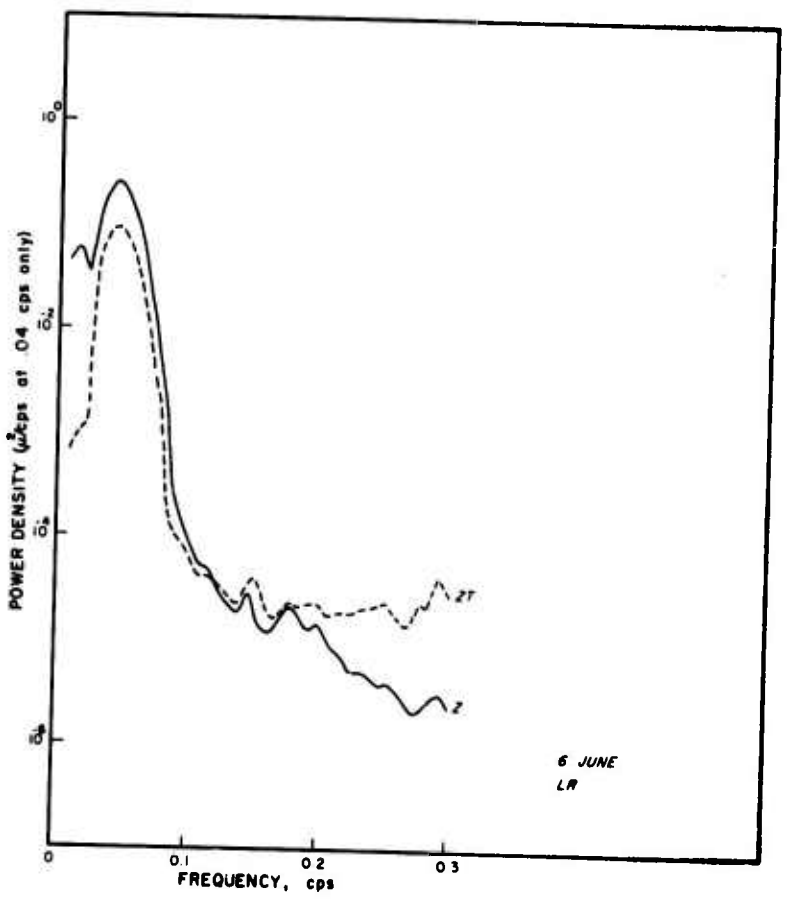

FIGURE 14. (CONT'D.) POWER SPECTRA OF RAYLEIGH WAVES RECORDED SIMULTANEOUSLY ON THE ALPS AND TRIAX SYSTEMS.

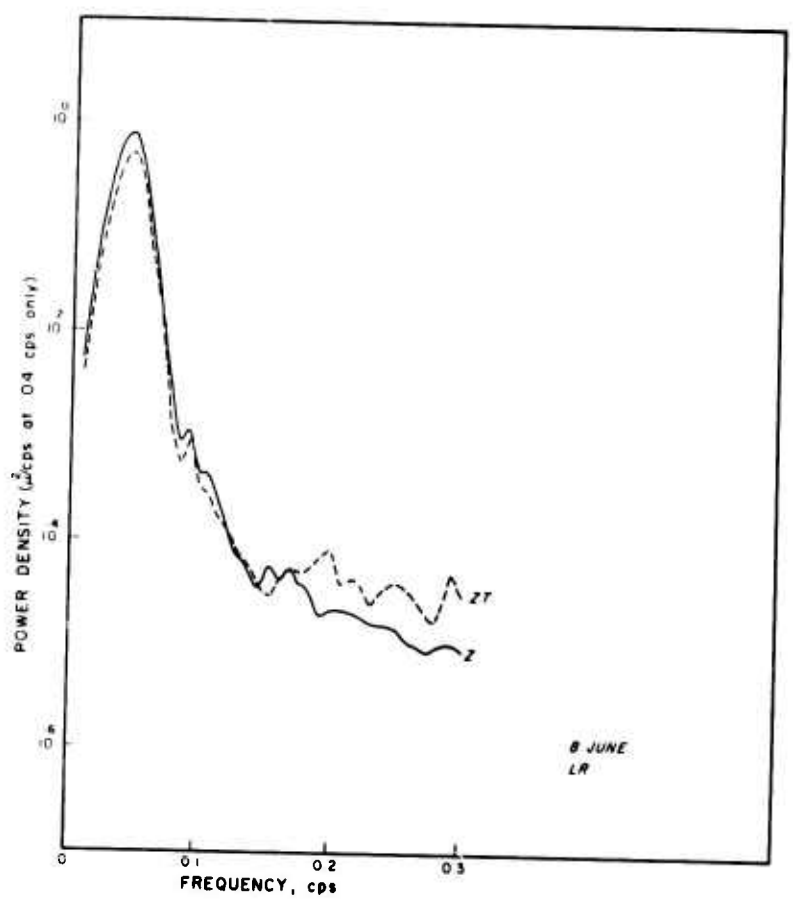

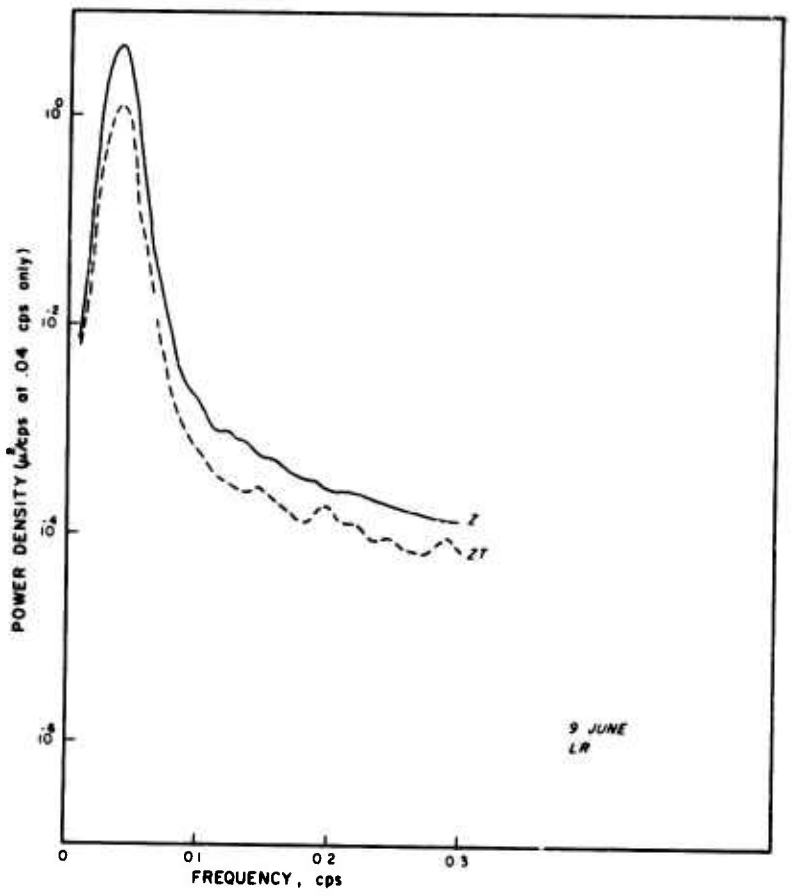

FIGURE 14. (CONT'D.) POWER SPECTRA OF RAYLEIGH WAVES RECORDED SIMULTANEOUSLY ON THE ALPS AND TRIAX SYSTEMS.

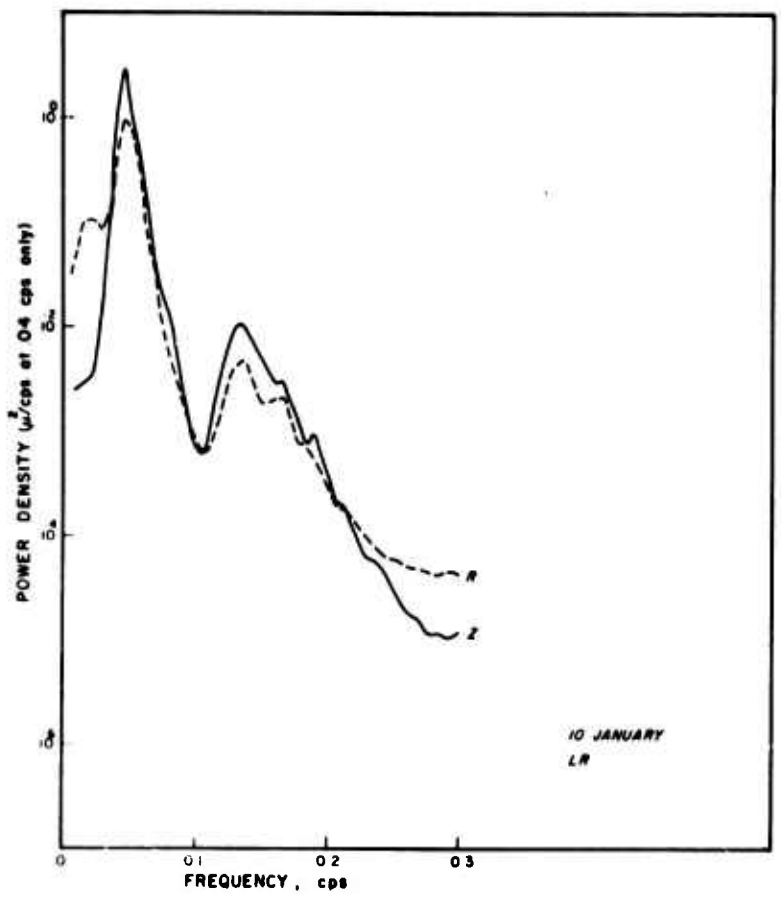

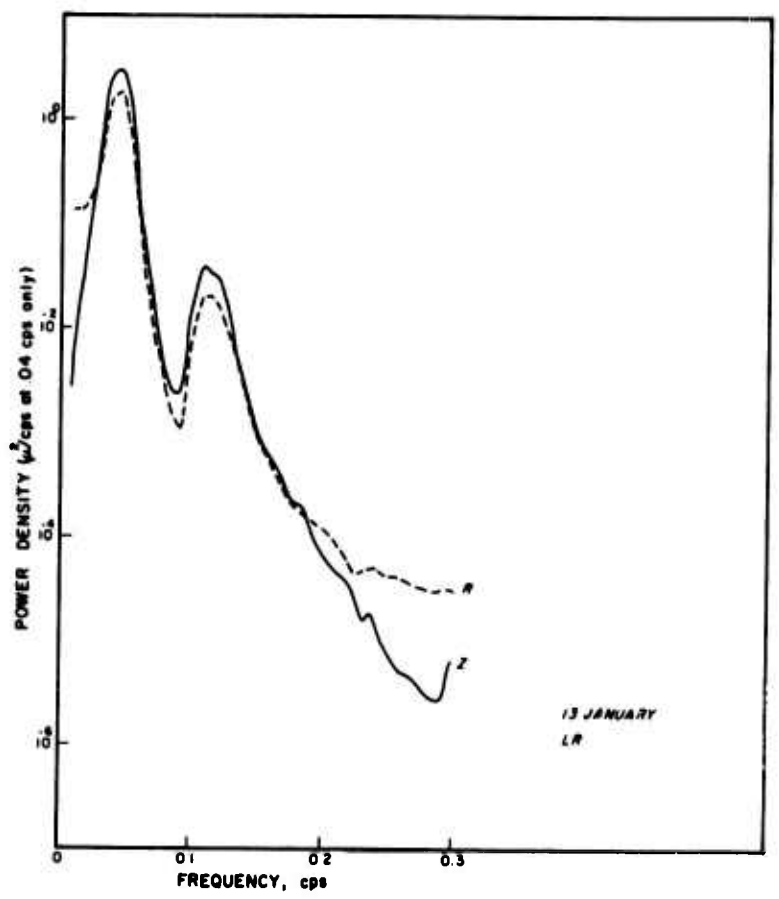

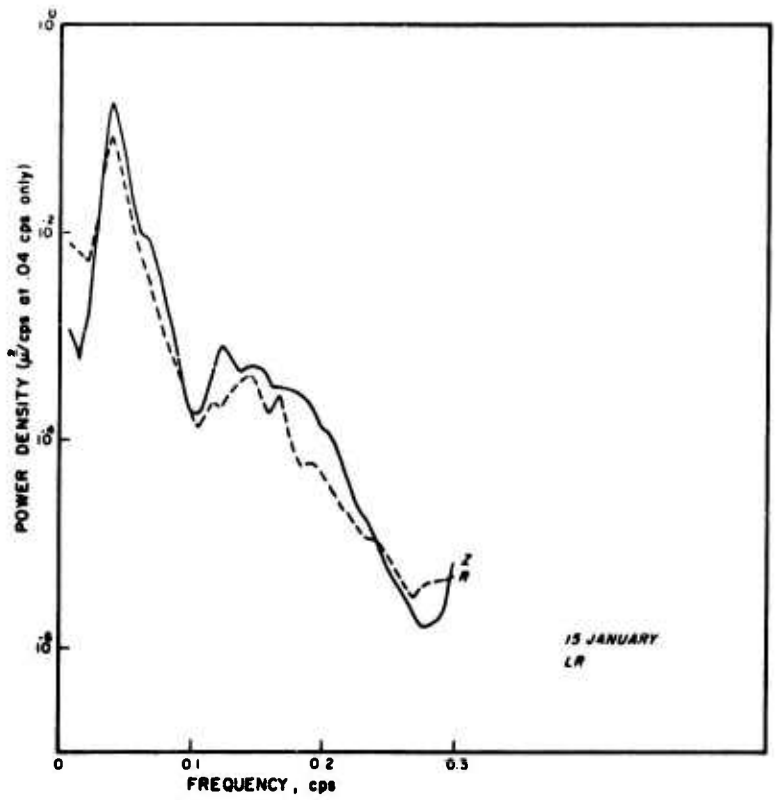

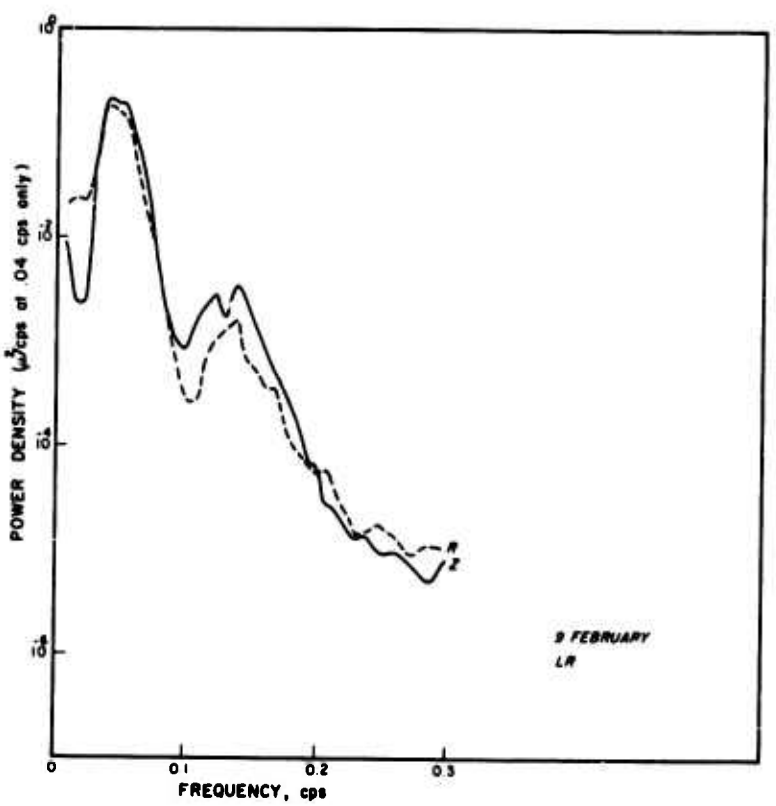

FIGURE 15. POWER SPECTRA OF RAYLEIGH WAVES RECORDED SIMULTANEOUSLY ON THE ALPS VERTICAL AND RADIAL COMPONENTS.

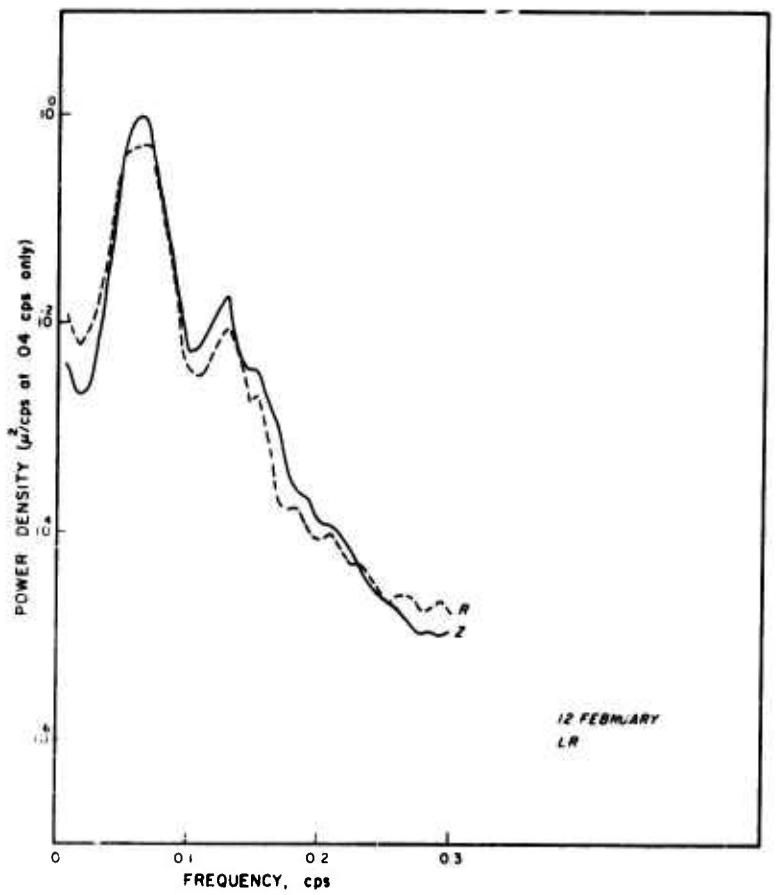

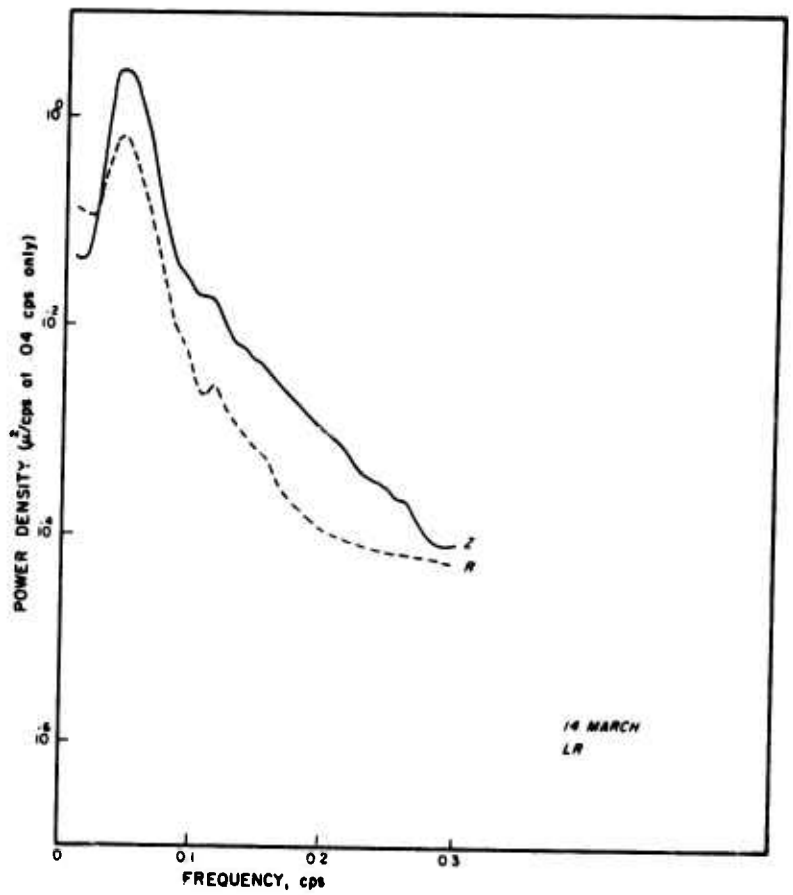

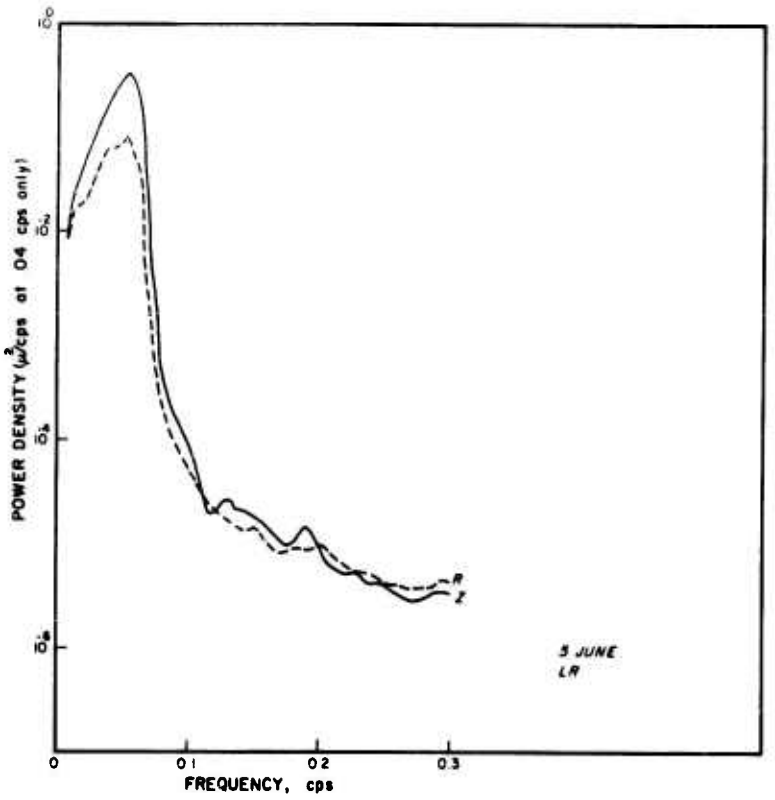

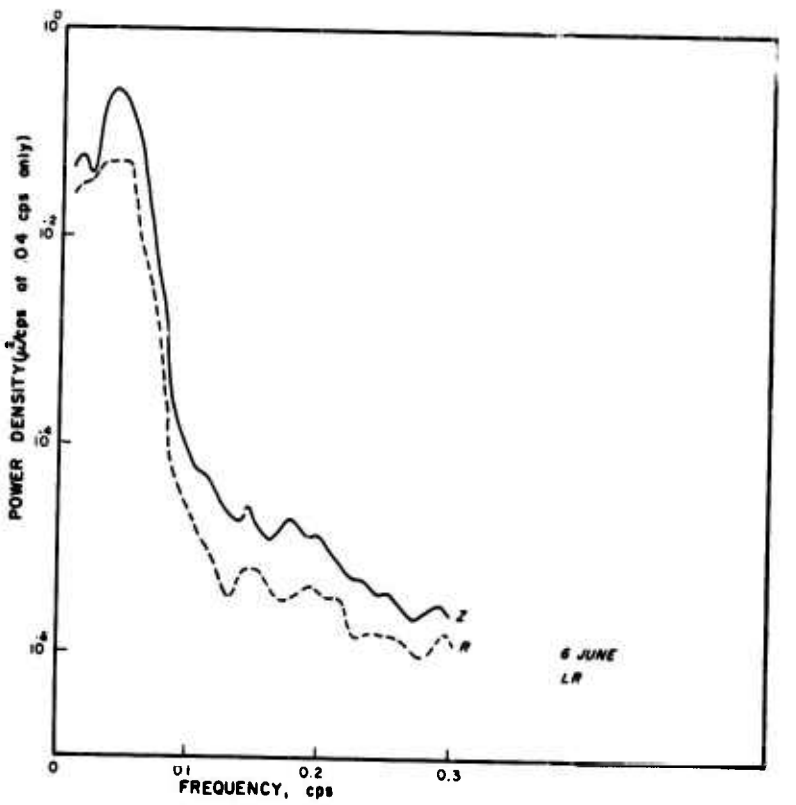

FIGURE 15. (CONT'D.) POWER SPECTRA OF RAYLEIGH WAVES RECORDED SIMULTANEOUSLY ON THE ALPS VERTICAL AND RADIAL COMPONENTS.

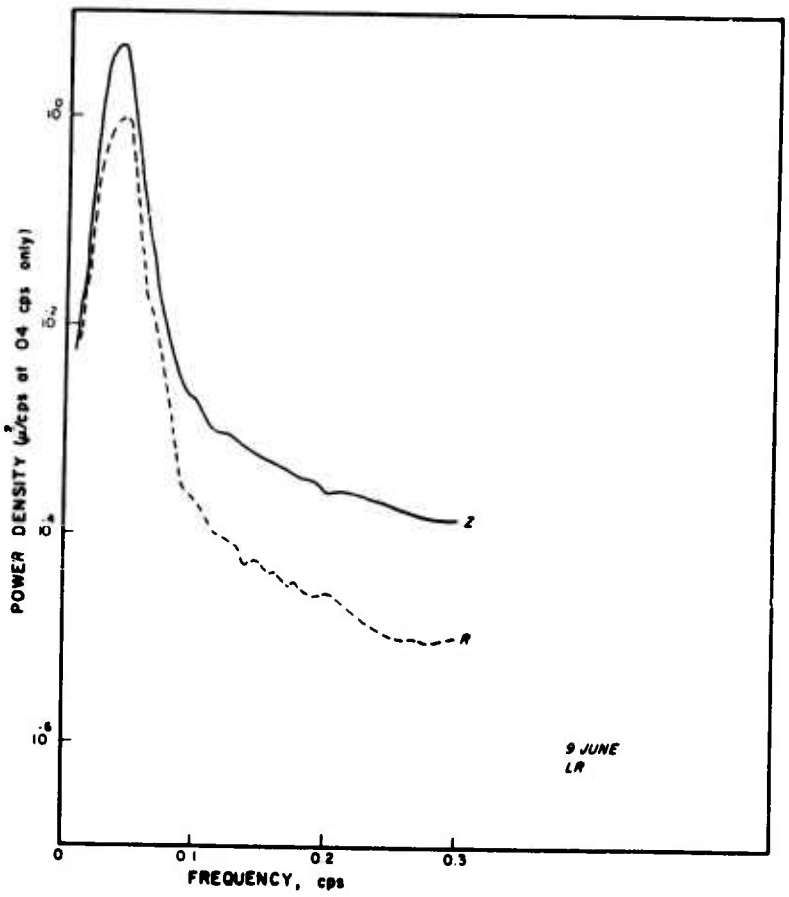

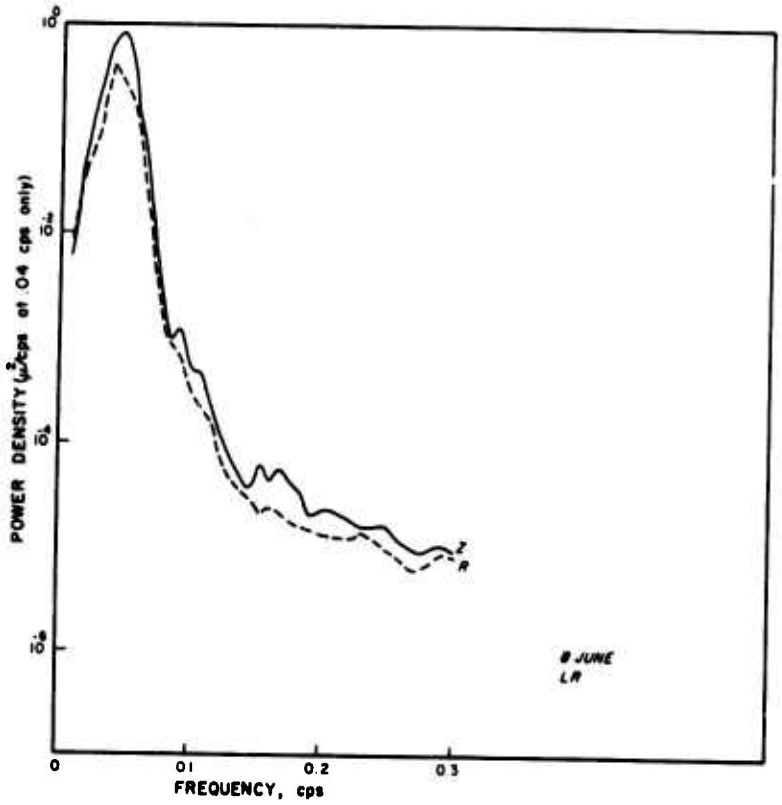

FIGURE 15. (CONT'D.) POWER SPECTRA OF RAYLEIGH WAVES RECORDED SIMULTANEOUSLY ON THE ALPS VERTICAL AND RADIAL COMPONENTS.

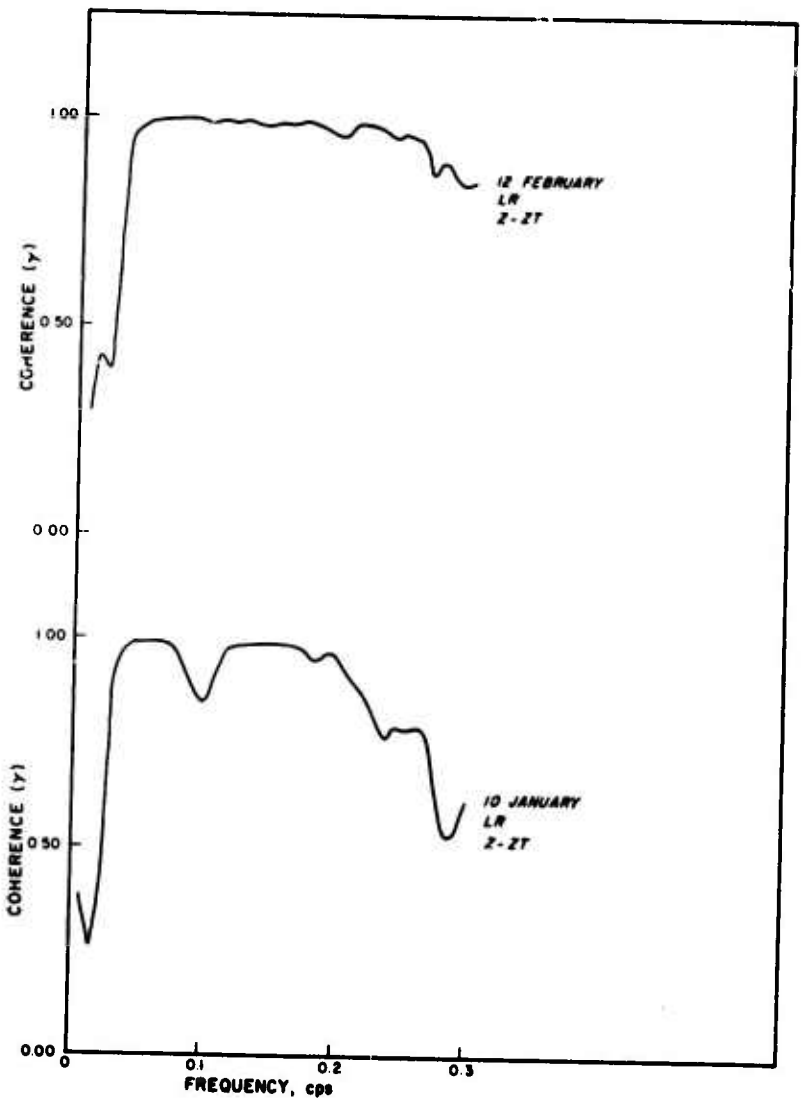

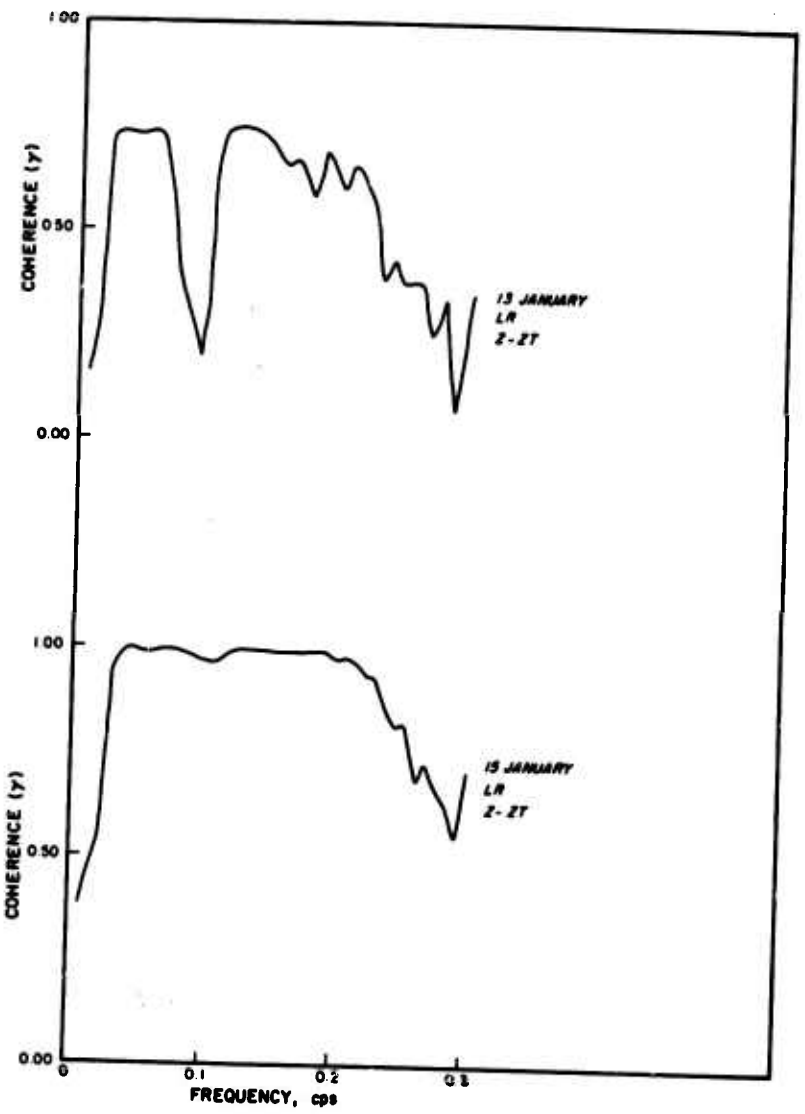

FIGURE 16. COHERENCE BETWEEN ALPS AND TRIAX COMPONENTS FOR SEVERAL SIGNALS.

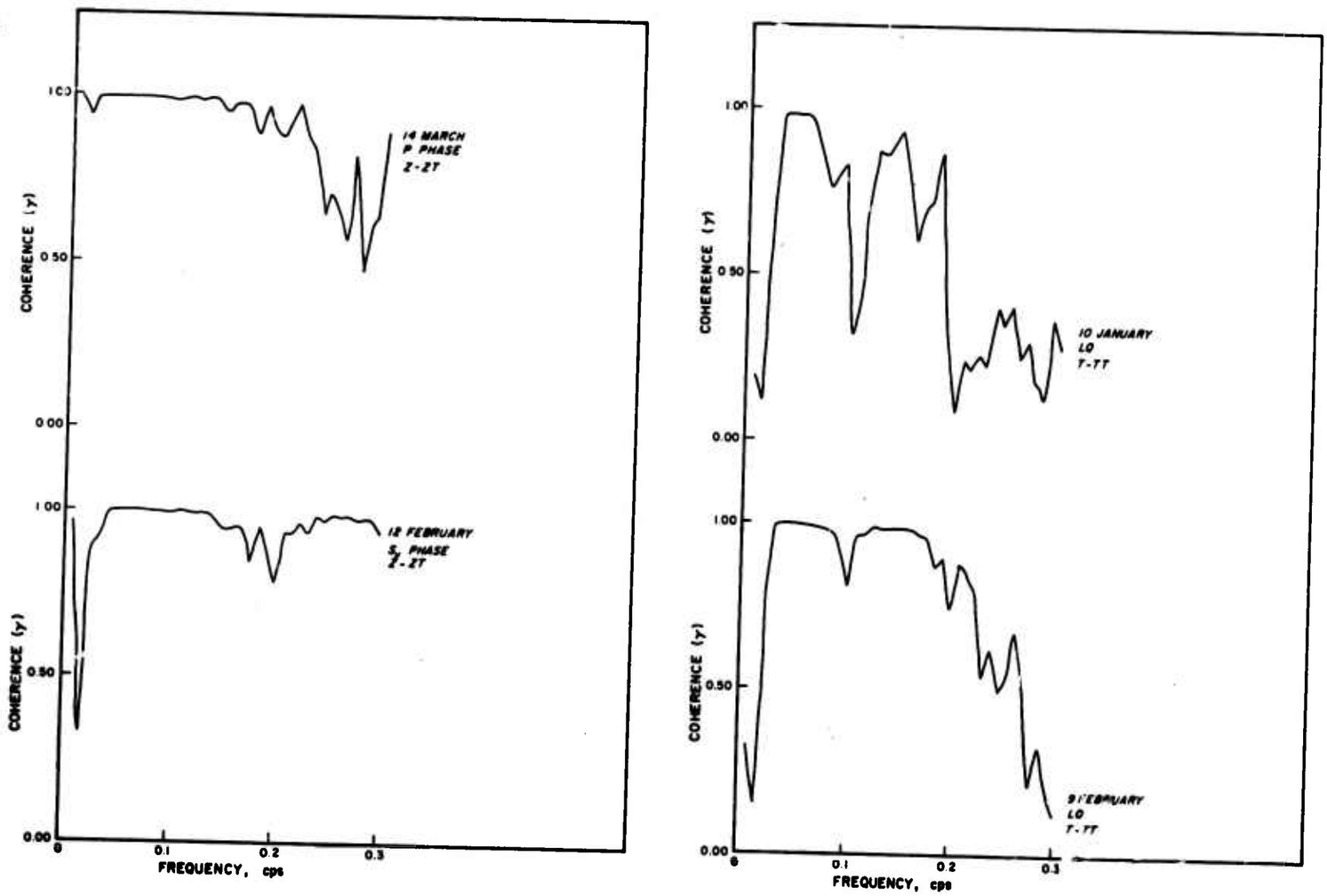

FIGURE 16. (CONT'D.) COHERENCE BETWEEN ALPS AND TRIAX COMPONENTS FOR SEVERAL SIGNALS.

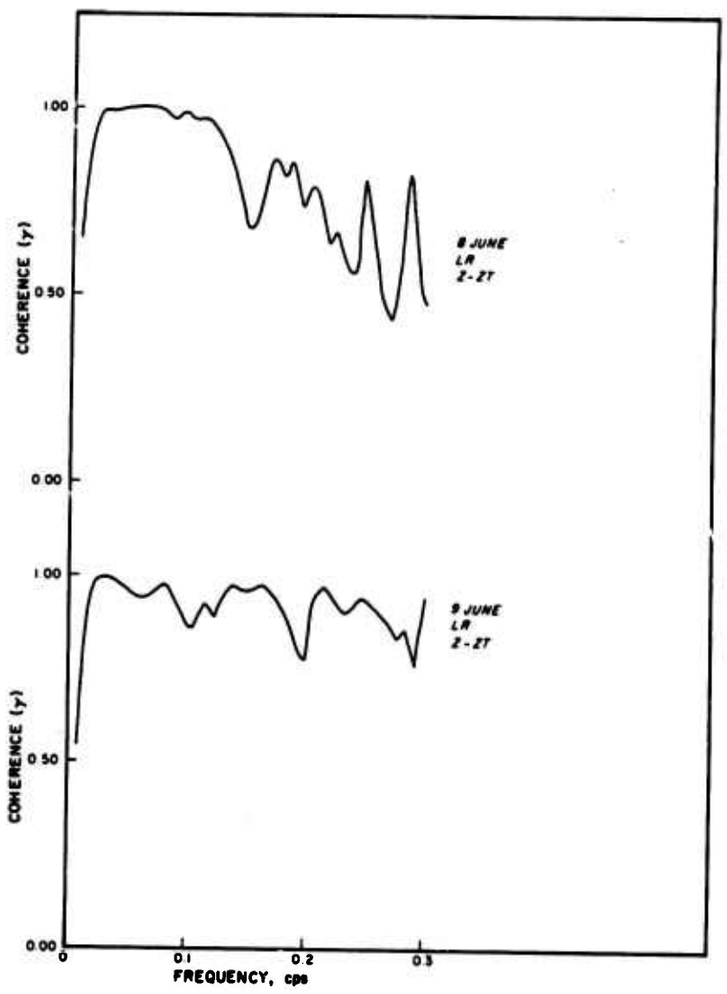

FIGURE 16. (CONT'D.) COHERENCE BETWEEN ALPS AND TRIAX COMPONENTS FOR SEVERAL SIGNALS.

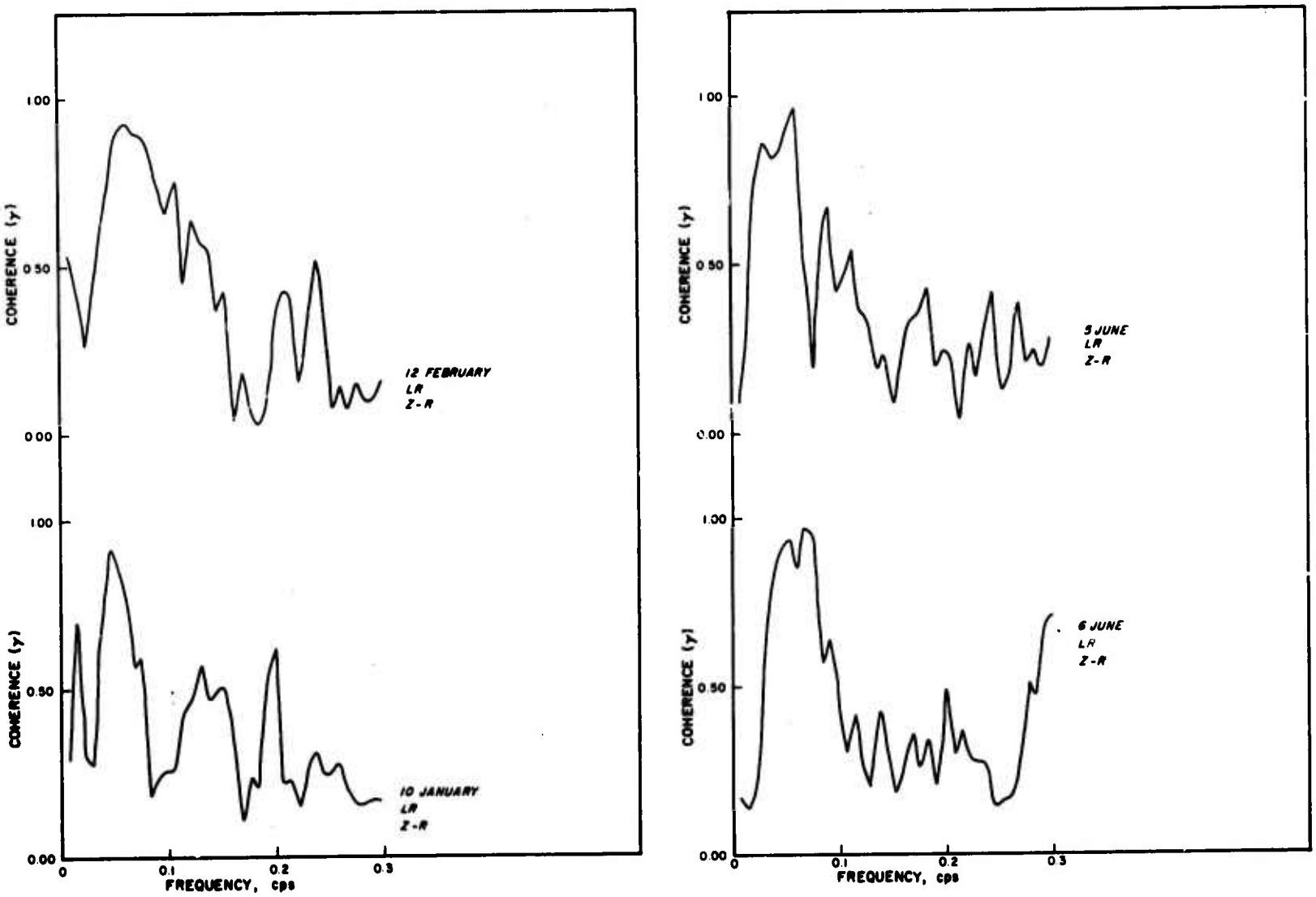

FIGURE 17. COHERENCE BETWEEN ALPS VERTICAL AND ALPS RADIAL COMPONENTS FOR SEVERAL SIGNALS.

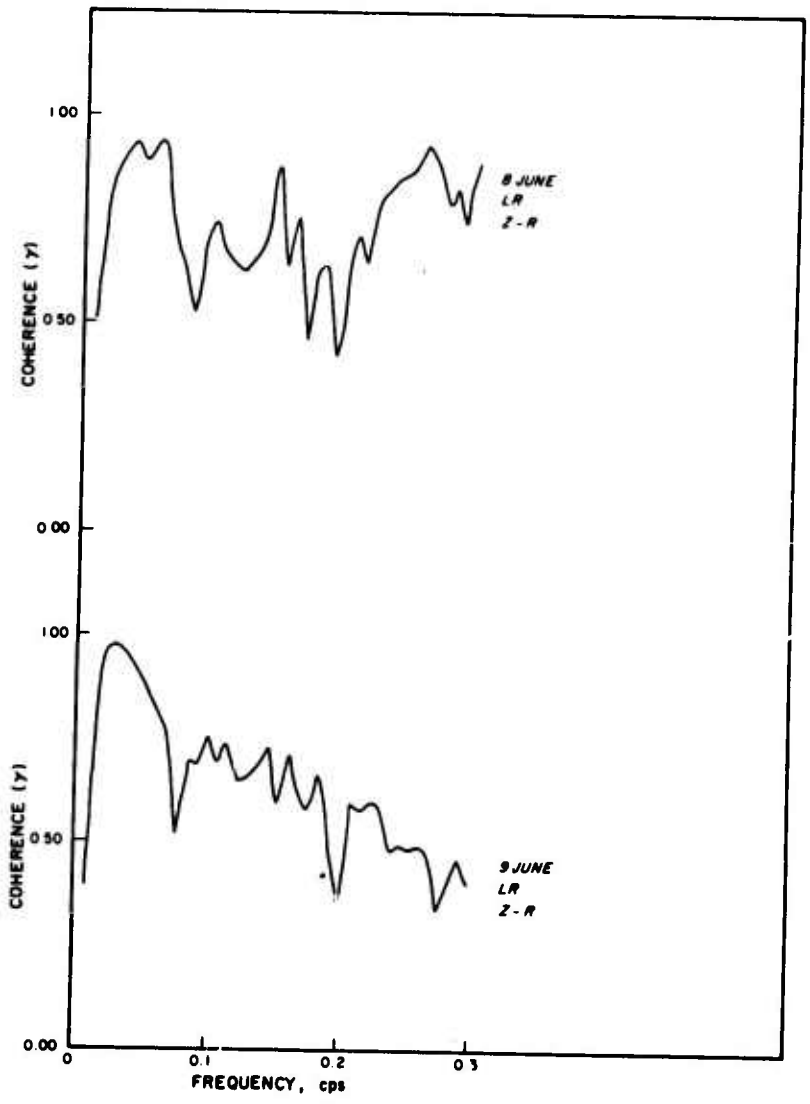

FIGURE 17. (CONT'D.) COHERENCE BETWEEN ALPS VERTICAL AND ALPS RADIAL COMPONENTS FOR SEVERAL SIGNALS.

Unclassified

Security Classification

DOCUMENT CONTROL DATA - R&D

(Security classification of title, body of abstract and indexing annotation must be entered when the overall report is classified)

1. ORIGINATING ACTIVITY (Corporate author)
TELEDYNE INDUSTRIES, INC.
ALEXANDRIA, VIRGINIA

2a. REPORT SECURITY CLASSIFICATION
Unclassified

2b. GROUP

3. REPORT TITLE
A LONG-PERIOD NOISE STUDY AT
MURPHY DOME, ALASKA
(LRSM Site FB-AK and ALPA Site 3-4)

4. DESCRIPTIVE NOTES (Type of report and inclusive dates)
Scientific

5. AUTHOR(S) (Last name, first name, initial)
Von Seggern, D. H.

6. REPORT DATE
6 January 1970

7a. TOTAL NO. OF PAGES
61

7b. NO. OF REFS
8

8a. CONTRACT OR GRANT NO.
F33657-69-C-0913-PZ01

b. PROJECT NO.
VELA T/9706

c. ARPA Order No. 624

d. ARPA Program Code No. 9F10

9a. ORIGINATOR'S REPORT NUMBER(S)
247

9b. OTHER REPORT NO(S) (Any other numbers that may be assigned this report)

10. AVAILABILITY/LIMITATION NOTICES
This document is subject to special export controls and each transmittal to foreign governments or foreign nationals may be made only with prior approval of Chief, AFTAC.

11. SUPPLEMENTARY NOTES

12. SPONSORING MILITARY ACTIVITY
ADVANCED RESEARCH PROJECTS AGENCY
NUCLEAR MONITORING RESEARCH OFFICE
WASHINGTON, D. C.

13. ABSTRACT

Long-period signals and noise samples recorded at Murphy Dome, Alaska, on standard LRSM instruments and the Geotech triaxial seismometer were subjected to spectral analysis. System noise tests showed that recorded seismic noise was limited to a band from .02 to 0.3 cps. Spectra representing many recording periods between January and August 1969 revealed the background noise to be of variable character and the RMS to range from 2.5 millimeters to 5.2 millimeters on a trace magnified 10^5 times with the standard LRSM system response. Due to its location at depth the triaxial instrument significantly reduced background noise on horizontal components caused by atmospheric pressure changes. Coherence between triaxial components of motion and corresponding LRSM components was excellent for most signals analyzed.

14. KEY WORDS

Seismic Noise
Coherence
Triaxial Seismometer
Microbarograph
Propagating Noise
ALPA

Unclassified

Security Classification